FINAL REPORT

Validation of Command-Detonation Munition Residues Testing

Project ER20-5018

October 2023

Samuel A. Beal, Ph.D., and Matthew F. Bigl, M.S.
USACE ERDC-CRREL

Charles A. Ramsey, M.S.
EnviroStat, Inc.

REPORT DOCUMENTATION PAGE

Form Approved
OMB No. 0704-0188

1. REPORT DATE *(DD-MM-YYYY)*	**2. REPORT TYPE**	**3. DATES COVERED** *(From - To)*
31-05-2023	ESTCP Final Report	4/1/2020 – 5/31/2023

4. TITLE AND SUBTITLE

Validation of Command-Detonation Munition Residues Testing

5a. CONTRACT NUMBER

5b. GRANT NUMBER

5c. PROGRAM ELEMENT NUMBER

6. AUTHOR(S)

Samuel A. Beal, Matthew F. Bigl, Charles A. Ramsey

5d. PROJECT NUMBER
ER20-5018

5e. TASK NUMBER

5f. WORK UNIT NUMBER

7. PERFORMING ORGANIZATION NAME(S) AND ADDRESS(ES)

US Army ERDC-CRREL
72 Lyme Rd
Hanover, NH 03755

EnviroStat, Inc.
PO Box 339
Vail, AZ 85641

8. PERFORMING ORGANIZATION REPORT NUMBER

9. SPONSORING / MONITORING AGENCY NAME(S) AND ADDRESS(ES)

Environmental Security Technology Certification Program
4800 Mark Center Drive, Suite 16F16
Alexandria, VA 22350-3605

10. SPONSOR/MONITOR'S ACRONYM(S)
ESTCP

11. SPONSOR/MONITOR'S REPORT NUMBER(S)

12. DISTRIBUTION / AVAILABILITY STATEMENT

DISTRIBUTION STATEMENT A. Approved for public release: distribution unlimited.

13. SUPPLEMENTARY NOTES

14. ABSTRACT

Command detonation allows a munition to be assessed for energetic residues early in the acquisition process, however this technology's representation of live-fire conditions has not yet been validated. The main objectives of this project were to 1) determine live-fire residue loading rates for two insensitive mortar munitions and 2) statistically compare these rates with previously determined rates for the same munitions using command detonation. Live-fire residue loading rates were successfully determine for a 60 mm IMX-104 munition (n=11 cartridges) and for an 81 mm IMX-104 munition (n=14 cartridges). Command detonation was found to have successfully reproduced total compound loading from live fire of the 60 mm munition ($p = 0.76$) but significantly underestimated live-fire loading from the 81 mm munition ($p < 0.01$). While command detonation underestimated loading of some residues, its utility was supported by the correct order-of-magnitude prediction of individual compound loading rates across both tested munitions.

15. SUBJECT TERMS
Munitions constituents; range sustainment; insensitive munitions

16. SECURITY CLASSIFICATION OF:			**17. LIMITATION OF ABSTRACT**	**18. NUMBER OF PAGES**	**19a. NAME OF RESPONSIBLE PERSON**
					Samuel A. Beal
a. REPORT	**b. ABSTRACT**	**c. THIS PAGE**			**19b. TELEPHONE NUMBER** *(include area code)*
UNCLASS	UNCLASS	UNCLASS	UNCLASS	100	(603) 646-4125

TABLE OF CONTENTS

LIST OF ACRONYMS

ACAT	Acquisition Category
AFS	Armaments Center Fuze Simulator
C4	Composition C-4; an explosive containing RDX and wax
CCDC AC	Combat Capabilities Development Command Armaments Center
CCV	Continuing Calibration Verification
Comp B	Composition B; an explosive containing RDX and TNT
CFS	CRREL Fuze Simulator
CHEETAH	A thermochemical model developed by Lawrence Livermore National Lab
CRREL	Cold Regions Research and Engineering Laboratory
DEVCOM AC	Combat Capabilities Development Command Armaments Center
DNAN	2,4-dinitroanisole
DOD	Department of Defense
DU	Decision Unit
EOD	Explosive Ordnance Disposal
ERDC	Engineer Research and Development Center
ERF	Eagle River Flats
ESOH	Environmental, Safety, and Occupational Health
ESTCP	Environmental Security Technology Certification Program
GPS	Global Positioning System
HMX	Octahydro-1,3,5,7-tetranitro-1,3,5,7-tetrazocine
HPLC	High Performance Liquid Chromatography
ICV	Initial Calibration Verification
IM	Insensitive Munition
IMP	Impact Fuze Setting
IMX-101	An IM formulation containing NTO, DNAN, and NQ
IMX-104	An IM formulation containing NTO, DNAN, and RDX
IPR	In-Progress Review
IQR	Interquartile Range
ITP	Inside the plume
JBER	Joint Base Elmendorf-Richardson
JPEO A&A	Joint Program Executive Office Armaments and Ammunition
LCEA	Lifecycle Environmental Assessment
LCS	Laboratory Control Sample
MIS	Multi Increment® Sampling, a registered trademark of EnviroStat, Inc.
MS	Matrix Spike
MSD	Matrix Spike Duplicate
NEPA	National Environmental Policy Act
NQ	Nitroguanidine
NTO	3-nitro-1,2,4-triazol-5-one
OB	Oxygen Balance
OTP	Outside the plume
PAX-21	An IM formulation containing RDX, DNAN, and ammonium perchlorate
PBXN-5	An explosive used as a booster in M734A1 fuzes
PBXW-14	An explosive used as a booster in M720A2 and M821A3 mortar munitions

PD	Point Detonating fuze
PESHE	Programmatic Environment, Safety and Occupational Health Evaluation
PEO	Program Executive Office
PM	Project Manager
PM CAS	Project Manager Combat Ammunition Systems
PRX	Proximity Fuze Setting
QA	Quality Assurance
QC	Quality Control
RDX	1,3,5-Trinitro-1,3,5-triazinane
RSD	Relative Standard Deviation
S&A	Safe and Arming Device
SERDP	Strategic Environmental Research and Development Program
SPE	Solid Phase Extraction
TNT	2,4,6-trinitrotoluene
UV	Ultraviolet

FIGURES

TABLES

ACKNOWLEDGMENTS

The authors are grateful to the following individuals and organizations for their support of this ESTCP project: Ashley Mossell, Kate Liddle Broberg, Art Gelvin, and Warren Kadoya for field and lab work; Megan Bishop, Jay Clausen, and Warren Kadoya for technical review; Brian Hubbard, Philip Samuels, Michael Walsh, and Erik Wrobel for scientific input; Fort Richardson Range Control and Ammunition Supply; the US Army 3rd Battalion 509th Infantry Regiment, 1st Battalion 501st Infantry Regiment, and 716th Explosive Ordnance Disposal Company; and the ESTCP program leaders, committee members, and support staff.

ABSTRACT

Introduction and Objectives

Loading of energetic residues during military training presents an environmental risk and potential threat to range sustainment. While conventional explosives (i.e., RDX, TNT) produce minimal post-detonation residues (<10 mg/round), some new insensitive high explosives have been found to produce gram-scale loading rates that may be environmentally significant. Command detonation allows a munition to be assessed for energetic residues early in the acquisition process, before the item is certified for live fire from a weapon. However, the ability for this technology to accurately represent residue loading as it occurs during training has not yet been validated. Application of this technology during life cycle environment assessment would help the DOD address potential future range sustainment issues and environmental liabilities.

The objectives of this project were to: 1) determine live-fire residue loading rates for two insensitive munitions as they are produced during military training; 2) statistically compare loading rates between these actual live-fire tests and previous command-detonation tests of the same munitions using two different fuze simulators (SERDP Project ER-2219); and 3) transfer validation study results to armaments and ammunition stakeholders.

Technology Description

Command detonation enables a munition to be fired remotely in a static position at a testing location where residues can be collected and then analyzed. The key uncertainties in this practice are whether the required replacement of the munition's fuze with a fuze simulator and the static upright positioning accurately represent residue production as it occurs during live fire. Previous command-detonation tests of the study munitions (60 mm and 81 mm IMX-104 mortar) used fuze simulators developed by ERDC-CRREL and the Armaments Center, each initiated in nose-up orientation with military blasting caps. Snow was used as a sampling medium as it provides visual evidence for the spatial extent of deposited soot and residue, and this medium provides extremely sensitive method detection limits (typically less than 1 mg/cartridge).

Performance and Cost Assessment

Loading rates of IMX-104 compounds were successfully determined from live fire of 60 mm (n = 11 cartridges) and 81 mm (n = 14 cartridges) mortar munitions that were initiated upon impact with snow, and then sampled and analyzed in the same manner as previous command-detonation tests. Command detonation was found to have successfully reproduced total compound loading from live fire of the 60 mm munition ($p = 0.76$) but significantly underestimated live-fire loading from the 81 mm munition ($p < 0.01$). While command detonation underestimated loading of some residues, its utility was supported by the correct order-of-magnitude prediction of individual compound loading rates across both tested munitions. The cost of implementing this technology to new, in-development munitions was estimated as minor relative to costs associated with potential future remediation efforts, range restrictions, and acquisition modifications.

Implementation Issues

Implementation of this technology would introduce an additional performance test in the development of new munitions. Minimization in effort and cost can be derived through tailoring

test logistics (i.e., test area and sampling medium) to data quality objectives (e.g., detection limits and targeted vulnerable receptors), while also examining opportunities to leverage existing test methods.

Publications

Beal, S.A., Bigl, M.F., Ramsey, C.A., Kadoya, W.M., Gelvin, A., and K. Liddle Broberg (accepted) Representation of live-fire energetic residues from insensitive mortar munitions using command-detonation testing, *Propellants, Explosives, Pyrotechnics*.

Beal, S.A. Bigl, M.F., and C.A. Ramsey (2023) Live-fire validation of command-detonation residues testing using an 81 mm IMX-104 munition. ERDC/CRREL TR-23-2, Hanover, NH. **DOI:** 10.21079/11681/46913

Beal, S.A. Bigl, M.F., and C.A. Ramsey (2022) Live-fire validation of command-detonation residues testing using a 60 mm IMX-104 munition. ERDC/CRREL TR-22-13, Hanover, NH. **DOI:** 10.21079/11681/45266

EXECUTIVE SUMMARY

INTRODUCTION

Reducing the source loading of munitions constituents on training ranges benefits the Department of Defense (DOD) by minimizing environmental impacts that could threaten range sustainment and incur significant remediation costs. On indirect fire and bombing ranges, the primary source of unconsumed explosives is currently low-order functioning (i.e., partial detonation, deflagration, dud) that releases dissolved energetic compounds from large particles of explosive filler (or intact unexploded ordnance) over the course of months to decades (*Beal and Bigl, 2023; Chendorain et al. 2005, Walsh et al. 2010*). For conventional explosives (i.e., TNT, RDX), intended high-order functioning has been found to deposit extremely minimal quantities of residual energetic compound relative to the original filler mass (<0.001 %; *Walsh et al. 2011a*). However, the requirement for new ammunition to meet insensitive munition (IM) criteria has led to the development of some munitions with significant, gram-scale residue loading rates following high-order detonation (*Walsh et al. 2018a*). In addition, some compounds used in these IM have high environmental mobility that raises concern for potential impacts to groundwater and surface water runoff (*Taylor et al. 2015; Arthur et al. 2018*). Environmental impacts on ranges from conventional energetics in the past have restricted training activities and incurred significant remediation costs (*Walsh et al. 2014a*).

The occurrence of unconsumed energetic material following detonation, where temperatures exceed 4000 K and pressures exceed 10 GPa, is unexpected and not readily predicted by theory (*Abdul-Karim et al. 2014*). Thermochemical models are commonly used to calculate condensed and gaseous-phase detonation products, which are in turn used to predict detonation performance of explosive formulations, but these models assume complete explosive consumption and therefore do not predict residue formation (e.g., *Fried and Souers, 1994*). Empirical testing is therefore required to assess residue loading rates and, due to the complexity of modern munitions, each munition should be tested individually to represent variables in explosive mass, diameter, and explosive train (i.e., initiating charge to booster to main fill).

Live-fire testing is logistically difficult and critically cannot be performed early in the acquisition process when changes are most easily and cost-effectively made. Command detonation provides the only method for performing residue testing early in the acquisition process, before certification for fire from a weapon, and in a static position in a controlled testing environment. Crucially, reproduction of the fuze-initiated explosive train with a fuze simulator is required. The key uncertainties in this practice are whether residue production is affected by replacement of the munition's standard fuze with a fuze simulator and orienting the munition in a static position.

OBJECTIVES

The primary objective of the performed work was to validate the use of command detonation for munition residues testing using two IM (60 mm and 81 mm mortar with IMX-104 filler) that were previously characterized by command detonation using two different fuze simulators during SERDP Project ER-2219. These study munitions have completed the certification process and are being integrated into ammunition supplies, which allowed us to determine actual residue loading from live-fire training and then to perform statistical comparisons with prior command-detonation data.

The secondary objective of this work was to transfer the results of this validation study to munition acquisition, research, and development stakeholders at Joint Program Executive Office Armaments and Ammunition (JPEO A&A), Project Manager Combat Ammunition Systems (PM CAS), and Combat Capabilities Development Command Armaments Center (DEVCOM AC). Study results aimed to inform stakeholders of live-fire representation by previous command-detonation tests and potential methods for integrating residue testing in the environmental assessment for new munitions.

TECHNOLOGY DESCRIPTION

The command-detonation technology involves application of a fuze simulator to a study munition in a static position. An ideal fuze simulator matches the explosive charge composition and output of the safe and arming (S&A) device and booster used in the munition's fuze. Previous work has shown that external initiation, such as using a demolition block or shaped charge, produces significantly greater residue loading than initiation through the fuze well for both conventional munitions and IM (*Walsh et al. 2008; 2014b*). Fuze simulators applied to studying post-detonation residues have been developed by the Cold Regions Research and Engineering Laboratory (CRREL) using a field-adjustable Composition C-4 (C4) booster (Figure 1; *Walsh et al. 2011b*) and by DEVCOM AC using a fuze-matching polymer bonded explosive booster. Both fuze simulators have been applied with a standard M6/M7 blasting cap for initiation. The fuze simulators developed by CRREL (CFS) and DEVCOM AC (AFS) have well-constrained residue loading data in application to 60 mm and 81 mm munitions filled with IMX-104, an insensitive high explosive containing the compounds 3-nitro-1,2,4-triazol-5-one (NTO), 2,4-dinitroanisole (DNAN), and 1,3,5-trinitroperhydro-1,3,5-triazine (RDX).

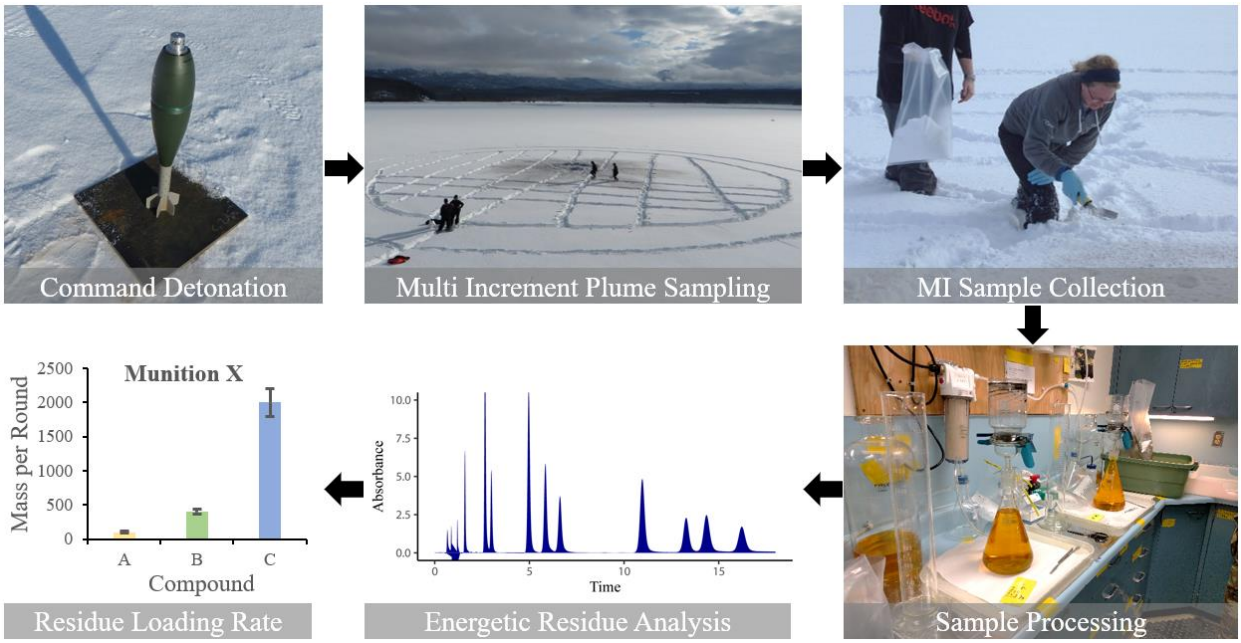

Figure 1. Schematic of command detonation residues testing method, starting from top left.

Command-detonation tests typically position the study item on a steel plate or ice block to minimize cratering (Figure 1). Following detonation, the produced residues can be sampled following a variety of different approaches and methods. For this validation study, sampling of

residues deposited on snow was used as it provides a robust and sensitive method that was also used previously in command-detonation tests of the study munitions. The visible plume of deposited soot and residue on snow allows the entire depositional area to be representatively sampled using Multi Increment® sampling. Measured compound concentrations in melted and processed snow samples are used in combination with areal measurements of the plume to calculate compound loading rates on a per-cartridge basis.

PERFORMANCE ASSESSMENT

We determined live-fire detonation residues from 60 mm and 81 mm IMX-104 mortar cartridges over two respective field campaigns. Cartridges were fired from mortar systems, exactly as they are during training, and then sampled following the same protocols that have been used in determining command-detonation residues for these munitions previously. The impact fuze setting for live-fired cartridges was found to produce a well-defined depositional plume of residue and soot with minimal or no cratering (Figure 2), which was similar in presentation to plumes produced from previous command-detonation tests. In contrast, a single 60 mm cartridge was fired with a 2-meter airburst using the proximity setting that produced no visible deposition. Subsequently, all test cartridges were fired with the impact fuze setting.

Figure 2. Post-detonation cloud from live fire of an 81 mm munition (M889A4) with impact setting; and multi increment sampling the deposited soot and residue plume on snow.

In total, 9 plumes covering 11 live-fire impact detonations of the 60 mm IMX-104 munition and 13 plumes covering 14 live-fire impact detonations of the 81 mm IMX-104 munition were successfully sampled (Figure 3). Sampling quality assurance comprised ‘outside-the-plume’ samples surrounding each detonation plume and background samples outside the target area. Each plume was sampled in triplicate to assess method uncertainty, which was minimal for all sampled plumes ranging from 2 to 25 % relative standard deviation (RSD). Uncertainty in the estimate of total loading rate, calculated across all sampled plumes for each munition, was 24 % RSD for the 60 mm munition and 35 % for the 81 mm munition. This level of precision met the success criteria of less than 50 % and bettered precision from previous command-detonation tests.

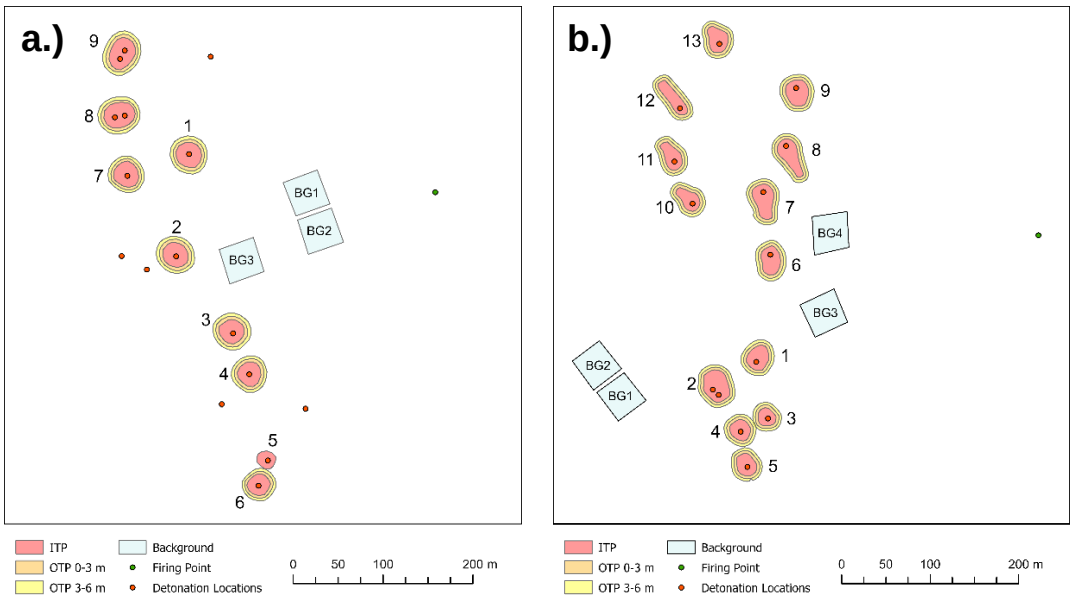

Figure 3. Plume locations and areas in the target region from live-fire tests of the a.) 60 mm munition and b.) 81 mm munition, as measured by real-time kinematic survey.

Newly collected live-fire and previously collected command-detonation data were aggregated to perform statistical tests on loading rates of each constituent IMX-104 compound. Validation success was measured as no significant difference in total residue loading rates between live fire and at least one of the fuze simulators. Total residue loading rates are compared between live-fire and all command-detonation tests in Figure 4. For the 60 mm munition, there was no significant difference in total residue loading rates between live fire and command detonation with the AFS (p = 0.76), which met the validation success criteria. The CFS with 12 g C4 booster significantly underestimated total residue loading from detonation of the 60 mm munition, potentially due to its greater booster mass. For the 81 mm munition, both fuze simulators significantly underestimated total residue loading rates as it occurs during training, which led the validation success criteria not to be met for this munition.

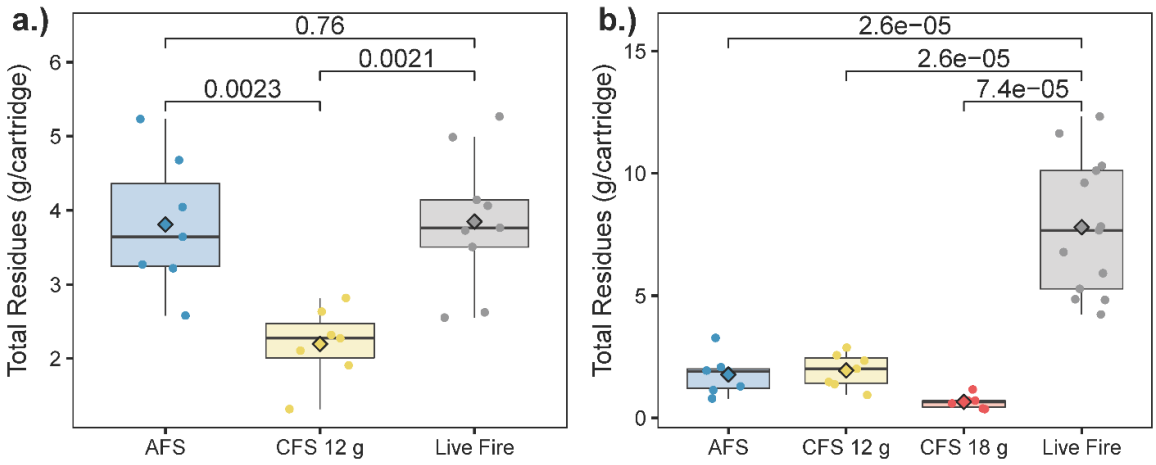

Figure 4. Comparison of total residue loading rates between live-fire and command-detonation tests of a.) the 60 mm munition and b.) the 81 mm munition. *P* values for Mann-Whitney tests are listed, individual plume estimates shown as points, and means for each fuzing type shown as diamonds.

Total residue loading was controlled by NTO—the dominant residual compound by two orders of magnitude (Table 1). The minor residue compounds RDX and DNAN were at times well-represented or underestimated by previous command-detonation tests. For the 60 mm munition, while NTO loading was an exact match between the AFS and live fire, RDX and DNAN loading rates were significantly underestimated with both fuze simulators by factors of 3–6. Conversely, for the 81 mm munition NTO was significantly underestimated by command detonation, but RDX and DNAN loading rates were generally not significantly different between representative command detonation (AFS and CFS 12 g) and live fire.

Table 1. Summarized average residue loading rates using all tested fuzing types for the 60 mm IMX-104 (M720A2) and 81 mm IMX-104 (M821A3/M889A4) munitions. Values are rounded to appropriate significant figures based on plume-average standard deviations shown in parentheses.

Caliber	Plumes/ Cartridges	Fuze	Mean Loading Rate (mg/cartridge)				
			HMX	RDX	DNAN	NTO	Total
60 mm	9/11	Live Fire	1.9 (0.6)	12 (4)	30 (10)	3800 (900)	3800 (900)
	7/7	AFS	0.4 (0.3)	2 (1)	7 (4)	3800 (900)	3800 (900)
	7/7	CFS 12 g	2 (2)	4 (5)	5 (1)	2200 (500)	2200 (500)
81 mm	13/14	Live Fire	2 (2)	20 (20)	60 (60)	8000 (3000)	8000 (3000)
	7/7	AFS	1 (1)	10 (20)	50 (80)	1700 (700)	1800 (800)
	7/7	CFS 12 g	2 (2)	20 (20)	30 (30)	1900 (700)	1900 (700)
	6/6	CFS 18 g	0.9 (0.5)	8 (4)	8 (8)	600 (300)	700 (300)

The two main variables that could explain observed differences in residue loading between command detonation and live fire are: 1) cartridge orientation effects on deposition of fine particles; and 2) accurate representation of the fuze explosive train.

In positioning the study cartridges nose-up during previous command-detonation tests, emission may have been promoted especially for fine-particle constituents such as DNAN and RDX. Observed differences in RDX and DNAN phase-partitioning for the 60 mm munition following sample melt (i.e., aqueous mass in filtrate versus solid mass on filters) suggested that the nose-down orientation during live-fire impact may have more completely retained produced fine residues.

Slight deviations from the fuze's explosive train in previous command-detonation tests may have propagated to significant differences in residues of explosive filler. While the previously tested fuze simulators matched or represented the booster used in the munitions' fuze, the military blasting caps that were used to initiate the boosters in these fuze simulators significantly exceeded the explosive mass of the detonators in the fuze S&A device. This potential over-initiation of the cartridges during command detonation may have led to the observed underestimation of live-fire residues, particularly for the larger mass 81 mm munition.

Despite differences in loading rates for some compounds and munitions, this study showed that command detonation can accurately predict compound loading to the correct order of magnitude. This level of accuracy is likely sufficient for environmental impact prediction, but improvements in the command-detonation test setup can likely lead to closer representation of live fire. Namely, orientation in a nose-down orientation just above the sampling surface, and use of detonators that closely match the explosive train of the issued fuze, could improve future command-detonation tests.

COST ASSESSMENT

The costs of integrating this technology in the acquisition process for a new munition is estimated to be approximately $70K in direct costs only. Overall costs are likely to depend greatly on the ability to leverage existing item tests and the tailoring of test setups to meet targeted data quality objectives. For example, if the high sensitivity of testing on snow is not required and an existing temperate field test can be leveraged, then costs are likely to fall under $70K. These minimal testing costs should be compared against the potential costs incurred if testing is not performed and a study munition is found to deposit significant damaging quantities of energetic residue. These no-action costs are difficult to estimate but could involve: 1) acquisition changes (estimated >$1M); 2) remediation efforts (e.g., >$1.2B at Joint Base Cape Cod; *MA ARNG [2019]*); and/or 3) range closures and associated impacts to training access and readiness (*Walsh et al. 2014a*). Given the low cost of residue testing relative to potential no-action liabilities and the findings of extremely high loading rates from some IM, implementation of this technology appears both critical and minimally intensive.

IMPLEMENTATION ISSUES

Accurate representation of a fuze-initiated firing train presents some challenges when applied in a static configuration required for command detonation. While previous attempts to match the fuze booster charge were applied with reasonable results, differences in the initiation charge stemming from the use of common military blasting caps may have caused observed underestimation of compound loading. Application of commercial-of-the-shelf exploding bridge-wire detonators of similar output charge to the study fuze's S&A device could improve data representativeness.

Several methods of sampling energetic residues released from command-detonation are available, each with their own advantages and disadvantages. The use of deposition on snow in this study followed the method used in previous command-detonation tests of the munition. This method assumes complete recovery of produced residues from the snow surface surrounding the detonation point, but in this open-air setting emission for long-range atmospheric transport was a possibility. A previous study indicated this emitted fraction is low (7 %; *Walsh et al. 2018b*), and we additionally demonstrated that elemental carbon can be a surrogate for residue recovery. Integration in the development and qualification process for new munitions can consider the array of sampling methods available to best address their data quality objectives and leverage related performance tests to reduce overall costs.

Implementation of the command-detonation technology for residue testing, regardless of the sampling method, can provide meaningful data to guide acquisition and range management decisions. Recent stakeholder interest in applying this technology to previously untested IM highlights this technology's value. As the DOD develops improved explosive formulations and replenishes munition stockpiles, integration of this technology in the acquisition process is poised to identify and manage potential environmental issues proactively to ensure future range sustainment.

1. INTRODUCTION

1.1 BACKGROUND

Live-fire training with munitions is an essential component of warfighter readiness. However, munition firing and detonation releases energetic residues that may accumulate in high concentrations at the soil surface or mobilize off-site. Environmental impacts from energetic residues have resulted in training restrictions and expensive remediation efforts on installations in the past (*Walsh et al. 2014a*). Controlling source loading of energetic residues is therefore fundamental to sustaining training ranges, and this control is especially needed as the military transitions from using conventional munitions to new insensitive munitions (IM) that have favorable performance characteristics but often contain explosive compounds with significantly greater environmental mobility (*Taylor et al. 2015; Arthur et al. 2018*).

Conventional munitions containing the explosive formulations Composition B (2,4,6-trinitrotoluene [TNT] and 1,3,5-trinitroperhydro-1,3,5-triazine [RDX]) and TNT have been found to deposit minimal residues following detonation (<1 to 19 mg per round; Table 2). For conventional munitions, the bulk of energetic residues deposited on ranges are derived from munition malfunctioning (i.e., low-order), which is characterized by partial detonations or duds that slowly release their energetic filler over months to decades, respectively (*Beal and Bigl, 2023; Chendorain et al. 2005, Walsh et al. 2010*). However, command-detonation tests during SERDP Project ER-2219 found that tested mortar and howitzer IM deposited significant quantities (>1 g per round) of unconsumed energetic material following intended high-order functioning (*Walsh et al. 2013a; 2014b; 2018a*). The two current IM filler formulations used by the DOD are IMX-101 (containing the compounds 3-nitro-1,2,4-triazol-5-one [NTO], 2,4-dinitroanisole [DNAN], and nitroguanidine [NQ]) and IMX-104 (containing NTO, DNAN, and RDX). The compounds NTO and NQ have relatively high solubility and low affinity for soil compared to their conventional counterparts (*Taylor et al. 2015, Arthur et al. 2018*), which raises concern of their likelihood for groundwater and surface water transport.

The presence of unreacted energetic material following detonation is unexpected given the high energy environment (in excess of 4000 K and 10 GPa), and mechanistic theory explaining residue formation is critically missing (*Abdul-Karim et al. 2014*). This uncertainty precludes prediction by modeling. Common thermochemical models (e.g., CHEETAH; *Fried and Souers, 1994*) that are used to calculate detonation products and explosive performance make the reasonable assumption of no unreacted energetic remaining following detonation. Empirical post-detonation residue testing is therefore the only method of estimating residue loading for munitions. Life cycle environmental assessments (LCEAs) for recent new munitions have seldom included empirical residue testing of any type, and the absence of this information makes determination of environmental impact during use stage (i.e., training) highly uncertain (*Walsh et al. 2018b*).

While live-fire testing reflects the real-world conditions in which residues are deposited, this method of testing is logistically difficult as it requires operating in a dudded impact area, and live fire cannot occur early in the acquisition process when rounds are not yet certified. Command-

detonation residue testing is the only current effective technology for addressing environmental impact early in the acquisition process.

Table 2. Summarized total energetic residues from selected CRREL high-order detonation tests. Command-detonation tests used the fuze simulators: AFS developed by DEVCOM Armaments Center and CFS with variable C4 booster masses developed by CRREL. Previous live-fire tests used point detonating (*PD*) fuzes with nomenclature noted as available.

Caliber (mm)	Munition	HE Filler	HE Compounds	*Fuze*/ Simulator	DUs/ Rnds (*n*/*n*)	Residues (mg/round)	Reference
60	M888	Comp B	RDX/TNT	*PD (M935)*	6/7	0.07	*Walsh et al. 2006*
	M768	PAX-21	AP/RDX/ DNAN	CFS 14 g	7/7	14,000	*Walsh et al. 2013a*
	M720A2	IMX-104	NTO/RDX/ DNAN	CFS 12 g	7/7	2,200	*Walsh et al. 2014b*
	M720A2	IMX-104	NTO/RDX/ DNAN	AFS	7/7	3,800	*Walsh et al. 2018a*
81	M374	Comp B	RDX/TNT	*PD*	2/14	9.5	*Hewitt et al. 2003*
	M374A2	Comp B	RDX/TNT	CFS 23 g	3/3	10	*Walsh et al. 2011a*
	M889A2	Comp B	RDX/TNT	CFS 12 g	6/6	<0.8	*Walsh et al. 2018a*
	M821A3	IMX-104	NTO/RDX/ DNAN	CFS 12 g	7/7	1,900	*Walsh et al. 2014b*
	M821A3	IMX-104	NTO/RDX/ DNAN	CFS 18 g	6/7	700	*Walsh et al. 2018b*
	M821A3	IMX-104	NTO/RDX/ DNAN	AFS	7/7	1,800	*Walsh et al. 2018a*
105	M1	Comp B	RDX/TNT	*PD*	9/13	0.2	*Hewitt et al. 2003*
120	M933	Comp B	RDX/TNT	*PD (M745)*	8/9	21	*Walsh et al. 2005a*
155	M107	Comp B	RDX/TNT	*PD*	7/7	0.3	*Walsh et al. 2005b*
	M107	TNT	TNT	*PD*	7/7	<0.02	*Walsh et al. 2005b*
	M1122	IMX-101	NTO/NQ/ DNAN	CFS 50 g	7/7	154,000	*Walsh et al. 2018a*
	M1122	IMX-101	NTO/NQ/ DNAN	AFS	3/7	87,000	*Walsh et al. 2018a*

The technology evaluated in this project included a method of initiating munition high-order functioning by command detonation and a coupled method of quantitatively measuring deposited residues. This technology enables munitions to be tested prior to certification for firing from a weapon system, so it can occur early in the acquisition cycle when changes are most practical and efficient. Although new munitions are subjected to environmental assessment prior to large-scale production and usage on ranges, testing for solid residues is not commonly performed (*Walsh et al. 2018b*). This demonstration sought to validate the technology and advise its adoption by program managers early in the acquisition process for new munitions.

The potential derivative benefits of this demonstration are the avoidance of environmental cleanup liabilities, the sustainment of training ranges, and increased cost efficiency in defense acquisition. As an example, a mortar munition containing the IM filler PAX-21 was identified to deposit high amounts of perchlorate following high-order detonation, but this testing occurred during a non-routine research study and after approximately 180,000 cartridges had been acquired (*Walsh et al., 2013b*). Integration of this technology early in the acquisition cycle would have saved substantial acquisition costs in addition to the avoidance of potentially significant environmental liability.

1.2 OBJECTIVE OF THE DEMONSTRATION

The primary objective of the performed work was to validate the use of command detonation technology for munition residues testing. We approached this technology validation by measuring energetic residue loading rates from live-fire training with 60 mm and 81 mm mortar IM that have well-established command-detonation loading rates using two different fuze simulators. These munitions have completed the certification process and are being integrated into ammunition supplies, replacing stockpiles of munitions containing current standard (Comp B) explosive fillers.

The secondary objective of this work was to transfer the results of this validation study to the munition acquisition stakeholders at Joint Program Executive Office Armaments and Ammunition (JPEO A&A), Project Manager Combat Ammunition Systems (PM CAS), and Combat Capabilities Development Command Armaments Center (DEVCOM AC). Study results were aimed to inform stakeholders on potential methods for residue testing integration in the environmental assessments for new munitions.

1.3 REGULATORY DRIVERS

This command-detonation residue testing method addresses several regulations that cover the mandate for IM, the determination of environmental impact for Army actions, and the considerations of environmental impact in range sustainment. Relevant excerpts or paraphrased sections of these regulations are listed below:

DOD Directive 5000.01 (August 2018) "The Defense Acquisition System"

E1.1.1.11. Integrated Test and Evaluation

> "Test and evaluation shall be integrated throughout the defense acquisition process. Test and evaluation shall be structured to provide essential information to decision-makers, assess attainment of technical performance parameters, and determine whether systems are operationally effective, suitable, survivable, and safe for intended use…"

E1.1.23. Safety

> "… All systems containing energetics shall comply with insensitive munitions criteria."

DOD Instruction 5000.02 (November 2013) "Operation of the Defense Acquisition System"

E3.16a. Programmatic ESOH Evaluation (PESHE)

> "The Program Manager, regardless of acquisition category (ACAT) level, will prepare and maintain a PESHE to document data generated by ESOH analyses conducted in support of program execution. The PESHE will include at a minimum identification of ESOH risks and their status; and, identification of hazardous

materials, waste, and pollutants (discharges/emissions/noise) associated with the system and its support as well as the plans for minimization and/or safe disposal."

32 CFR Part 651 (AR-200-2) "Environmental Analysis of Army Actions"

Section 651.14 calls for early integration of environmental impacts through NEPA analysis to drive decision-making by PEOs and PMs.

DOD Directive 4715.11 (August 2018) "Environmental and Explosives Safety Management on Operational Ranges within the United States"

4.2: "Ensure the long-term viability of operational ranges while protecting human health and the environment."

4.5: "Design and use operational ranges and the munitions used on them, to the extent practical, to minimize both potential explosive hazards and harmful environmental impacts and to promote resource recovery and recycling."

5.4.3: "Establish and implement procedures to assess the environmental impacts of munitions use on operational ranges."

5.4.15: "Where prior hydrologic and hydrogeologic assessments create a reasonable belief that munitions constituents may migrate off an operational range, conduct an additional, appropriate assessment, including testing and analysis, as necessary, to determine whether a release or substantial threat of a release of munitions constituents from an operational range to off-range areas has occurred or is about to occur."

DOD Directive 3200.15 (December 2013): "Sustainment Access to the Live Training and Test Domain."

"Preserve and sustain access and operational use of the live training and test domain needed to support current and future requirements through:

… Management that incorporates sound environmental principles and range sustainment considerations."

2. TECHNOLOGY

2.1 TECHNOLOGY DESCRIPTION AND DEVELOPMENT

The technology seeking validation here was the static command detonation of munitions using a fuze simulator for the determination of energetic residues. Common mortar and howitzer munitions are issued with a fuze that arms after firing and initiates at the target. However, to test munitions without firing from a weapons system, the issued fuze must be replaced with a fuze simulator that allows the munition to be initiated in a static position and on command. Initiation by external charges (i.e., blow-in-place) has been shown insufficient in this application as it produces significantly greater residues than initiation through the fuze well for both conventional munitions and IM (*Hewitt et al. 2005*; *Walsh et al. 2008; 2014b*).

During SERDP Project ER-1481, Mr. Michael Walsh developed a fuze simulator to enable command detonation of mortar and artillery munitions, and this technology was then later applied to IM for SERDP Project ER-2219. This CRREL fuze simulator (CFS) is constructed of aluminum with a milled well for a booster charge, a hole for blasting cap insertion, and a male threaded base that matches the issued fuze (*Walsh et al. 2011b*; Figure 5). The explosive train of the CFS uses a standard M6/M7 blasting cap transferred to a field-adjustable mass of Composition C-4 (C4) explosive in the booster well, which in turn initiates the study munition's main fill or auxiliary booster (if applicable).

Figure 5. A CFS packed with C4 explosive (left), a CFS threaded onto a 60 mm body (middle), and an actual fuze on a 60 mm cartridge (right).

The C4 booster mass in the CFS was found to be a major control on munition functioning, with a reduced mass capable of initiating a partial detonation (*Bigl et al. 2020; Walsh et al. 2018a*). Thus, the selection of C4 mass remains a major variable that could affect residue production significantly, even within the category of observable high-order functioning (*Walsh et al. 2018b*). Although the mass of explosive used in the issued fuze can be used as a reference, differences in explosive formulation, density, and geometry have an undetermined effect on residual quantity. Ideally, command-detonation tests would use a fuze simulator that closely matches the explosive train of the issued fuze to best represent live-fire conditions.

The finding of high residue deposition rates for IM using the CFS led to subsequent command-detonation tests using a fuze simulator developed by DEVCOM AC (designated here as AFS). The AFS used a 9 g booster of PBXN-5 (an HMX-based explosive) that matches the composition of the booster used in the M734A1 multi-option fuze issued with the studied 60 mm and 81 mm mortar IM. Command-detonation tests using the AFS were performed on seven cartridges each of 60 mm (M720A2) and 81 mm (M821A3) IMX-104 mortar munitions, and the same setup and sampling methods were used as earlier tests with the CFS (*Walsh et al. 2018a*). For the 60 mm munition, the AFS produced residues that were slightly greater but the same order-of-magnitude as the CFS, with the predominant and differential residual component being NTO (Figure 6). For the 81 mm munition, residue loading rates with the AFS were generally equivalent to those produced by the CFS with 12 g C4 booster, whereas loading rates with the 18 g CFS were significantly lower. Overall, these tests demonstrated that the different fuze simulators produced residue loading rates on the same order-of-magnitude despite differences in booster mass and composition.

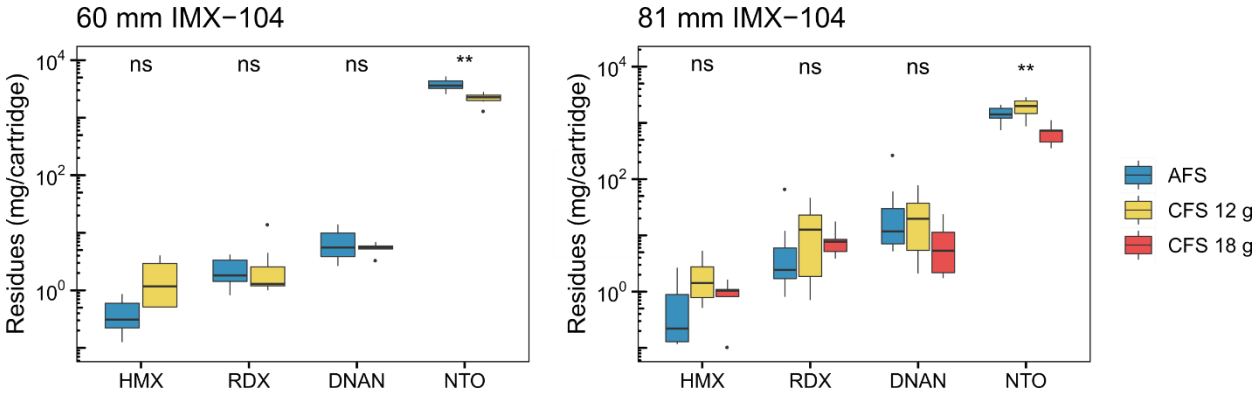

Figure 6. Command detonation residue loading rates of the 60 mm M720A2 (left) and 81 mm M821A3 (right) IMX-104 mortar rounds using the CRREL (CFS) and DEVCOM AC (AFS) fuze simulators (*Walsh et al., 2018a*). Kruskal-Wallis rank sum test significance levels are noted (ns: $p > 0.05$; **: $p \leq 0.01$).

Validation of the command-detonation technology through comparison with live fire has so far been limited to a small set of data on 81 mm Comp B mortar munitions. The first tests using the CFS on Comp B-filled M374A2 ($n = 3$) produced detonation residues of ~10 mg/cartridge, which were in good agreement with loading rates determined on M374 by live fire (~9 mg/cartridge; $n = 2$; Table 1; *Hewitt et al., 2005; Walsh et al., 2011a*). Later command-detonation tests on another munition of the same caliber and filler (M889A2) produced residues below the method detection limit (<0.8 mg/cartridge; $n = 6$; *Walsh et al. 2018a*). The limited live-fire data and near or below detection loading rates for these conventional munitions provide incomplete validation of the command-detonation technology, with uncertainty in application to IM.

Coupled with the command-detonation technology is a method of sampling post-detonation material, quantifying energetic residues, and calculating residue loading rates (i.e., amount of energetic residue produced per round fired). Approaches to this problem have included: detonation in an enclosed chamber that contains the produced solid residue; collection of residue adhered to witness plates; and sampling of the ground surface that contains deposited residue. The advantages of each method are discussed in the following section, however the latter method applied to a snow surface was selected for this validation study and is discussed in detail.

A robust and sensitive method for conducting these tests on snow and ice was developed and successfully applied to more than thirty munition configurations by CRREL and Defence Research and Development Canada Valcartier (*Walsh et al. 2017a*). The first step of this methodology involves demarcation of the visual detonation residue/soot plume area to determine a decision unit (DU) for Multi Increment® Sampling (MIS). The plume perimeter is traced with a high-precision GPS (i.e., real-time kinematic) to measure total DU area. Sampling teams collect MI samples, each comprised of approximately 100 increments, following the MIS pattern across the DU (Figure 7). The sampling tool is a square-sided flat-bottomed scoop with fixed dimensions that, in combination with the number of increments collected, allows the determination of total sampled area. Collected snow samples are processed by melting, filtering, and extraction following established methods (*Walsh et al. 2012*). Processed samples are then analyzed for their energetic composition by high performance liquid chromatography (HPLC) with ultraviolet (UV) detection. While legacy energetics (e.g., HMX and RDX) and DNAN are amenable to conventional reverse phase separation (i.e., EPA Method 8330B), the polar IM compounds NTO and NQ are resolvable by porous graphitic carbon and hydrophilic interaction techniques (*Walsh 2016*).

Figure 7. In-progress MI sampling of an 81 mm command detonation plume area.

The method of sampling deposited residues was indirectly supported through comparison of blast-chamber and snow samples from separate command-detonation tests of the 60 mm PAX-21 mortar cartridge (M720A1 and M768). Discrete samples of residue from the blast chamber detonations of two cartridges yielded an average of 14 g perchlorate per cartridge, and multi increment snow samples of seven cartridge detonations averaged 13 g perchlorate per cartridge (*Walsh et al. 2018b*).

The combined technology for validation in this study is described visually in Figure 8. Moving clockwise from the top left: a study munition is set up at a testing location and command detonated; the detonation plume is sampled following MIS procedures in triplicate; the samples are processed to isolate aqueous and solid fractions, concentrate aqueous analytes, and extract solid residues; processed samples are analyzed for energetic composition; and residue loading rates are calculated for each energetic compound.

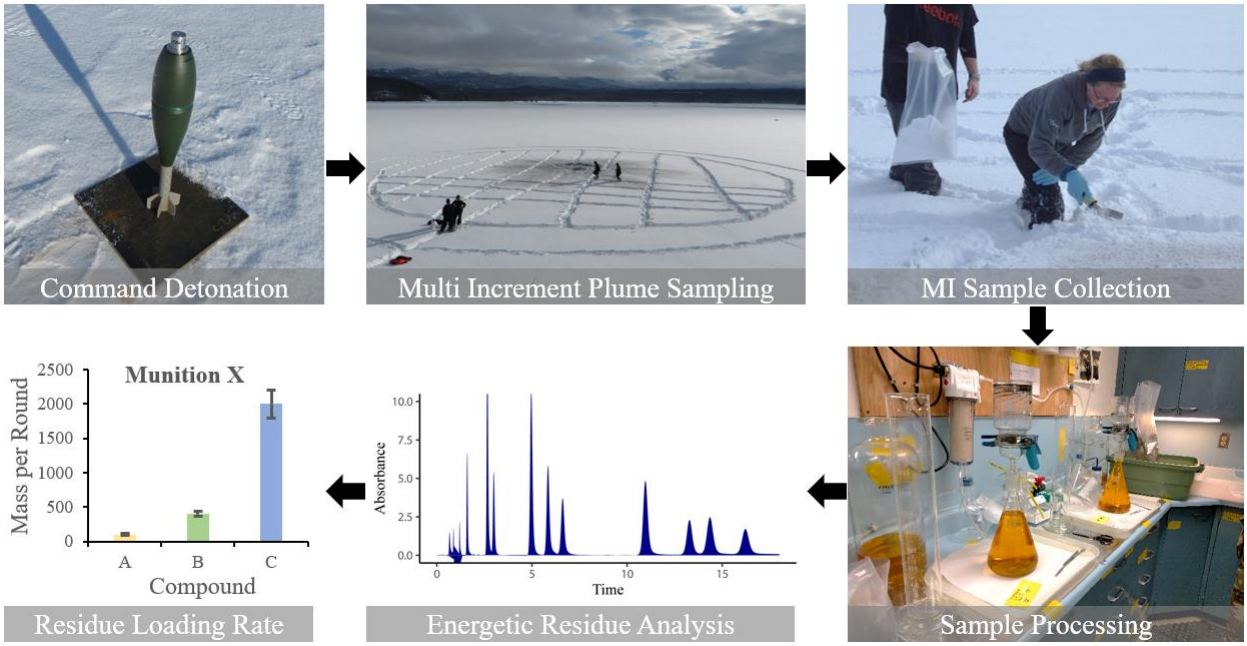

Figure 8. Schematic of command detonation residues testing method, starting from top left.

The technology was developed through several significant advances accomplished during previous SERDP projects, summarized below:

2000-2005: SERDP ER-1155

- Blow-in-place and live-fire detonations of mine, mortar, and howitzer rounds on snow. Plume areas were sampled in discrete units and analyzed.
- Developed method for cleanly collecting, filtering, and analyzing snow samples.

2005-2011: SERDP ER-1481

- Developed methods for Multi Increment® Sampling of detonation plumes on snow.
- Tested additional explosives and propellants using this new defensible sampling method. (*Walsh et al. 2007, Walsh et al. 2012*).
- Developed CRREL fuze simulator for command-detonation studies.

2011-2018: SERDP ER-2219

- Applied the CFS to IM and found high deposition rates for some munitions (i.e., M768 PAX-21 and M1122 IMX-101).
- Confirmed representative simulation of the CFS by testing IMX-104 mortar rounds and M1122 with a fuze simulator supplied by DEVCOM AC (AFS).
- Developed analytical methods for NTO, NQ, DNAN, and DNAN transformation products in post-detonation residue (*Walsh 2016*).

The ultimate intended application of this technology is in the LCEA and PESHE processes for new munitions, which are managed by defense acquisition stakeholders. Ideally, this validation would facilitate early integration of this testing technology in the acquisition process before significant costs are incurred. The primary stakeholders are PM CAS and JPEO A&A, located at Picatinny Arsenal, New Jersey.

2.2 ADVANTAGES AND LIMITATIONS OF THE TECHNOLOGY

The main advantages of implementing command-detonation testing early in the acquisition cycle are the avoidance of unnecessary acquisition costs and mitigation of environmental impacts. As an example, command-detonation testing of the 60 mm PAX-21 mortar munition allowed the Army to avoid environmental liabilities estimated on the order of $1B, but testing earlier in the acquisition process could have also avoided acquisition costs of greater than $40M (*Walsh et al., 2013b*).

Environmental impacts from detonation are considered in LCEAs typically only as the degraded gaseous and solid-carbon products. While unconsumed solid energetic residues are known to occur (*Jenkins et al. 2002, Hewitt et al. 2003, Walsh et al. 2005a, Walsh et al. 2005b*), their formation is not predicted by thermochemical modeling given the extremely high temperatures and pressures. Omission of energetic residues from assessments of conventional munitions are likely reasonable given their minimal loading rates (Table 1), however the assumption of >99.99% filler degradation may not apply to some of the new IM. Walsh et al. (*2018b*) reviewed five munition LCEAs and found that three modeled combustion products, two measured blast chamber gaseous products and aerosols, and only one additionally measured blast chamber solid residue. The modeling approach ignores unconsumed filler and therefore residual energetic material, and the empirical atmospheric sampling approach relies on uncertain extrapolation to ground deposition. As a result, only empirical testing for deposited solid residues can fully assess environmental impact from detonation.

Command detonation enables empirical solid residue tests to be performed in a specified area, either a prepared testing surface outdoors or inside a blast chamber. Further, this command-detonation can be performed early in the acquisition process, before a munition is certified for live-fire from a weapon system. The main limitations of the command-detonation technology are the cost and logistical effort of conducting the tests. Recent costs for testing a munition by CRREL are approximately $180–300K for a munition, consisting of replicate analyses of seven detonation plumes with appropriate quality control (QC), analysis, and reporting. To date, these tests have benefitted from support from Army Explosive Ordnance Disposal (EOD) teams. For tests using the AFS, fuze simulator development costs were also provided at no charge. Scale-up of testing to include multiple munitions in a single event has the potential to dramatically reduce per-munition testing costs.

Test setting has a significant control on both cost and data quality. The ideal setting of testing on a clean snow surface adds a layer of complexity in logistics planning but affords the greatest quality control and sensitivity (lower limit <10 mg/round). Alternative test settings have been conducted in the past but have significant disadvantages compared to snow. Testing on soil has detection limits approximately two to three orders of magnitude higher (gram-level) than testing on snow, as well as the potential of preexisting contamination and inability of seeing the visual plume extent (*Persico et al. 2022)*. Collection in fixed pans (e.g., *Taylor et al. 2004*) or on witness plates (e.g., *Abdul-Karim et al. 2016*) has the disadvantage of only collecting discrete portions of the plume area, though the distribution of energetics is known to be spatially heterogeneous (*Walsh et al. 2017b*). Blast chamber tests of 60 mm mortar cartridges filled with PAX-21 compared well with tests performed on snow (*Walsh et al., 2013a*), but prior contamination is likely an issue for testing lower-depositing munitions in these chambers. Further, maximum net explosive weight limits on

certain blast chambers may restrict larger caliber munitions. While focused solely on residues deposited on snow, this validation study supports command-detonation residue testing using any of these setups.

3. PERFORMANCE OBJECTIVES

Table 3. Performance Objectives: Validation of Command-Detonation Munition Residues Testing.

Performance Objective	Data Requirements	Success Criteria	Results
Quantitative Performance Objectives			
Tasks 1-2. Live-fire tests of 60 mm and 81 mm IMX-104 mortar munitions	DNAN, NTO, RDX, and HMX masses from triplicate MI samples from ≥ 7 DUs covering ≥ 7 live-fire detonation plumes, per munition	Relative standard deviation of < 50 % for total residue loading rate, for each munition	**Met** for 60 mm: 24 % RSD **Met** for 81 mm: 35 % RSD
Task 3. Validate command detonation testing	Compiled loading rates of DNAN, NTO, RDX, and HMX from live fire tests and from command detonation tests, for each munition	Mean total loading rates not significantly different between live fire and command detonation	**Met** for 60 mm: $p = 0.76$ **Not met** for 81 mm: $p < 0.0001$
Qualitative Performance Objectives			
Determination of optimal fuze setting	Visual inspection of live-fire detonation plumes using proximity and impact fuze settings	Identification of fuze setting with least surface disturbance based on visual inspection	Impact fuze setting produced soot and residue plume with minimal cratering. Proximity setting produced no visible deposited soot and residue
Acceptance of validation test results by stakeholders	Feedback from DEVCOM AC personnel and JPEO A&A and PM-CAS managers on results and potential integration of technology into their LCEA and PESHE processes	Documented future steps in incorporating or improving command detonation residues testing for use in acquisition process	Stakeholder support of command-detonation residue testing of 155 mm M795 IMX-101 munition

3.1 PERFORMANCE OBJECTIVE: Live-Fire Tests of 60 mm and 81 mm munitions.

During Tasks 1 and 2 we measured live-fire detonation residues from 60 mm and 81 mm IMX-104 mortar cartridges, respectively. Cartridges were fired from mortar systems, exactly as they are during training, and then sampled following the same protocols that have been used in determining command-detonation residues for these munitions.

For each munition, at least seven DUs covering at least seven detonation plumes were sampled in triplicate following MIS theory and analyzed for the IMX-104 compounds DNAN, NTO, RDX, and HMX. Combined with area measurements, per-cartridge individual compound and total residue loading rates were determined for each replicate sample and averaged for each plume. Associated with these samples, appropriate QC to include background and outside-the-plume samples were also collected.

Successful determination of live-fire detonation residue rate was assessed based on the relative standard deviation (RSD) from the minimum seven DUs, using a success criterion of less than 50 %. Command detonation tests typically yield RSDs 22–46 % for $n = 7$ replicates (*Walsh et al., 2018a*), and we expected similar precision from live fire.

3.2 PERFORMANCE OBJECTIVE: Validate Command Detonation Testing

In Task 3, we statistically compared results for the tested munitions between live fire and command detonation with the AFS, and between live fire and command detonation with the CFS. Statistical tests were performed on each IMX-104 compound and the total loading rates.

The data required to perform the statistical tests were the DNAN, NTO, RDX, and HMX loading rates determined by the live-fire tests and by the command-detonation tests using the AFS and the CFS. For the 60 mm IMX-104 munition, these data include loading rates from at least seven plumes by live fire, seven plumes by the AFS, and seven plumes by the 12 g CFS. For the 81 mm IMX-104 munitions, these data include loading rates from at least seven plumes by live fire, seven plumes by the AFS, seven plumes by the 12 g CFS, and six plumes by the 18 g CFS.

The results of statistical mean comparison tests (i.e., t-test or Mann-Whitney test) on live-fire and command-detonation loading rates were used to determine success. No significant difference in total compound loading rates between live-fire and any of the command-detonation tests defined success.

4. SITE DESCRIPTION

4.1 SITE LOCATION AND HISTORY

The live-fire tests occurred on the Eagle River Flats (ERF) impact area at Joint Base Elmendorf-Richardson (JBER) in Anchorage, Alaska. This site has been used over the past 20 years in multiple SERDP projects to conduct munitions residues testing, including the command-detonation tests of the 60 mm and 81 mm IMX-104 munitions with the CFS and AFS as part of SERDP Project ER-2219. CRREL maintains a field laboratory on JBER for sample processing. The ERF has the ideal test location characteristic of tidal flooding that forms a thick sheet (~75 cm) of ice in the winter months, capping any previous detonation material and allowing for a clean testing surface.

JBER is located in south-central Alaska and borders the municipality of Anchorage and the Knik Arm of Cook Inlet (Figure 9). JBER covers an area of approximately 300 km^2 and has been used for military training since 1939. The ERF (61.32°, -149.71°) within JBER is a ~10 km^2 impact area and is currently used for indirect fire training during winter months, although there are plans to open this training to all-seasons following a planned final Environmental Impact Statement in 2024. Munitions currently fired at the range include 60 mm, 81 mm, and 120 mm mortars and 105 mm howitzers. Firing points are located on bluffs surrounding the ERF. The munitions tested in this study were fired into the Area C portion (Figure 10) where previous command-detonation tests of these munitions occurred during SERDP Project ER-2219. This section of the impact area is relatively accessible by road. CRREL has conducted research studies and remediation efforts related to munitions on ERF since the late 1980s.

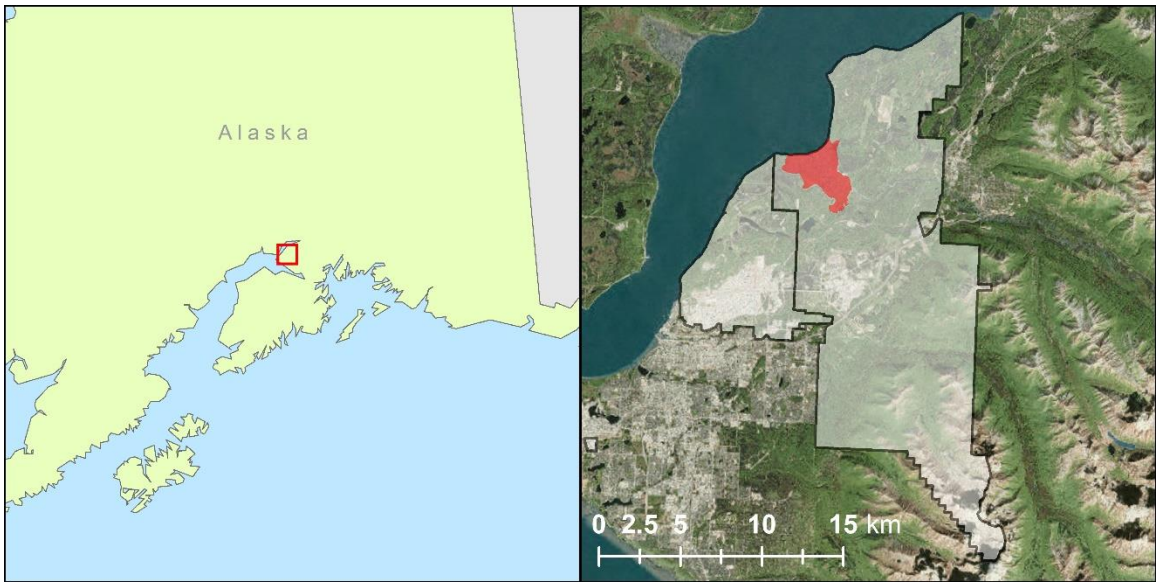

Figure 9. Location of JBER in Alaska (left; red box) and an aerial image of JBER (white) and the ERF impact area (red).

Figure 10. Aerial photograph of ERF. Multiple firing points are located on bluffs surrounding the estuary. The target area (red box) is located in the upper center part of the estuary (Area C) in this photograph.

4.2 SITE GEOLOGY/HYDROGEOLOGY

JBER lies in an alluvial plain known as the Anchorage Lowland (*Yehle et al. 1991*). The surficial geology of Fort Richardson is described by Hunter et al. (*2000*) as extremely complex and is characterized by glacial deposits and glacial erosion events. The ERF is an estuarine salt marsh that undergoes tidal flooding on an approximately two-week period. In 2021 and 2022, multiple flooding tides occurred during the winter testing months (Figure 11). These flooding tides formed an ice layer between the potentially contaminated soil/sediment and clean overlying snow. Testing was performed during the week-long periods of low tides immediately following a period of flooding tides.

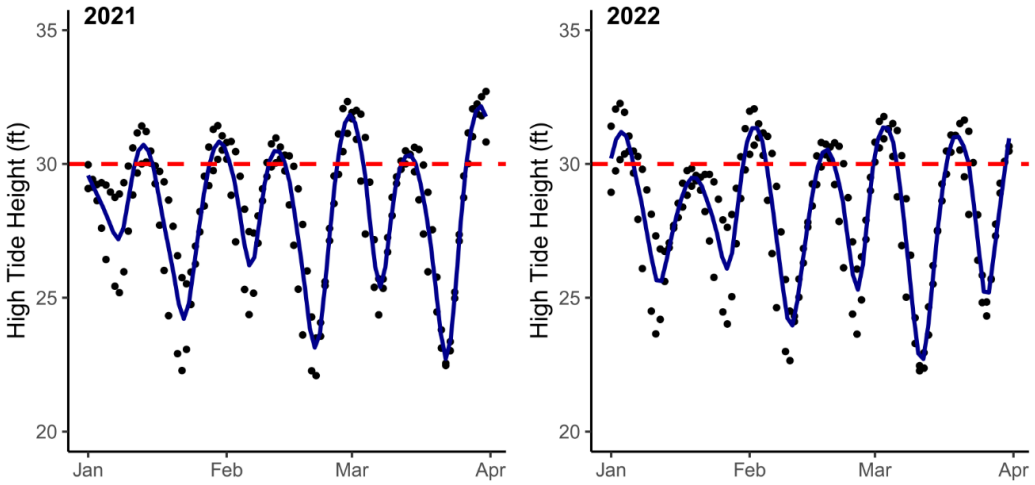

Figure 11. Predicted high tide heights in Anchorage, AK, during the winter field seasons. Heights above 30 feet are considered flooding on ERF and create an ideal surface for testing and accessibility. Source: NOAA Tides and Currents.

The sampling approach required a minimum snow depth of 1 cm to representatively remove increments using the sampling tool. Average snow depth in Anchorage, AK, is 10 inches by January 1st and approximately 18 inches by March 31st, bracketing the windows of our field seasons (*NOAA 2023*).

4.3 CONTAMINANT DISTRIBUTION

The plume areas for the 60 mm and 81 mm IMX-104 munitions, as determined by prior command-detonation tests with the AFS in nose-up vertical orientation, are listed in Table 4. The plume areas for the 81 mm munition are significantly larger than those for the 60 mm munition. The plumes produced by live fire were expected to have approximately the same dimensions as those by command detonation. Areas directly outside the visible plume area typically have energetic concentrations near or below the method detection limits and were used primarily as QC checks.

Table 4. Visible inside-the-plume (ITP) and outside-the-plume (OTP) areas for M720A2 and M821A3 munitions determined by command detonation with the AFS (*Walsh et al. 2018a*). Reported values are average ± one standard deviation on *n* = 7 detonations.

Munition	ITP (m^2)	OTP 0-3 m (m^2)	OTP 3-6 m (m^2)
M720A2	249 ± 91	284 ± 90	275 ± 40
M821A3	766 ± 64	420 ± 180	407 ± 14

5. TEST DESIGN

5.1 CONCEPTUAL EXPERIMENTAL DESIGN

Sixteen 60 mm and fourteen 81 mm IMX-104 cartridges were fired from mortar systems into the ERF impact area on snow in the winters of 2021 and 2022, respectively. These live-fire tests were divided in two subsequent tasks for logistical reasons and separated with a Go/No-Go decision after the first 60 mm test in 2021. After each firing, select plume areas were demarcated into a total of at least seven DUs for each munition, depending on the overlap of visible plumes. Each DU was sampled following MIS theory using snow-sampling scoops. The samples were processed in a laboratory on JBER to isolate the solid and aqueous fractions, and to perform solid phase extraction (SPE) on the aqueous fractions. Samples were analyzed for IMX-104 compounds (DNAN, NTO, RDX, and HMX), as well as DNAN transformation products, at the CRREL laboratory in Hanover, New Hampshire, using established analytical methods for these analytes. Quality control was exercised throughout using background samples, laboratory control samples, matrix spikes, and frequent blanks for each processing step. Per-cartridge residue loading rates were determined using analyzed concentrations, sample volumes, sampled areas, and plume areas. Finally, the newly determined live-fire residue loading rates for each munition were statistically compared with prior-determined command-detonation loading rates using the CFS and AFS. The results of these comparisons were used to assess the representation of live-fire conditions by command detonation.

5.2 BASELINE CHARACTERIZATION

Prior to live-fire activities, the target areas were visually inspected for recent disturbance from training activities. Detonations could be clearly seen on the snow surface, and, if present, the target area was adjusted to focus on undisturbed snow. At least two background MI samples were collected from the snow surface just outside the target area prior to live-fire activities. For the 81 mm munition, background samples were also collected in the middle of the firing schedule and after all cartridges had been fired. All background samples were processed following the same methods for regular samples. Baseline data are reported in Appendix C.

5.3 DESIGN AND LAYOUT OF TECHNOLOGY COMPONENTS

5.3.1 Live-Fire Tests of 60-mm and 81-mm IMX-104 Munitions

Cartridges of the study munitions were fired from mortars by a unit of the 4th Infantry Brigade Combat Team (Airborne), 25th Infantry Division, into Area C of the ERF at the desired target locations over the course of three to four days. The 716th EOD Company cleared the area of any unexploded ordnance before research personnel approached the site and monitored sampling activities.

Initially in Task 1, two cartridges of the 60 mm study munition were fired at the southern extent of the target area to determine the optimal fuze setting. The M734A1 multi-option fuze, issued with the M720A2 60 mm IMX-104 mortar cartridge, has discrete settings for impact (IMP), proximity (PRX), and delay. Prior live-fire residue tests used point-detonating (PD) fuzes, equivalent to the IMP setting, but the PRX setting had not been assessed in regard to surface presentation and disturbance. The PRX setting has a height of burst of 2 m for the 60 mm and 81 mm mortar cartridges. For this initial test, one cartridge used the IMP setting and the other the

PRX setting. The level of surface disturbance and visible plume characteristics were assessed by observing the detonations through zoom lens and walking the residue plumes. The fuze setting with the most prominent residue/soot plume and minimal disturbance was used for subsequent cartridge firings.

The ideal target placement for detonations (Figure 12) would allow approximately 50 meters spacing and ensure quality control samples could be collected for each cartridge detonation. The target area was accessed by a temporary plowed ice road from an access road at the edge of the estuary. The target area was relatively free of obstruction, with the exceptions of a line of target armored personnel carriers and a wood tower with extensive fragment damage.

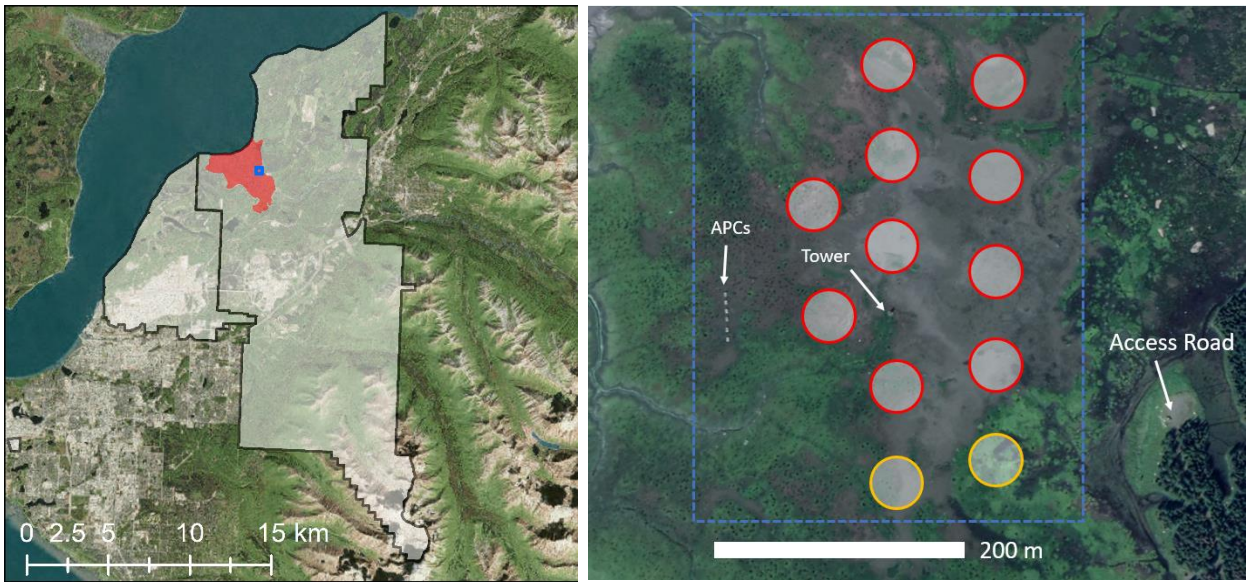

Figure 12. Left panel: location of the ERF impact area (red) and target area (blue box) on JBER (transparent). Right panel: proposed idealized target plume locations for two fuze-setting test rounds (yellow) and ten sampled rounds (red).

5.3.2 Sample Collection using MIS

Each plume area was sampled using MIS theory based on established protocols (*Walsh et al. 2012*). The DU for each MI sample was first mapped by walking the perimeter of visible plume area, and then measured with a high-precision Trimble GPS to determine the area of the plume (A_p). Each MI sample consisted of approximately 100 increments collected across the visible plume area (Figure 13). MIS uses a systematic random approach, meaning a random starting point with systematic distances between increments that cover the entire DU. In this case the DUs were the demarcated plume areas. Sampling lanes were maintained using intermittent flagging along the perimeter of the DU, and systematic distances between increments were maintained using individual pacing. Each plume area DU was sampled in triplicate. The second replicate was collected in a perpendicular path to the first replicate, and the third replicate followed a path that was 45° to the first and second replicate paths.

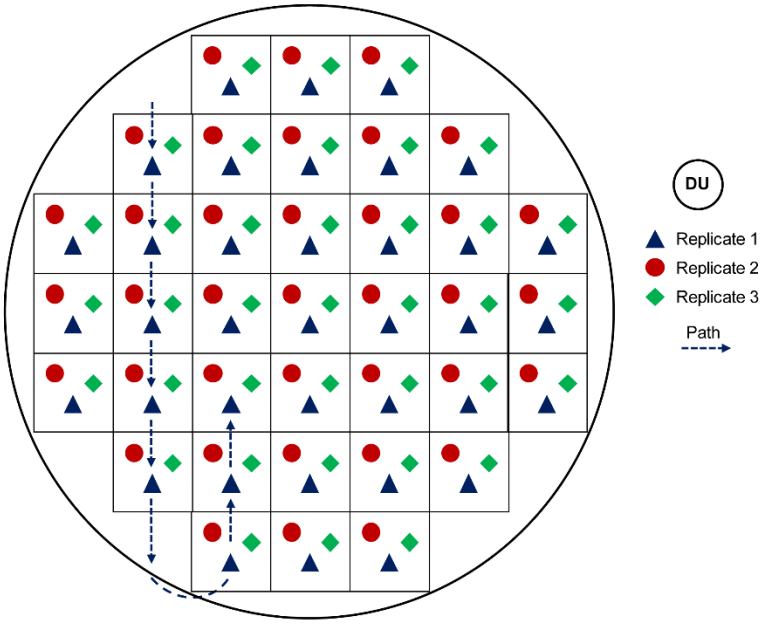

Figure 13. Simplified MIS layout of a circular plume area DU. Replicate MI samples will be made up of ~100 increments each instead of the 37 shown here.

Each increment consisted of a single scoop of the snow surface using a square-sided stainless-steel scoop (10 cm length, 10 cm width, 2.5 cm depth). This upper snow layer generally contains all of the post-detonation material (Figure 14). The increments were collected using a two-person team, with one person scooping and pacing and the other person collecting the increments in a polyethylene bag and using a mechanical counter to track the number of increments. The area of the sampling tool (A_s) combined with the number of increments allowed the determination of the area sampled.

Figure 14. Example of complete residue collection with a 2.5-cm deep snow scoop (20-cm x 20-cm scoops pictured).

5.3.3 Sample Processing and Analysis

Each sample was processed and analyzed following the same methods as used in prior command-detonation tests of these munitions (*Walsh et al. 2012; Walsh, 2016; Walsh et al. 2018a*). The first step of processing was melting and vacuum filtering using glass fiber filters (Figure 15). The aqueous and solid fractions were isolated, and the total aqueous volume (V_{aq}) recorded. The entire solid material and a 40 ml aliquot of the aqueous fraction were set aside for analysis. A 500 ml

aliquot of the aqueous fraction was subjected to SPE for a 100-fold concentration of compatible analytes HMX, RDX, and DNAN. In the analytical laboratory, the solid fraction was extracted with a known volume (V_e) of 1/1 (v/v) acetonitrile/water. Direct aqueous, SPE extracts, and solid extracts were analyzed for the concentrations (C) of NTO, RDX, HMX, DNAN, and DNAN transformation products using established HPLC methods.

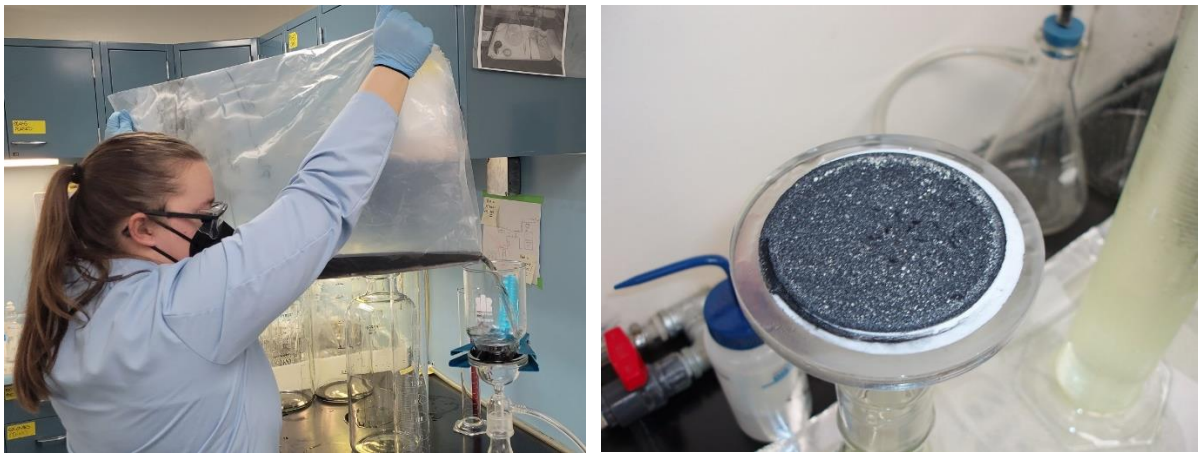

Figure 15. Processing post-detonation snow samples in the JBER laboratory. Left: filtering a melted snow sample into a vacuum filtration apparatus. Right: solid residue on a glass fiber filter from an IMX-104 snow sample.

5.3.4 Determination of Residue Loading Rate

The residue loading rates (R) for each IMX-104 compound (NTO, DNAN, RDX, and HMX) in a plume or plume set were determined through the equation below.

$$R_i = \frac{A_p}{nA_s}\left(C_{i,aq}V_{aq} + C_{i,e}V_e\right)$$

The total residue loading rate was the sum of the loading rates for each compound. As three replicates were collected from each plume, an average and standard deviation could be calculated for each plume to assess uncertainty. If multiple cartridge detonations were combined in a single DU due to plume overlap, then the loading rates were divided by the number of cartridges included. Loading rates from at least seven DUs were averaged to determine a mean loading rate for a munition. Also, from these seven or more DUs, a relative standard deviation (standard deviation / average) was calculated to provide an estimate of uncertainty in the loading rate determination.

5.4 FIELD TESTING

Live-fire field testing for the 60 mm munition occurred during January 2021 (Table 5) and the 81 mm munition during January-February 2022 (Table 6). Ammunition supply requests were made for 16 of M720A2 with PBXW-14 supplementary charge and M734A1 MO fuze (DODIC BA44) and 15 of M821A3 with PBXW-14 supplementary charge and M734A1 MO fuze (DODIC CA61) through the Total Ammunition Management Information System for delivery to the JBER-Richardson Ammunition Supply Point (ASP). This ammunition remained in the ASP until withdrawn by the training unit on the days of the tests. The M821A3 provided did not include fuzes, so a late change was made to use the M889A4 with M783 point detonating/delay fuze

(DODIC CA63). The sole difference between the M889A4 and M821A3 munitions is the fuze—the M821A3 uses the M734A1 multi-option fuze and the M889A4 uses the M783 point detonating/delay fuze. Both fuzes use a lead and booster charge composed of PBXN-5. The M889A4 is the preferred training munition due to its lower cost. Munitions were withdrawn from the ammunition supply point and handled by the infantry unit.

For both Task 1 and Task 2 field tests, the field team assembled at JBER and immediately began preparations of the field site, to include plowing the access road and, if possible, out to the target area on the estuary. Safety briefs were provided by range control to all personnel—a requirement for access to the impact area. Background samples were collected just outside the target area prior to any firing. Firing was scheduled to occur over three days with an additional day as a make-up for any contingencies. This flexibility in scheduling permitted a delay in the firing schedule for Task 2 that allowed fresh snowfall to expand target areas that were previously uncovered bare ice. Samples were stored outside or in a shipping container (below freezing) covered in tarpaulins until the day prior to processing, when they were brought to room temperature in the field laboratory to melt overnight. Sample processing occurred over four days, after which the processed samples and QC were shipped in coolers to the CRREL analytical laboratory in Hanover, NH.

Table 5. Gantt chart of actual Task 1 field activities for the 60 mm IMX-104 munition live-fire test.

Activity	January 2021													Feb.	
	19	20	21	22	23	24	25	26	27	28	29	30	31	1	2
Safety and Range Safety Briefs															
Field Lab Cleaning and Prep															
Site Preparation at ERF (Plowing)															
Background Sample Collection															
Fuze Setting Test															
Live Fire and Sampling															
Sample Melt Start															
Sample Processing and QC															
Processed Sample Shipment to Lab															
Sample Receipt and Storage															

Table 6. Gantt chart of actual Task 2 field activities for the 81 mm IMX-104 munition live-fire test.

Activity	January 2022											Feb.						
	21	22	23	24	25	26	27	28	29	30	31	1	2	3	4	5	6	7
Safety and Range Safety Briefs																		
Field Lab Cleaning and Prep																		
Site Preparation at ERF (Plowing)																		
Background Sample Collection																		
Live Fire and Sampling																		
Sample Melt Start																		
Sample Processing and QC																		

Processed Sample Shipment to Lab																	
Sample Receipt and Storage																	

5.5 SAMPLING METHODS

5.5.1 Plume Areas and Decision Units

The plume areas were visually demarcated by walking the perimeters of the areas surrounding detonation points with visibly discolored snow surfaces from soot and residues (Figure 16). This inside the plume (ITP) area contained almost all of the detectable energetic residues. Outside-the-plume areas (OTPs) were demarcated by a two-person team holding a measuring tape and walking the perimeter of the ITP from 0 to 3 m and 3 to 6 m from the ITP edge. The DUs for MIS were the ITP, 0-3 m OTP, and 3-6 m OTP for each plume or plume set. Figure 17 shows the conceptual design of these DUs for a singly resolved plume and for two overlapping plumes. For each ITP DU, triplicate MI samples were collected, each consisting of approximately 100 increments following the MIS patterns in Figure 13. Triplicate MI samples were collected from at least two OTP DUs, otherwise singular OTP samples were collected from each plume, each consisting of approximately 60-100 increments. At least seven plumes or plume sets were sampled in this fashion for each tested munition.

Figure 16. The post-command detonation plume from an 81 mm mortar cartridge with demarcated ITP area and 0 to 3 m OTP area.

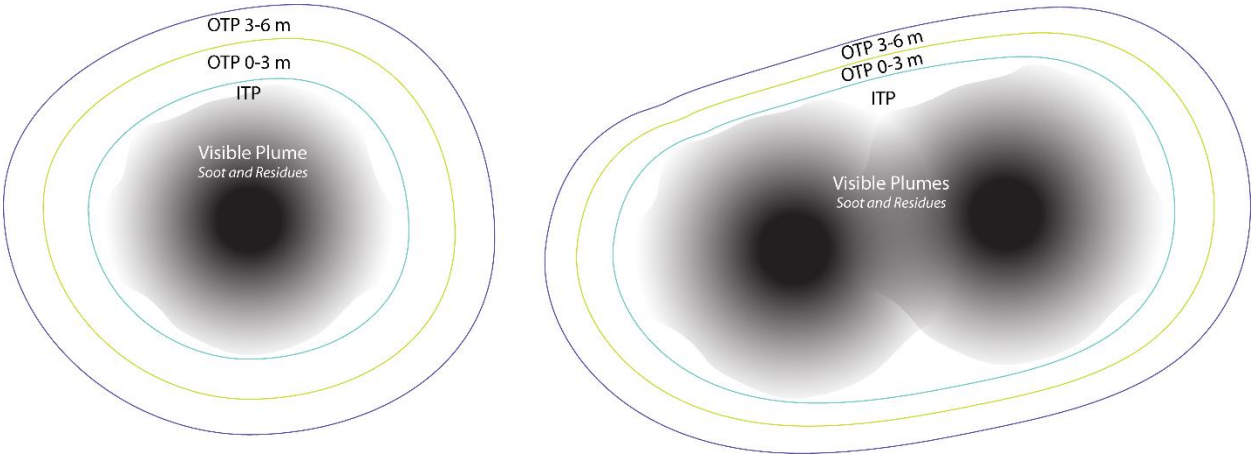

Figure 17. Schematics of sampling DUs for a single separated plume (left) and two overlapping plumes (right). Not to scale.

5.5.2 Samples

The number of samples and sample types are listed in Table 7. From each plume or plume set, three replicate MI samples were collected from the ITP DU and singular MI samples were collected from the OTP 0-3 m and OTP 3-6 m DUs. For at least two of the plumes, triplicate OTP MI samples were collected. For each munition, and respective test year, at least three background samples were collected. In the case that plume patterns and testing logistics permitted more than seven plumes or plume sets to be sampled for each munition, the additional plumes were sampled in the same manner and total number of samples increased.

Table 7. Minimum number of multi increment samples and analytes for each live-fire munition test.

Munition	Sample Type	DUs	Reps	MI Samples (*n*)	Process Fraction Matrices	Analytes for each Sample Fraction
60 mm IMX-104	ITP	≥ 7	3	21	Aqueous filtrate, filter solids	NTO, RDX, HMX, DNAN
	OTP 0-3 m	≥ 7	1–3	9	Aqueous filtrate, filter solids	NTO, RDX, HMX, DNAN
	OTP 3-6 m	≥ 7	1–3	9	Aqueous filtrate, filter solids	NTO, RDX, HMX, DNAN
	Background	3	1	3	Aqueous filtrate, filter solids	NTO, RDX, HMX, DNAN
	Min. Total			49		
81 mm IMX-104	ITP	≥ 7	3	21	Aqueous filtrate, filter solids	NTO, RDX, HMX, DNAN
	OTP 0-3 m	≥ 7	1–3	9	Aqueous filtrate, filter solids	NTO, RDX, HMX, DNAN
	OTP 3-6 m	≥ 7	1–3	9	Aqueous filtrate, filter solids	NTO, RDX, HMX, DNAN
	Background	3	1	3	Aqueous filtrate, filter solids	NTO, RDX, HMX, DNAN
	Min. Total			49		

5.5.3 Sample Processing

The snow samples were melted at room temperature overnight in their sample bag with a second clean new over-bag to prevent sample loss due to bag punctures from frag and cross contamination between ITPs, OTPs, and different plumes. The double-bagged samples were also placed in clean bins to allow sample recovery in case of outer-bag puncture. Each melted sample (approximately 2–9 L, dependent on number of increments and snow density) was vacuum filtered using Whatman GF/A glass fiber filters. Of the aqueous filtrate, a 500 ml aliquot was reserved for SPE, a 40 ml aliquot for NTO analysis, and a 500 ml aliquot for archive, all in glass amber bottles/vials (Table 8). The filter(s) and solid residue were placed into new amber glass jars using clean tweezers. SPE was performed using a vacuum manifold and Waters Sep-Pak RDX cartridges, preconditioned with acetonitrile and water, and eluted with 5.00 ml of acetonitrile. SPE extracts were adjusted to 5.00 ml volume with acetonitrile for a 100-fold concentration factor of HMX, RDX, and DNAN. The solids with filters were extracted with 20–50 ml of 1/1 (v/v) acetonitrile/water on a shaker table for 18 hours to fully dissolve the IMX-104 constituent compounds. All filtration and sample handling glassware were thoroughly cleaned between each usage using Micro-90 soap solution and MilliQ Type I water.

Table 8. Processed sample fractions.

Sample Fraction	Volume (ml)	Container	Analytes
Aqueous Filtrate	40	40 ml amber vial	NTO
Aqueous SPE	5.00	500 ml amber bottle to 7 ml borosilicate glass vial	DNAN, RDX, HMX
Filter Solids	-	4-ounce amber glass jar	NTO, DNAN, RDX, HMX

5.5.4 Quality Assurance / Quality Control in Processing

Samples were processed following a progression from expected lowest to highest concentration: background samples, OTP samples, and then ITP samples. Before processing any samples, two filtration blanks composed of 2 liters of MilliQ Type I water were processed identically to subsequent samples. Similarly, two filtration blanks were processed at the mid-point of sample processing and after all samples had been processed. Complete cleaning of the glassware was judged based on concentrations below the method detection limits (Table 9). Potential contamination during SPE was assessed by SPE blanks, consisting of 500 ml of MilliQ Type I water, run every 20 samples. Also every 20 samples, a sample triplicate was processed by SPE, and matrix spike (MS) and matrix spike duplicates (MSD) were performed on the same sample used for triplicates. Laboratory control samples (LCS) were processed through SPE every 20 samples and consisted of 500 ml of MilliQ water spiked to 4 µg/l with DNAN, RDX, and HMX. The same QC samples were performed for direct aqueous analysis of NTO, with aliquots for matrix spikes and LCS spiked at 0.5 mg/l for LCS and 0.5–5 mg/l for matrix spikes. Recovery acceptance criteria followed DOD Quality Standards Manual 5.4 (*DOD, 2021*) EPA Method 8330B for HMX and RDX and the generic limits of 70–130% for DNAN and NTO.

Table 9. Quality control samples performed for each field test.

QC Sample	Frequency	Analyte	Acceptance Criteria
Pre-Filtration Blank	2/munition	HMX, RDX, DNAN, NTO	< MDL
Mid-Filtration Blank	2/munition	HMX, RDX, DNAN, NTO	< MDL
Post-Filtration Blank	2/munition	HMX, RDX, DNAN, NTO	< MDL
SPE Blank	1/20 samples	HMX, RDX, DNAN	< MDL
SPE Sample Triplicate	1/20 samples	HMX, RDX, DNAN	RSD < 20 %
SPE Sample MS/MSD	1/20 samples	HMX, RDX, DNAN	70–130 % RPD < 20 %
SPE LCS	1/20 samples	HMX, RDX, DNAN	70–130 %
Aqueous Sample Triplicate	1/20 samples	NTO	RSD < 20 %
Aqueous Sample MS/MSD	1/20 samples	NTO	70–130 % RPD < 20 %
Aqueous Sample LCS	1/20 samples	NTO	70–130 %

5.5.5 Sample Analysis

The processed samples were analyzed following methods established in Walsh (*2016*) using HPLC with UV detection on an Agilent 1260 Infinity and Infinity II. The filter solids extract and the aqueous fraction were analyzed for NTO in 3/1 (v/v) acetonitrile/water following an HPLC method adapted from Le Campion (*1997*) and U.S. Army Public Health Command Standard Operating Procedure DLS810. This method separates NTO on a porous graphitic carbon column (Thermo Hypercarb, 150 x 4.6 mm, 5 µm) with 3/1 (v/v) acetonitrile/water with 0.1 % trifluoroacetic acid at 28 °C. The pH of this eluent (pH 2) keeps the NTO weak acid (pKa 3.7) protonated during separation and analysis. DNAN, RDX, HMX, and DNAN transformation products were analyzed in 3/1 (v/v) water/acetonitrile on a C8 reverse phase column (Waters NovaPak, 150 x 3.9 mm, 4 µm) using 15/85 (v/v) isopropanol/water with 0.1 % acetic acid. This method follows EPA Method 8330B for RDX and HMX and has also been found to apply to DNAN and the DNAN transformation products 2,4-dinitrophenol, 2-methoxy-5-nitroaniline, 4-methoxy-3-nitroaniline, 2-methoxy-5-nitrophenol, and 4-methoxy-3-nitrophenol (*Chow et al. 2009; Walsh, 2016; Taylor et al. 2017*). The detection limits for each analyte are presented in Table 10 and used to estimate the total residue detection limit. Concentrations of compounds detected by the primary methods were confirmed using two different secondary methods that have different separation mechanisms and elution orders for all four IMX-104 compounds. For NTO, hydrophilic interaction liquid chromatography (HILIC, Waters XBridge BEH Amide, 100 x 4.6 mm, 2.5 µm) was used; and for HMX, RDX, and DNAN a CN column (Agilent Poroshell 120 EC-CN, 150 × 3.0 mm, 2.7 µm) was used. Further details on analytical conditions and chromatography are presented in Appendix E.

Table 10. Method detection limits and estimated total residue limits. Assumes 2 l filtrate volume, 20 ml filter extract volume, and A_s/A_p of 0.0026.

Analyte	Aqueous (µg/l)	Filter Extract (µg/l)	Estimated Total (mg/cartridge)
NTO	10	5	8
DNAN	0.2	10	0.2
RDX	0.2	10	0.2
HMX	0.2	10	0.2

5.5.6 Calibration of Analytical Equipment

Each HPLC method was calibrated following EPA Method 8330B and DOD QSM 5.4 guidance, including initial calibration, independent calibration verification, and continuing calibration verifications every 10 samples. Analytical standards for NTO, DNAN, RDX, and HMX were obtained from Accustandard, Absolute Standards, and Restek. Independent calibration verification used a separate lot standard (HMX and RDX) or dissolved neat material obtained via Picatinny Arsenal (NTO and DNAN). Reagent-grade standards of the DNAN transformation products from Sigma Aldrich were used to qualitatively assess the presence of these compounds.

5.5.7 Data Analyses

Loading rates for each energetic compound (NTO, DNAN, RDX, and HMX) were calculated for each MI sample following the equation in Section 5.3.4. For each plume, a plume average was determined from the three replicate MI samples as:

$$\bar{x}_p = \frac{1}{n}\sum_{i=1}^{n} R_i$$

A munition average and standard deviation were determined from $n \geq 7$ plumes as:

$$\bar{x}_m = \frac{1}{n}\sum_{i=1}^{n} \bar{x}_{p,i}$$

$$\sigma = \sqrt{\frac{1}{n-1}\sum_{i=1}^{n}\left(\bar{x}_{p,i} - \bar{x}_m\right)^2}$$

Relative standard deviation was determined as $\sigma / \bar{x}_m$.

The residue loading rates for each compound were statistically compared between newly determined live-fire and previous command-detonation tests. For each test pair, an unpaired two sample Mann-Whitney ranked sum test was performed to determine if the two groups are significantly different. This nonparametric statistical method was used due to limited sample sizes and non-normal data distributions for some fuze types. Specifically, a two-sided test was performed to test the hypotheses:

$$H_0: R_{LF} = R_{FS}$$

$$H_a: R_{LF} \neq R_{FS}$$

where R_{LF} is the live-fire residue loading rate for a compound and R_{FS} is the corresponding rate for one of the fuze simulators. All tests were performed on plume-averaged data using the 'wilcox.test' function in the 'stats' package for R (*R Core Team, 2022*). A 95 % confidence level was used and the null hypothesis (H_0) rejected only if the test *p* value is less than or equal to 0.05.

5.6 SAMPLING RESULTS

5.6.1 Live-fire 60 mm IMX-104 Sampling Results

Sixteen cartridges of M720A2 60 mm IMX-104 were fired and all exhibited high-order functioning. The first two fired cartridges compared the PRX and IMP fuze settings (qualitative results discussed in Section 6.2.1). The remaining fourteen cartridges were fired using the IMP setting to the target area. Targets were adjusted in the field to avoid areas in the impact area with bare ice cover. Nonetheless, some targeting issues resulted in plumes that were not sampled due to impacting areas of bare ice. Only plumes that encompassed all snow (i.e., no ice patches) were sampled. These demarcated plumes were numbered sequentially according to sampling order (Figure 18). Plumes 1 through 7 covered single-cartridge detonations, and Plumes 8 and 9 covered two each closely landing cartridge detonations.

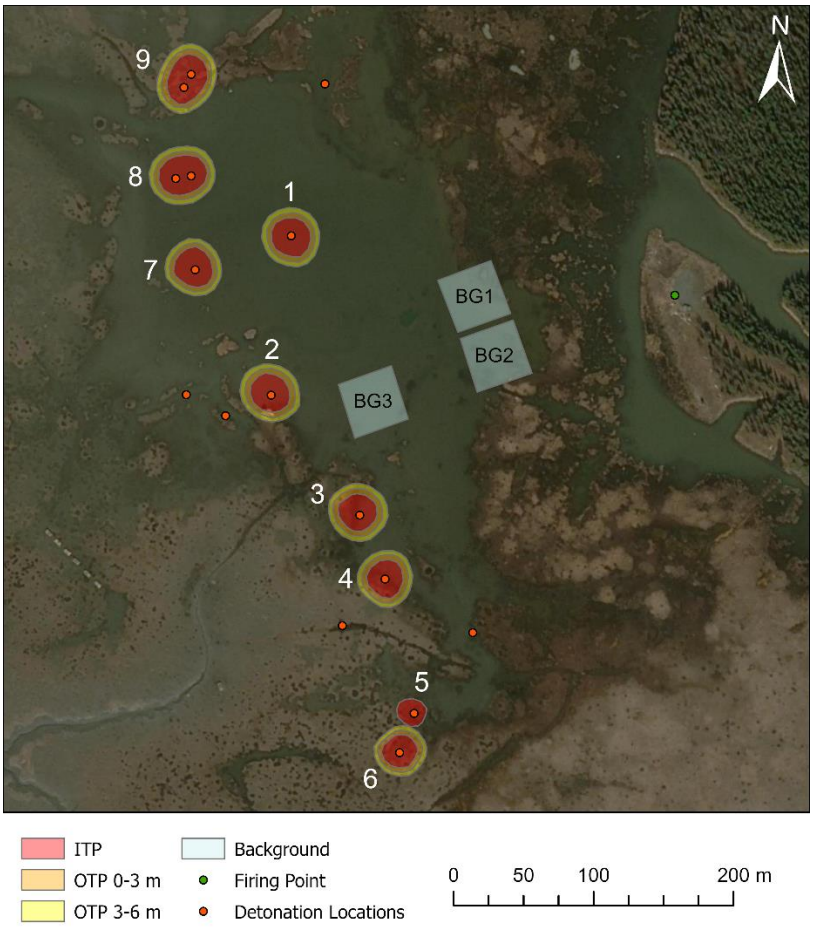

Figure 18. Plume locations and areas in the target region measured by real-time kinematic survey for the 60 mm munition.

Actual plume areas and number of increments are listed for each plume in Table 11. The demarcated ITP plume sizes (Table 11) were greater than previous ones determined in command-detonation studies (190–450 m^2; *Walsh et al. 2018a*). This difference may have resulted from a difference in residue and soot dispersion, or to the subjective determination of visible plume edge. Sample increments ranged from 77 to 156 and met the project minimum of 60 increments for representative sampling.

Table 11. Areas and MIS increments for each 60 mm detonation plume. Note: Plume 5 did not have OTP samples due to overlap with bare ice; Plumes 8 and 9 covered residues from two cartridge detonation each.

Plume	ITP		OTP 0-3 m		OTP 3-6 m	
	Area (m^2)	Increments (*n*)	Area (m^2)	Increments (*n*)	Area (m^2)	Increments (*n*)
1	632	82–90	327	76	409	97
2	613	86–89	363	97	401	102
3	571	77–114	360	83–101	412	81–97
4	547	84–88	334	85–94	350	96–115
5	322	81–88	-	-	-	-
6	460	84–156	256	93	310	93
7	614	91–105	292	83–98	356	84–102
8	787	78–99	315	88	438	85
9	772	82–120	372	81	442	102

All IMX-104 analytes were detected in all nine plumes, presented in Table 12. Consistent across all plumes, the residual compound masses ranked NTO >> DNAN > RDX > HMX. The OTP decision units for each plume contained negligible residues relative to the ITP, which supports the assumption of complete sampling of deposited residues. No transformation products of DNAN were found in any of the samples, which indicates no degradation of this compound.

Table 12. Average energetic residue loading rates for each 60 mm plume. Values in parentheses are standard deviations of triplicate MIS estimates. Note: Plumes 8 and 9 each include two cartridge detonations.

Plume	DU Type	Residues (mg/plume)			
		HMX	RDX	DNAN	NTO
1	ITP	1.6 (0.1)	12 (2)	35 (3)	3700 (100)
	OTP 0-3	0.3	<0.3	<0.3	20
	OTP 3-6	<0.4	3.7	<0.4	<11
2	ITP	2.1 (0.2)	14.0 (0.3)	44.8 (0.9)	5200 (200)
	OTP 0-3	0.8	0.4	0.6	29
	OTP 3-6	0.4	0.7	<0.4	<11
3	ITP	1.8 (0.3)	13 (3)	40 (10)	3400 (600)
	OTP 0-3	<0.4	<0.4	<0.4	<11
	OTP 3-6	<0.4	<0.4	<0.4	<12
4	ITP	2.2 (0.6)	19 (7)	50 (10)	4100 (800)
	OTP 0-3	<0.3	<0.3	<0.3	<10
	OTP 3-6	<0.4	<0.4	<0.4	<12
5	ITP	1.4 (0.4)	11 (4)	30 (7)	4000 (500)
6	ITP	1.4 (0.2)	10 (1)	33 (5)	2500 (100)
	OTP 0-3	<0.3	<0.3	0.4	12
	OTP 3-6	<0.3	<0.3	<0.3	<8
7	ITP	1.3 (0.2)	7 (2)	19 (4)	3700 (600)
	OTP 0-3	<0.3	<0.3	<0.3	<10
	OTP 3-6	<0.3	<0.3	<0.3	<10
8	ITP	2.1 (0.2)	14.0 (0.3)	44.8 (0.9)	5200 (200)
	OTP 0-3	<0.3	1.5	<0.3	11
	OTP 3-6	<0.4	<0.4	<0.4	<12
9	ITP	3.5 (0.5)	21 (2)	65 (4)	9800 (1000)
	OTP 0-3	<0.4	4.7	<0.4	17
	OTP 3-6	<0.4	<0.4	<0.4	16

Table 4 and Figure 19 summarize the per-cartridge residue loading rates and uncertainties in each plume. NTO loading rates were two orders of magnitude greater than the next highest compound DNAN. HMX and RDX loading rates were on the order of 1 to 10 mg/cartridge, approaching the detection limit, and were similar in magnitude to previous high-order detonation residue tests of Comp B (Table 2). Total residue estimates largely reflect NTO, given its predominance, and uncertainties in this total residue estimate within each plume were acceptable with RSDs less than or equal to 20 %. The minor residue compounds HMX, RDX, and DNAN also had acceptable precision within plumes (< 37 % RSD), which indicates minimal sampling and processing errors and representative characterization of the DUs. Across all plumes, precision for each compound estimate were acceptable with RSDs of 24 % to 33 %, which met the demonstration plan's success criteria of less than 50 % and bettered the precision of prior command-detonation tests. The overall precision demonstrated here provides confidence that the live-fire deposition rates are broadly representative of the munition.

Table 13. Average estimated live-fire energetic residue loading rates and precision for the 60 mm munition.

Plume	Residues (mg/cartridge)					RSD (%)				
	HMX	RDX	DNAN	NTO	Total	HMX	RDX	DNAN	NTO	Total
1	1.9	16	35	3700	3700	7	9	10	4	4
2	3.3	15.0	46	5200	5300	6	2	2	3	3
3	2.0	13	40	3500	3500	15	24	25	19	19
4	2.2	19	50	4100	4100	27	36	28	20	20
5	1.4	11	30	4000	4100	31	37	24	12	12
6	1.4	10	34	2500	2600	11	12	16	5	6
7	1.4	7	19	3700	3800	12	25	23	17	17
8	1.3	7.7	22.4	2600	2600	8	2	2	3	3
9	1.9	14	32	4900	5000	12	9	7	10	10
Ave.	**1.9**	**12**	**30**	**3800**	**3800**	-	-	-	-	-
SD	0.6	4	10	900	900	-	-	-	-	-
RSD (%)	33	32	29	24	24	-	-	-	-	-

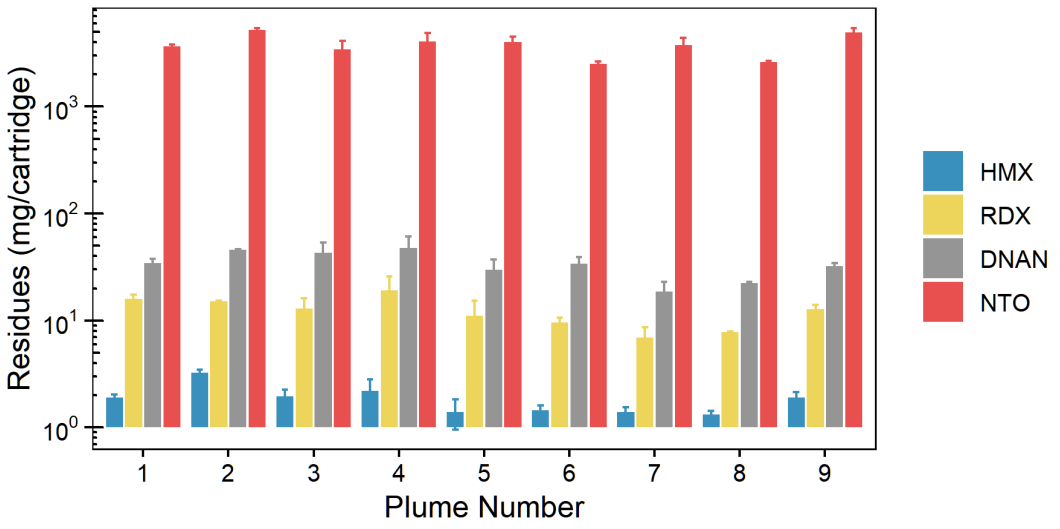

Figure 19. Average estimated energetic residue loading rate for each 60 mm plume. Error bars represent one standard deviation.

5.6.2 Live-fire 81 mm IMX-104 Sampling Results

Fourteen cartridges of M889A4 81 mm IMX-104 were fired using zero propellant charges, and all exhibited high-order functioning. The M783 fuzes on all cartridges were set to point detonating (i.e., impact). The impact locations and sampling plume areas are shown in Figure 20, labeled sequentially in order of day of firing and sampling. All plumes were single cartridge resolved, with the exception of Plume 2 that covered two cartridge detonations. The plume shapes surrounding the impact location provide a general indication of predominant wind direction and speed. Wet conditions at the lower-lying areas of the site prompted initial tests (Plumes 1–5) to focus on higher elevation areas with deep snowpack. A pause in firing for a day allowed the lower-lying areas of the site to freeze over, with subsequent thin snow cover providing ideal conditions for Plumes 6–13.

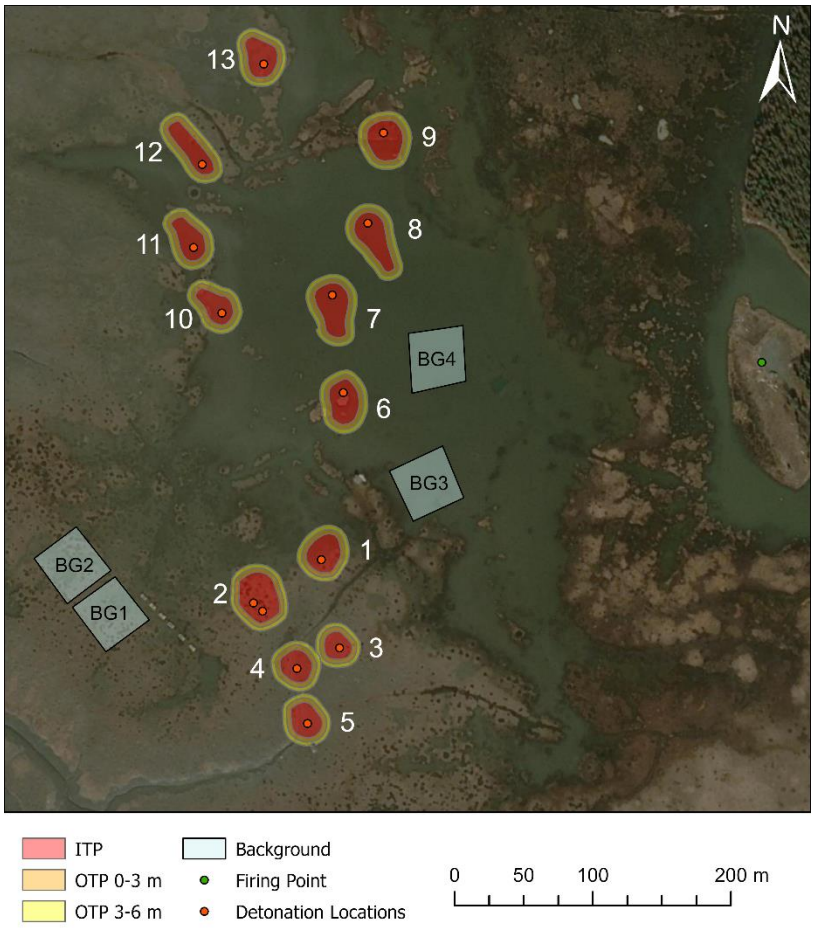

Figure 20. Plume locations and areas in the target region measured by real-time kinematic survey for the 81 mm munition.

Actual areas and number of increments are listed for each plume in Table 14. The demarcated ITP plume sizes (Table 14) are within the range of ones determined during previous command detonations of the M821A3 (300–890 m^2; *Walsh et al. 2018a*).

Table 14. GPS-measured areas and MIS increments collected for each 81 mm detonation plume. Note: Plume 2 covered residues from two cartridge detonations.

Plume	ITP		OTP 0-3 m		OTP 3-6 m	
	Area (m^2)	Increments (*n*)	Area (m^2)	Increments (*n*)	Area (m^2)	Increments (*n*)
1	540	89–121	288	104	345	99
2	843	119–140	344	73–92	389	95–108
3	324	87–102	239	80–88	273	76–80
4	426	81–125	273	89	314	95
5	451	93–113	275	91	301	96
6	568	99–105	323	91–97	366	73–89
7	711	93–130	370	76	391	75
8	672	92–118	395	90	403	83
9	617	96–150	321	101	346	87
10	445	90–91	294	79–96	332	86–88
11	492	90–142	314	108	342	88
12	553	95–145	380	95	386	85
13	526	101–110	305	98	333	85

All IMX-104 analytes were detected in all thirteen plumes of the 81 mm munition (Table 15). As has been observed in all tests of IMX-104 munitions, the compound NTO was the dominant residual component by two orders of magnitude. Masses of the other compounds followed a consistent trend of DNAN > RDX > HMX. Masses of each compound in the OTP decision units were negligible compared to the ITPs, which supports complete sampling of deposited residues. Transformation products of DNAN were not observed in any of the samples, indicating no degradation of this compound.

Table 15. Average energetic residue masses within each 81 mm plume's decision units. Values in parentheses are standard deviations of triplicate MIS estimates. Note that Plume 2 includes two cartridge detonations.

Plume	DU Type	Residues (mg/plume)			
		HMX	RDX	DNAN	NTO
1	ITP	6.4 (0.7)	80 (9)	240 (30)	11000 (2000)
	OTP 0-3	0.2	0.5	3.4	108
	OTP 3-6	<0.1	0.3	0.8	28
2	ITP	2.5 (0.3)	30 (10)	90 (20)	8000 (2000)
	OTP 0-3	<0.2	0.5 (0.8)	<0.2	44 (4)
	OTP 3-6	<0.1	<0.1	<0.1	28 (4)
3	ITP	1.7 (0.4)	22 (2)	48 (8)	10000 (600)
	OTP 0-3	<0.1	0.1 (0.0)	0.6 (0.1)	66 (9)
	OTP 3-6	0.3 (0.1)	<0.2	<0.2	18 (4)
4	ITP	1.3 (0.2)	9.6 (0.5)	31 (7)	4700 (100)
	OTP 0-3	<0.1	0.2	1.4	110
	OTP 3-6	0.4	<0.2	0.4	47
5	ITP	3.1 (0.4)	23 (3)	100 (10)	4500 (600)
	OTP 0-3	0.5	1.5	10	130
	OTP 3-6	0.3	<0.2	0.8	24
6	ITP	3.0 (0.2)	31 (3)	79 (9)	7600 (700)
	OTP 0-3	<0.2	0.2 (0.1)	0.8 (0.4)	50 (20)
	OTP 3-6	0.3 (0.1)	<0.2	0.2 (0.0)	16 (3)
7	ITP	1.8 (0.3)	23 (4)	42 (9)	12200 (300)
	OTP 0-3	<0.2	<0.2	0.4	47
	OTP 3-6	0.3	<0.2	0.3	31
8	ITP	0.8 (0.1)	7 (1)	17 (2)	5200 (800)
	OTP 0-3	<0.2	<0.2	0.2	32
	OTP 3-6	0.2	<0.2	<0.2	7
9	ITP	1.7 (0.1)	16.8 (0.7)	47 (2)	6600 (400)
	OTP 0-3	<0.2	0.2	1.0	95
	OTP 3-6	0.2	<0.2	0.3	35
10	ITP	0.9 (0.1)	8 (1)	14.3 (0.9)	5800 (800)
	OTP 0-3	<0.2	<0.2	0.2 (0.0)	30 (8)
	OTP 3-6	<0.2	<0.2	<0.2	10 (10)
11	ITP	2.0 (0.3)	25 (3)	50 (10)	9000 (1000)
	OTP 0-3	<0.1	0.1	0.5	30
	OTP 3-6	0.1	<0.1	<0.1	11
12	ITP	2.5 (0.6)	22.8 (0.4)	60 (8)	7600 (800)
	OTP 0-3	<0.2	<0.2	0.4	13
	OTP 3-6	<0.3	<0.3	<0.3	10
13	ITP	1.2 (0.2)	14 (3)	23 (3)	10000 (2000)
	OTP 0-3	<0.2	<0.2	0.6	78
	OTP 3-6	<0.2	<0.2	<0.2	21

Table 16 and Figure 21 summarize the per-cartridge residue loading rates and uncertainties in each 81 mm plume. Uncertainty associated with each plume's estimate, derived from the triplicate samples taken from each plume's ITP DU, are shown as RSDs in Table 16. The low RSDs associated with each compound's estimate within plumes (< 32 %) indicate minimal uncertainty related to sampling and analysis. Uncertainty in loading rate estimates among all plumes includes variability related to cartridge-to-cartridge differences in detonation and potentially variability in

plume-surface recovery of produced residues. This uncertainty was relatively high for HMX, RDX, and DNAN, in part due to Plume 1, but the overall uncertainty characterized by NTO and total residues RSD (35 %) met the success criteria of less than 50 % and bettered previous command detonation tests of the study munition (RSDs: 46 % AFS; 36 % CFS 12 g; 45 % CFS 18 g). Overall, the precision in the live-fire data, both within individual plumes and among all plumes, provides confidence that the live-fire loading rate estimates are broadly representative of the munition.

Table 16. Average estimated live-fire energetic residue loading rates and precision for the 81 mm munition.

Plume	Residues (mg/cartridge)					RSD (%)				
	HMX	RDX	DNAN	NTO	Total	HMX	RDX	DNAN	NTO	Total
1	6.7	80	240	11000	12000	11	11	13	16	16
2	1.4	16	46	4000	4000	11	32	17	25	25
3	2.0	22	49	10000	10000	19	10	16	6	6
4	1.7	9.9	33	4800	4900	9	5	21	2	2
5	3.9	25	110	4700	4800	10	14	9	12	12
6	3.3	31	80	7700	7800	7	11	11	9	9
7	2.1	23	43	12300	12300	12	16	22	2	2
8	0.9	7	17	5300	5300	14	19	14	16	16
9	1.9	17	48	6700	6800	7	4	5	6	6
10	1.0	8	14.5	5900	5900	14	15	6	13	13
11	2.1	25	50	10000	10000	13	12	23	12	12
12	2.7	22.8	60	7600	7700	24	2	14	10	10
13	1.2	14	23	10000	10000	13	20	12	19	19
Ave.	**2.4**	**23**	**63**	**7700**	**7800**	-	-	-	-	-
SD	1.6	19	60	2700	2800	-	-	-	-	-
RSD (%)	65	81	96	35	35	-	-	-	-	-

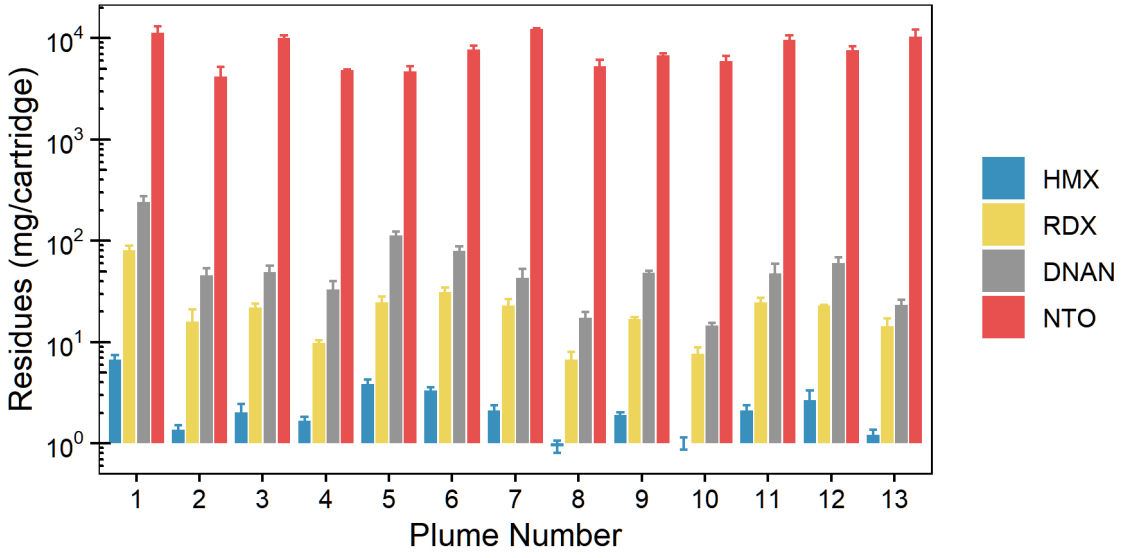

Figure 21. Average estimated energetic residue loading rate for each 81 mm plume. Error bars represent one standard deviation.

6. PERFORMANCE ASSESSMENT

6.1 QUANTITATIVE PERFORMANCE OBJECTIVES

6.1.1 Validation of Command Detonation with 60 mm IMX-104 Munition

Live-fire loading rates are compared with command-detonation loading rates for the 60 mm munition in Figure 22 and Table 17. The boxplots represent the data distribution of each compound for each fuze type. HMX, which is a component of the fuze, supplemental charge, and as an impurity in IMX-104, was minimal and near or below the detection limit for all fuze types. While RDX and DNAN loading rates were consistent between the AFS and CFS, both fuze simulators underestimated these compounds' live-fire loading rates by factors of 3–6. Still, these loading rates are extremely minimal and therefore unlikely to affect a management decision, however potential explanations for these observed differences are needed and discussed below. The main residue compound NTO exhibited identical loading rates between live-fire and AFS command-detonation tests.

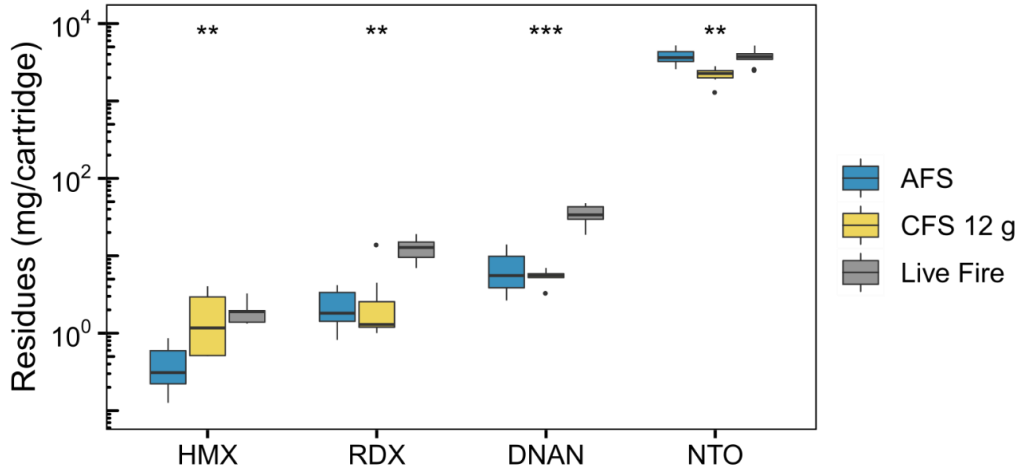

Figure 22. Boxplots of loading rates determined by live fire and command detonation of the 60 mm IMX-104 munition (M720A2). Previous command-detonation data with the AFS and CFS are presented in Walsh et al. *(2018a)*. Boxes represent the median and interquartile range (IQR), and whiskers represent no more than 1.5 times the IQR above and below the hinges. Data beyond the whiskers are marked as outlying points. Asterisks represent Kruskal-Wallis rank sum test significance levels (: $p \leq 0.01$; ***: $p \leq 0.001$).**

Table 17. Summarized average residue loading rates using all tested fuzing types for the 60 mm IMX-104 munition (M720A2). Values are rounded to appropriate significant figures based on plume-average standard deviations shown in parentheses.

Fuze	Mean Residues (mg/cartridge)				
	HMX	RDX	DNAN	NTO	Total
Live Fire	1.9 (0.6)	12 (4)	30 (10)	3800 (900)	3800 (900)
AFS	0.4 (0.3)	2 (1)	7 (4)	3800 (900)	3800 (900)
CFS 12 g	2 (2)	4 (5)	5 (1)	2200 (500)	2200 (500)

Statistical comparison of total residue loading rates was the metric used for determining validation success and is shown in Figure 23. This comparison between live fire and the AFS yielded a p value of 0.76, indicating no significant difference in these estimates, whereas comparison between live fire and the CFS yielded a significant difference ($p < 0.05$). The lack of significance difference

with the AFS allowed the success criteria for this objective to be met. These comparisons confirmed that command detonation using the AFS accurately reflected total energetic residue loading as it can occur during training. The significantly lower total loading rates using the CFS indicate that the 12 g C4 booster mass applied to this munition underestimated live-fire residue deposition. The successful validation of total residues by command detonation with the AFS for this 60 mm munition supported a Go decision and allowed for the project to continue with the Task 2 live-fire tests of the 81 mm IMX-104 mortar cartridge.

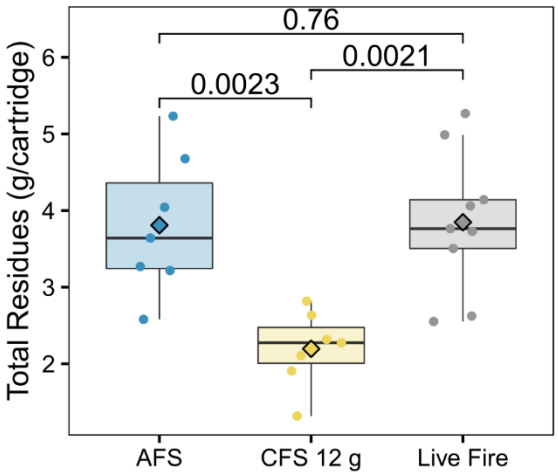

Figure 23. Comparison of total residue loading rates for the 60 mm munition (M720A2 IMX-104) between fuze types. *P* values for Mann-Whitney tests are listed, individual plume estimates shown as points, and means for each fuzing type shown as diamonds.

However, on an individual compound basis, only the NTO loading rate was similar between the AFS and live fire (Table 18). Significant differences in the (minor) loading rates of DNAN and RDX for both the AFS and CFS suggest a potential bias in their testing methodology that required further investigation.

Table 18. Summarized average residue deposition rates using all tested fuzing types for the 60 mm munition (M720A2 IMX-104). Values are rounded to appropriate significant figures based on estimate uncertainties. Values in bold are above the significance threshold ($p > 0.05$), indicating no significant difference.

Test Pairs	*P* Value				
	HMX	RDX	DNAN	NTO	Total
Live Fire – AFS	0.0002	0.0002	0.0002	**0.92**	**0.76**
Live Fire – CFS 12-g	**0.94**	0.0052	0.0002	0.0021	0.0021

There are only two major methodological differences between the live-fire and command-detonation tests: the initiation method and the physical orientation of the cartridges prior to detonation. The underestimation of DNAN and RDX by the AFS and CFS suggest potential loss of some of these residues outside of the sampled deposition areas during the command-detonation tests. Residues of DNAN and RDX were expected to be of relatively fine particle size, as DNAN is the molten matrix and a small crystal size of RDX is used in IMX-104, and therefore potentially susceptible to emission rather than deposition. Comparison of the initial liquid-solid partitioning between fuze types in the melted samples (Table 19) show much higher aqueous fractions for DNAN and RDX by live fire, which indicate the retention of fine particles that have high surface area and solubility. In positioning the cartridges nose-up and on 20 cm-thick blocks of solid ice,

the command-detonation setup may have promoted the air emission of fine particles composed of RDX and DNAN

Table 19. Initial proportion of energetic compounds in aqueous phase from tests of the 60 mm munition (M720A2 IMX-104). Results are the average of all ITP measurements with standard deviation in parentheses.

Fuze	Percent Fraction Aqueous (1σ)			
	HMX	RDX	DNAN	NTO
Live Fire	58 (9)	94 (4)	70 (6)	97 (2)
AFS	10 (10)	80 (10)	15 (6)	99.998 (0.001)
CFS 12 g	0 (0)	60 (10)	12 (4)	99 (2)

The same sampling protocol was applied to both methods of detonation (i.e., live fire and command detonation). In both cases, soot and residue plumes were clearly visible on the snow surface and could be representatively sampled using MIS. Differences from impact angle and cartridge orientation may have caused a difference in plume geometry reflective of residue deposition. The ITP plume areas from previous command-detonation tests were significantly smaller for the 60 mm IMX-104 munition (Figure 24). However, the quality control samples collected from the OTPs were consistently below detection limits or minimal relative to ITPs for all test types, which supports the assumption of complete collection of deposited residues from each test. The larger plume areas for the live-fire tests likely reflect the subjective demarcation of ITP plume edge or possibly an effect of cartridge orientation/position on residue dispersion. Regardless, the larger ITP areas by live fire did not affect the results, as concentrations in all ITP samples were well above method detection limits.

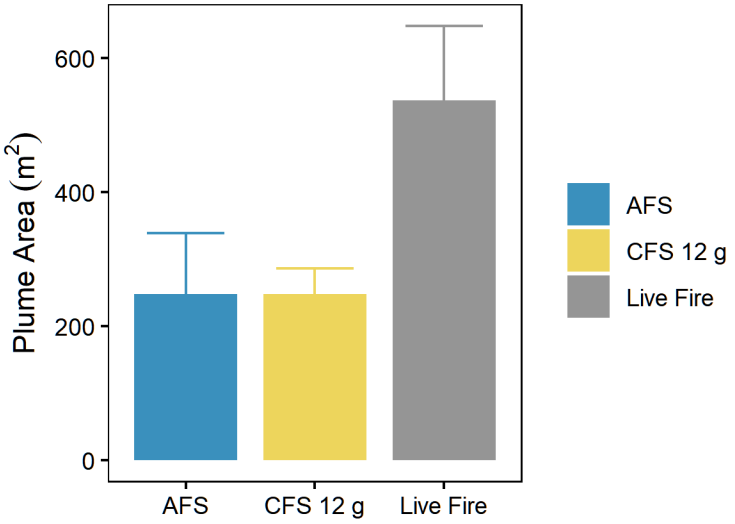

Figure 24. ITP areas of single-cartridge resolved detonations from command-detonation and live-fire tests of the 60 mm munition (M720A2 IMX-104). Error bars represent + 1 standard deviation.

Visual deposition patterns from both command detonation and live fire were similar, with no cratering and generally symmetrical even distribution, likely aided by low wind during testing (Figure 25). However, unlike command-detonation tests that had thoroughly covered snow at detonation centers, the live-fire detonations of the 60 mm munition tended to have bare, relatively clean snow at the impact point. This difference may have arisen from cartridge orientation, surface condition, or cartridge position (elevated on ice blocks for command detonation).

Figure 25. Examples of plume centers from command-detonation (left) and live-fire (right) tests of M720A2 60 mm IMX-104 mortar cartridges. Red arrow indicates the estimated impact point.

The last explanation for observed differences in DNAN and RDX could be from the firing train. While the fuze simulator boosters matched (AFS) or approximated (CFS) the issued fuze, the initiation charges to the firing trains were different. The M6/M7 blasting caps, used in the previous command-detonation tests with both the AFS and CFS, contain approximately 19 times the explosive mass of the safe and arming (S&A) device in the M734A1 fuze, and approximately 2 times the primary charge mass. Insights into how differences in initiation charge may have propagated to the main fill are explored through correlations in Figure 26. The live-fire loading of DNAN and RDX were tightly correlated, whereas these compounds were slightly decoupled with the AFS and unrelated for the CFS. Dissimilar consumption of the matrix compound DNAN and small crystalline compound RDX hint that the fuze simulators may not have perfectly replicated the live-fire firing train. Interestingly, loading of NTO was generally independent of the other energetic compounds for all fuze types, potentially explained by its large crystalline size in IMX-104 (*Taylor et al. 2013*).

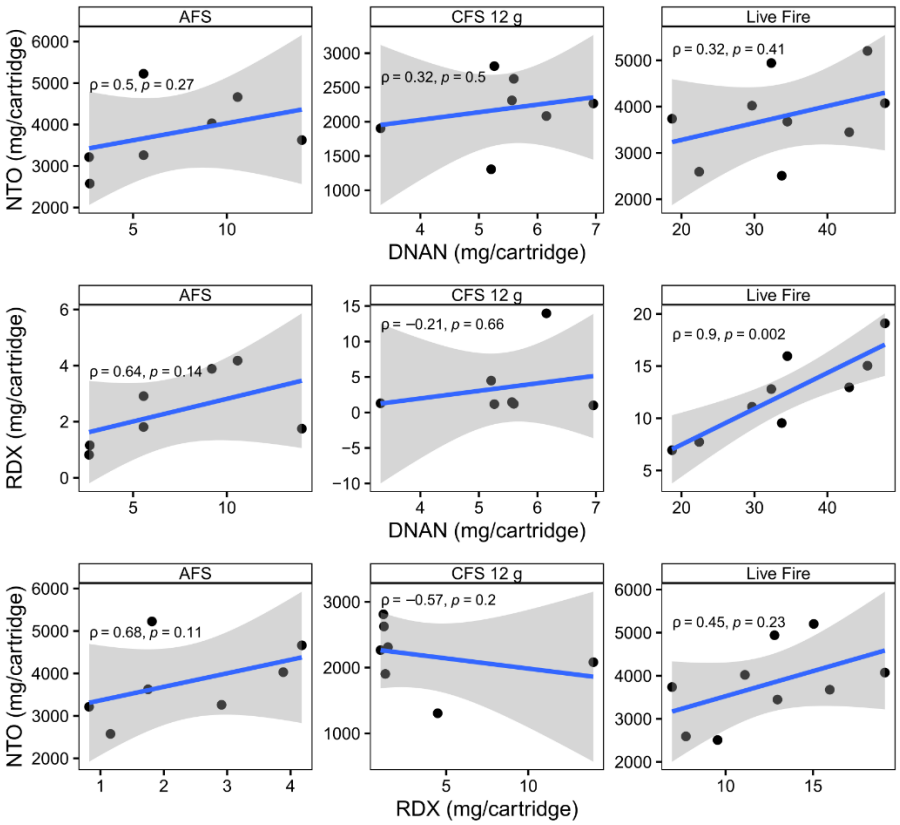

Figure 26. Inter-compound correlations for the 60 mm munition (M720A2 IMX-104) visualized with a linear model (blue line and grey 95 % confidence interval) and annotated with Spearman correlation coefficients (ρ) and *p* values.

Meeting the Task 1 success criteria for the 60 mm munition provided confidence in the command-detonation technology, yet the differences in the minor compound loading rates posed some uncertainty in the method's accuracy. Following these findings, two added efforts were planned for the subsequent 81 mm live-fire field season: 1) nose-down command-detonation tests with the CFS and 2) collection of elemental carbon as a surrogate material for residue recovery.

6.1.2 Validation of Command Detonation with 81 mm IMX-104 Munition

The live-fire loading rates for the M889A4 are compared with previously determined command-detonation loading rates for the M821A3 in Figure 27 and Table 20. Relative to the command-detonation tests, live-fire loading rates of HMX, RDX, and DNAN were generally similar if not slightly higher. However, NTO loading rates were consistently and significantly greater by live fire than by command detonation using any of the fuze simulators. The mean NTO loading rate by live fire was over 4 times greater than command-detonation tests using the AFS and the CFS with 12 g booster. The high booster mass used in the 18 g CFS was considered unrepresentative of the munition but provides end-member data for potentially over-driven detonations.

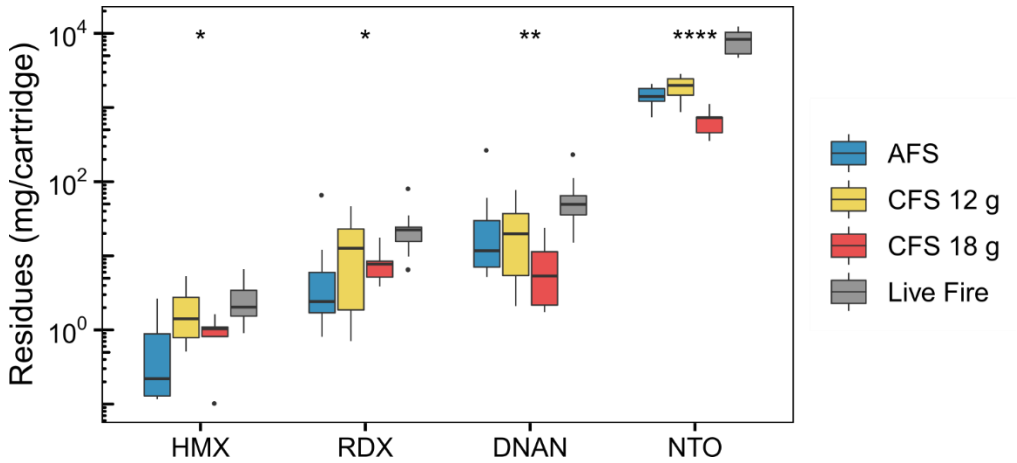

Figure 27. Boxplots of loading rates determined by live fire and command detonation of the 81 mm IMX-104 munition (M821A3/M889A4). Previous command-detonation data with the AFS and CFS are presented in Walsh et al. (*2018a, 2018b*). Boxes represent the median and IQR, and whiskers represent no more than 1.5 times the IQR above and below the hinges. Data beyond the whiskers are marked as outlying points. Asterisks represent Kruskal-Wallis rank sum test significance levels (*: $p \leq 0.05$; **: p: ≤ 0.01; ****: $p \leq 0.0001$).

Table 20. Summarized average residue loading rates using all tested fuzing types for the 81 mm IMX-104 munition (M821A3/M889A4). Values are rounded to appropriate significant figures based on plume-average standard deviations shown in parentheses.

Fuze	Mean Residues (mg/cartridge)				
	HMX	RDX	DNAN	NTO	Total
Live Fire	2 (2)	20 (20)	60 (60)	8000 (3000)	8000 (3000)
AFS	1 (1)	10 (20)	50 (80)	1700 (700)	1800 (800)
CFS 12 g	2 (2)	20 (20)	30 (30)	1900 (700)	1900 (700)
CFS 18 g	0.9 (0.5)	8 (4)	8 (8)	600 (300)	700 (300)

The large differences in NTO loading rates forced statistical tests to confidently ($p < 0.001$) reject the null hypothesis that total residue loading was not significantly different between each fuze simulator and live fire (Figure 28). These statistical results led the success criteria not to be met for this objective. However, loading rates for the other IMX-104 compounds compared more closely. DNAN loading rates were not significantly different between live fire and either the AFS or CFS 12 g at the 95 % confidence level, indicated by p values greater than 0.05 (Table 21). Live-fire loading rates of HMX and RDX were significantly different with the AFS but not with the CFS 12 g, though these compounds could have been derived from the fuze boosters and not the IMX-104 main filler.

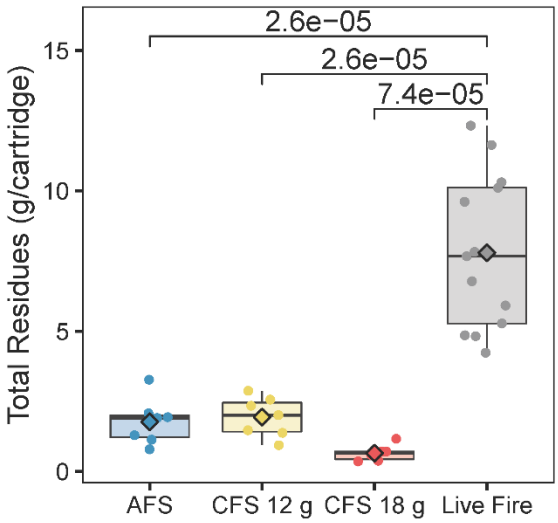

Figure 28. Comparison of total residue deposition rates for the 81 mm munition (M821A3/M889A4 IMX-104) between the different tested fuze simulators and live fire. *P* values for Mann-Whitney tests are listed, individual plume estimates shown as points, and means for each fuzing type shown as diamonds.

Table 21. Results of two-sided Mann-Whitney rank sum tests between live-fire and prior command detonation tests of the 81 mm munition (M889A4/M821A3 IMX-104). Values in bold are above the significance threshold ($p > 0.05$), indicating no significant difference.

Test Pairs	*P* Value				
	HMX	RDX	DNAN	NTO	Total
Live Fire – AFS	0.026	0.014	**0.067**	2.6x10-5	2.6x10-5
Live Fire – CFS 12 g	**0.503**	**0.275**	**0.097**	2.6x10-5	2.6x10-5
Live Fire – CFS 18 g	0.007	0.007	5.2x10-4	7.4x10-5	7.4x10-5

Unlike the 60 mm munition, all constituents were relatively equally partitioned between liquid and solid phases between representative fuzes (i.e., excluding the CFS with 18 g booster; Table 22). Slightly greater aqueous fractionation of DNAN by live fire suggest possible greater retention of fine particles, however loading rates for this compound were not significantly different between fuze types. Overall, these results suggest the residues recovered from each test were of the same general particle sizes. Preferential emission of NTO during command-detonation tests, potentially due to nose-up configuration, is unlikely due to its large particle size in IMX-104 (*Taylor et al. 2013*).

Table 22. Initial proportion of energetic compounds in aqueous phase from tests of the 81 mm munition (M889A4/M821A3 IMX-104). Results are the average of all ITP measurements with standard deviation in parentheses.

Fuze	Percent Fraction Aqueous (1σ)			
	HMX	RDX	DNAN	NTO
Live Fire	37 (9)	88 (4)	40 (10)	97 (2)
AFS	20 (20)	80 (20)	20 (5)	99.996 (0.003)
CFS 12 g	10 (20)	70 (10)	10 (6)	99 (2)
CFS 18 g	0 (0)	50 (20)	10 (10)	90 (10)

Differences in demarcated plume areas between live-fire and command-detonation tests of the 81 mm munition are shown in Figure 29. The plume areas from live fire were within the middle of

the range determined for the command-detonation tests, which exhibited considerable variability between fuze simulators.

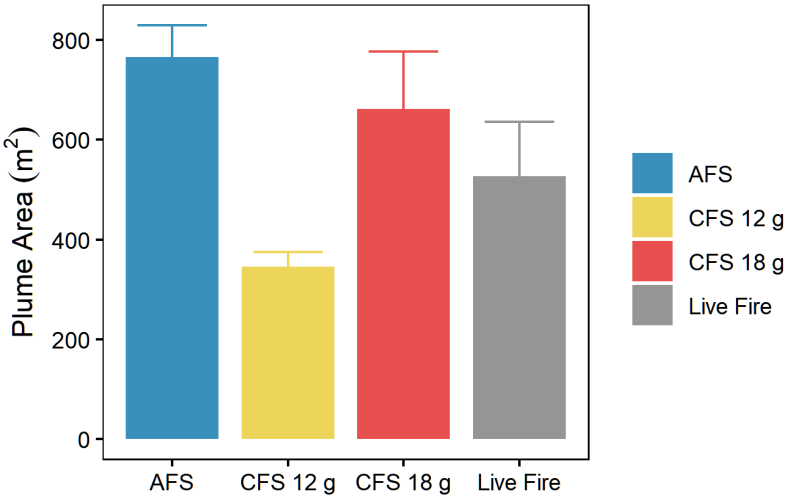

Figure 29. Areas of single-cartridge resolved plumes from command detonation and live-fire tests of the 81 mm munition (M821A3/M889A4 IMX-104). Error bars represent + 1 standard deviation.

Plume geometries were generally symmetrical for command detonations but assymmetric for live fire, likely due impact angle and wind conditions (Figure 30). As plume areas were similar, and sampling was agnostic of plume geometry, there were no apparent physical plume explanations for the observed differences in residue loading.

Figure 30. Examples of plume centers from command detonation tests of M821A3 (left) and live-fire tests of M889A4 (right) 81 mm IMX-104 mortar cartridges. Red arrow indicates the estimated impact point.

The same differences in initiation charges between command-detonation tests (M6 detonator) and the fuze S&A device apply to the M783 used in these 81 mm munition live-fire tests as applied to the 60 mm munition with the M734A1 fuze. In the case of the 81 mm munition, loading rates of DNAN and RDX were tightly correlated not only from live fire but also from command detonation with the AFS and CFS 12 g (Figure 31). The likely over-driven CFS 18 g command-detonation tests show non-linearity in DNAN and RDX loading. The matching DNAN-RDX linearity observed for the AFS and CFS 12 g support their representation of live-fire detonation. As was observed for the 60 mm munition, NTO loading was independent of DNAN and RDX loading by

live fire, however NTO is significantly correlated with both DNAN and RDX for tests with the AFS only. It is unclear whether this correlation is an anomaly or a reflection of the test setup.

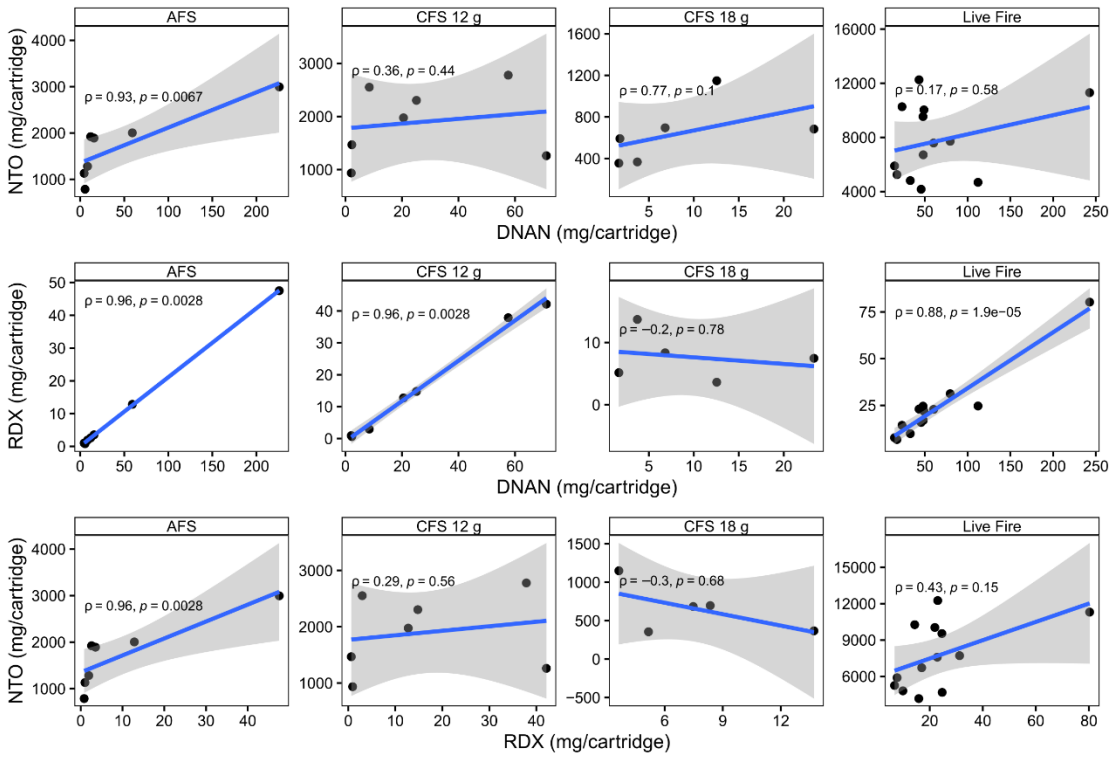

Figure 31. Inter-compound correlations for the 81 mm munition (M821A3/M889A4 IMX-104) visualized with a linear model (blue line and grey 95 % confidence interval) and annotated with Spearman correlation coefficients (ρ) and *p* values.

The effect of cartridge orientation was proposed as a source of error in the 60 mm munition tests and was planned to be tested with nose-down command-detonation tests during the 81 mm field work. Unfortunately, logistic constraints did not allow these add-on tests to be performed. Future static command-detonation tests in nose-down orientation, similar in position to live-fire impact, would potentially help explain underestimation by command detonation of NTO for the 81 mm and of DNAN/RDX for the 60 mm munition.

Following questions on quantitative recovery from this project's first in-progress review, we proposed that post-detonation deposited carbon could be compared to thermochemical combustion model predictions as a surrogate for energetic residue recovery, serving as a secondary means of quality assurance. Most military explosives have negative oxygen balance (i.e., they contain insufficient oxygen to fully oxidize their carbon) and therefore leave behind the dark soot plumes that we observed on the snow surface following detonation.

During the Task 2 live-fire tests with the 81 mm munition, fourth replicate MI samples from the ITPs of select plumes were collected for elemental carbon analysis. The sampled plumes had minimal cratering with no soil liberated and no vegetation. These samples were processed in the same manner as the other samples, with only the filtered solids submitted for analysis. Total elemental carbon in these samples was measured in triplicate by high temperature (990 °C)

combustion analysis at Midwest Micro Labs. Total carbon deposited was calculated in the same way as for energetic residues and is presented in Figure 32. Modeled products of IMX-104 detonation at total maximum density were provided by Philip Samuels, as calculated by the CHEETAH 6 Exp 6.3 thermochemical model (*Fried and Souers, 1996*). The amount of carbon deposited by the 81 mm munition was calculated from the provided solid carbon (as the diamond allotrope) detonation product fraction (mol C per kg IMX-104) and mass of IMX-104 in the 81 mm munition. The amounts of total carbon recovered from six of the seven sampled plumes were at or above the predicted 122 grams of carbon per cartridge, with the remaining plume just below at 101 g/cartridge. Total carbon recovery was unrelated to total energetic loading rate ($R = -0.2$, $p = 0.6$), which may have been due to deviation from model-predicted reaction or the unintentional inclusion of foreign carbon sources. However, the overall complete or excess recovery of model-predicted carbon soot, estimated to be of extremely fine particle size (*Bagge-Hansen et al. 2019*), supports the assumption of complete residue recovery from the snow surface surrounding the impact point.

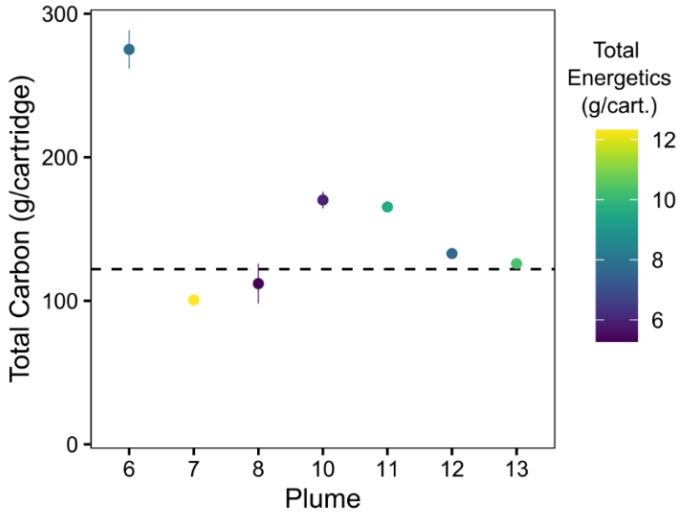

Figure 32. Estimated total carbon residues from the ITPs of select plumes of M889A4 81 mm IMX-104. Error bars represent ± 1 standard deviation on triplicate analyses of single replicate MI samples. Dashed line represents the amount of solid carbon (graphite) predicted by the Cheetah 6.0 thermochemical model.

Overall, while the success criteria for no significant difference in total residues was not met for the 81 mm munition, the data provided by command detonation were accurate to the correct order-of-magnitude. Given uncertainties in other aspects of munition functioning (i.e., partial detonation and dud rates), as well as the log-scale variability in loading rates across munitions (Table 1), this level of accuracy in loading rate prediction is likely sufficient to inform risk and environmental impact assessments. Nevertheless, improvements to future command-detonation test setups are proposed in Section 8 to better reflect residues produced during live-fire training.

6.2 QUALITATIVE PERFORMANCE OBJECTIVES

6.2.1 Fuze Setting Determination

The first two fired cartridge of the 60 mm munition compared the visual residue plumes produced by the IMP and PRX settings on the M734A1 multi-option fuze. The IMP setting detonates the projectile upon impact with the ground or target, whereas the PRX setting is an airburst at a mean

height of 2 m. Observed through telephoto lens, the dark residue cloud produced with the IMP setting was low-lying and solid material appeared to settle out immediately. Comparatively, the residue cloud from the PRX setting was produced above the ground surface and ultimately drifted and diffused away from the point of detonation (Figure 33). At the detonation site, the IMP setting produced a well-defined dark residue and soot plume on the snow surface with minimal to no cratering, whereas there was little evidence for any residues or soot on the snow surface above the PRX detonation. From these observations, the IMP setting was decided as optimum in preserving residues on the snow surface and the most comparable to prior command-detonation tests.

Figure 33. Residue and soot clouds immediately after detonation of a 60 mm munition (M720A2) using the IMP (left) and PRX (right) settings on the M734A1 multi-option fuze.

The M783 fuze for the 81 mm munition tests had settings only for point-detonating and delay, the former of which was selected for its equivalence to the IMP setting on the M734A1. The delay setting was untested but likely would have produced significantly greater cratering and liberation of potentially contaminated soil. Post-detonation clouds were generally similar between all cartridges and characterized by a dark component that settled out quickly and a fainter light component that drifted off-area along the wind direction (Figure 34). The darker component was assumed to comprise carbon soot and the majority of solid energetic residues, and the lighter component predominantly condensed gases (e.g., H_2O, CO, CO_2, N_2).

Figure 34. Two examples of post-detonation residue/soot/gas clouds from live-fired 81 mm cartridges (M889A4).

The effect of kinetic impact during live fire versus static positioning during command detonation was raised as a potential source of error during the first in-progress review (IPR). To address this question, the following simplified calculations were made for the 81 mm munition: first, assume the velocity at impact is approximately the same velocity at the muzzle when fired (66 m/s with Charge 0 for the M821 munition, as was used in Task 2, up to 305 m/s with Charge 4). The detonation velocity of IMX-104 is 7500 m/s (*Furnish et al. 2014*). Given a projectile length of approximately 0.4 m and assumed instantaneous initiation time (electric fuze), the projectile takes approximately $5x10^{-5}$ s to fully detonate. In that time, the projectile would have traveled approximately 3 to 15 mm beyond the initiation point, also assuming no influence of the impact medium. Negligible penetration is supported by the minimal cratering observed during the live-fire tests. This calculated penetration depth for a live-fired munition is less than the length of the fuze, and therefore its position above the impacting surface at the time of complete detonation is not significantly different from the position above the ice surface in which previous command detonation cartridges were set up. This similarity in positioning indicates that the distribution of residues would also be similar.

6.2.2 Stakeholder Results Acceptance

The results of this demonstration have been shared with armaments and ammunition stakeholders through multiple deliverables. Following data collection from each live-fire test (i.e., Task 1 and Task 2), reports containing all test data were submitted to JPEO A&A for internal distribution. All public technical reports and presentations were also submitted for technical review and advanced result briefing. An in-person briefing on the results of the project was scheduled to interested personnel at Picatinny Arsenal in May 2023.

General impressions by the stakeholders include acknowledgment of importance of residue testing and the desire to implement with minimal cost and time risks. The stakeholders have demonstrated their commitment to controlling energetic source loading on ranges by considering command-detonation residue tests of the M795 155 mm howitzer projectile with IMX-101 main fill. CRREL and DEVCOM AC partnered to test this munition in February 2023 with a modified standard fuze on a snow surface. Results of this test, combined with subsequent fate and transport modeling, will inform decision making on use of this munition during potential training on US ranges. For future and in-development munitions, cost-effective methods for integrating residue testing with adequate QC, as well as fate, transport, and impact modeling, were discussed as paths forward.

7. COST ASSESSMENT

7.1 COST MODEL

The purpose of this technology is to provide an efficient method, capable of integration early in the acquisition process for new munitions, that produces reproducible results representative of live-fire conditions. The costs of performing command-detonations test for new or existing munitions are affected by cost drivers, discussed in Section 7.2, but are estimated to be similar to those for the live-fire tests conducted as part of this study. Table 23 provides an overview of the cost model and associated costs tracked during the live-fire test of the 60 mm munition in this study.

Table 23. Cost model for performing residue testing on snow for a single munition.

Cost Element	Data Tracked During the Demonstration	Actual Demonstration Costs	
Command Detonation and Field Sampling	• Ammunition • Range Access • EOD Support • Personnel required, associated labor, and travel costs • Tools, GPS survey equipment, and consumable items needed for sample collection • Shipment costs for field supplies and samples • Travel costs	Field technician A, 175 h Field technician B, 175 h Field technician C, 175 h Project Chemist, 185 h Field Manager, 185 h	\$8,860 \$8,520 \$14,670 \$13,636 \$15,948
		Shipping to/from field	\$2,000
		Consumables	\$2,000
Sample Processing and Analysis	• Personnel required and associated labor • Consumable items (i.e., liquid handling, solvents, analytical columns)	Analytical Chemist, 160 h Lab Technician, 240 h	\$11,793 \$12,825
		Consumables	\$7,053
Waste Disposal	• Solvent types, volumes, holding containers, and disposal service	Holding Containers, 2ea Disposal Service, 10 gal	\$250 \$180
Data Analysis	• Personnel required and associated labor	Analytical Chemist, 80h	\$5,896

The cost element associated with field testing is the most significant and requires coordination between explosives experts and environmental sampling professionals. Access to a testing range and support from explosive ordnance disposal personnel are critical components of this element, along with acquisition of a suitable quantity ($n \geq 7$) of a study munition. This project benefited from these services and materiel provided at no charge, but routine application of this technology in a non-training environment could incur such costs. Secondary costs for field work include labor for field personnel qualified to collect MI samples and collect GPS survey data. Consumables during this stage are minimal, consisting of thick polyethylene sampling bags, sampling tools, labels, and personal protective equipment.

Sample processing and analysis requires significant labor for qualified personnel to filter samples, perform chemical extractions, and ultimately analyze sample fractions. Whereas commercial labs may be accustomed to accepting water and soil samples, processing of snow samples requires

specific methods to sensitively capture and measure constituent compounds. Once processed, established analytical methods (i.e., EPA Method 8330B and modifications thereof) can be applied and are available through commercial and research laboratories. Specific costs associated with analysis are disposable glassware, solvents, solid phase extraction cartridges, chromatographic columns, and associated instrument maintenance. This project benefited from existing analytical equipment at no direct cost. Processing and analysis generate hazardous waste, largely in the form of diluted flammable solvents with trace quantities of residual compounds.

Data analysis costs are solely in labor for an experienced chemist to integrate processing data (e.g., sample fraction volumes), field data (e.g., plume areas, increments), and analytical results. In addition, this chemist must interpret quality assurance and quality control data to ensure method acceptance criteria are met.

7.2 COST DRIVERS

The combined method of sampling (i.e., snow, soil, air) and study site (i.e., range with snow, range with clean soil, blast chamber) are the primary drivers of anticipated cost in applying this technology and present a high degree of variability. Selection of sampling method and associated site requirements (discussed in detail in Section 8.3) should ultimately address the data quality objectives of the assessment, which are informed by compound toxicity, compound mobility in the environment, and release pathway of concern (i.e., groundwater impacts, air emissions). Leveraging of existing full-scale empirical tests (e.g., performance tests, sensitivity tests) may save significant costs so long as the method and site meet the data quality objectives.

7.3 COST ANALYSIS

A simplified example is detailed below in Table 24 for command-detonation testing of 15 rounds of a novel munition using a fuze simulator. This example assumes testing at a site with snow cover, a local EOD who can handle the munition items, and sample processing/analysis equipment located nearby to minimize travel/shipping costs. An in-development munition is likely to require non-standard delivery to the study site. Testing 15 rounds over the course of 5 days assumes that the team can detonate and sample 3 rounds per day. The costs presented in the below example are direct, unburdened.

Table 24. Example cost data for command-detonation testing of a munition.

Cost Element	Cost
Munition shipment to study site	$10,000
Field Labor for 6 personnel over 5 days	$18,500
Sampling consumables	$2,000
Labor for analytical chemist	$12,000
Labor for laboratory technician	$13,000
Labor for data analysis/interpretation	$6,000
Laboratory consumables and waste disposal	$8,000
Total	**$69,500**

Several potentially unrealistic cost omissions are made in this analysis but cannot be predicted with certainty from a military research perspective. These omissions include costs associated with obtaining ammunition, tasking EOD technicians, site access, site travel, and lab equipment and facilities.

Costs of integrating command-detonation testing should be compared against the potential costs incurred if testing is not performed and a study munition is found to deposit significant damaging quantities of energetic residue. These no-action costs are difficult to estimate but could involve: 1) acquisition changes (estimated >$1M); 2) remediation efforts (e.g., >$1.2B at Joint Base Cape Cod; *MA ARNG 2019*); 3) range closures and associated impacts to training access and readiness (*Walsh et al. 2014a*). Given the low cost of residue testing relative to potential no-action liabilities, and the findings of high loading rates from some IM, implementation of this technology appears both critical and minimally intensive.

8. IMPLEMENTATION ISSUES

8.1 QUANTITATIVE RESIDUE RECOVERY

The testing methodology used in this study considered only the fraction of released residues that were deposited to the ground surface in the area surrounding detonation. As this testing was performed in open air, an unknown fraction of total produced residue remained lofted and was transported outside of the sampling area. Neglect of the latter atmospheric fraction was raised in the first IPR for this project. Several lines of evidence support the quantitative recovery of released residues using this testing methodology and are discussed below.

The particle size of released post-detonation residues of IMX-104 have been shown to be predominantly below 250 µm and consist predominantly of NTO (*Walsh et al. 2017b*). Residues of the other compounds are likely present as even smaller particles owing to their smaller crystal size (RDX) or matrix composition (TNT/DNAN). A previous modeling study of particulate transport from detonations (SERDP CP-1159) calculated that entrained soil particles with diameters less than 50 µm would be subject to emission, with the larger sized particles subject to deposition (*Brown et al. 2004*). This study only considered settling by gravity, however, and it did not consider dry and wet deposition processes that may have occurred with other solid combustion products (e.g., soot). Anecdotally, plumes generated while it was snowing during the live-fire 81 mm tests (Plumes 1-2) did not exhibit consistently enhanced loading rates compared to plumes formed without snow. The proximity fuze setting on the 60 mm munition, with a 2-meter height of burst, produced no visible soot plume on the snow surface. It is therefore apparent that dry deposition velocities of residual particles or aggregates require near-surface formation for interception with the ground surface.

Previous work has attempted to sample both residual fractions (emitted and deposited) simultaneously from command detonations. The EPA "Flyer" sensor and sampling package was used during SERDP Project ER-2219 suspended from wires (~2 m above ground level) for command detonations of C4 blocks and 81 mm IMX-104 mortar cartridges on snow (*Walsh et al. 2018b*). Shifting wind and Flyer mobility issues during the IMX-104 tests caused the Flyers to miss the munitions' aerial plumes; however, they did capture portions of the aerial plumes from five repeated detonations of two blocks of C4. Estimated atmospheric energetics from Flyer measurements, which were located approximately 20 m downwind from the site of detonation, were only 7 % of the deposited energetic mass (*Walsh et al. 2018b*). This minimal mass emitted from C4 blocks indicates near-complete recovery of total released residues from the snow surface surrounding the detonations.

Near quantitative recovery from the snow surface is also supported by comparison with limited available enclosed blast chamber data. During the LCEA for the M720A1 60 mm PAX-21 munition, two cartridges were command detonated in an enclosed chamber and the solid residues collected for analysis. Corrected extrapolation of analyses on sub-samples from these tests revealed perchlorate residues (7.8 and 17.5 g/cartridge) that were in good agreement with open-air tests on snow (14 ± 7 g/cartridge of perchlorate, n = 7 cartridges; *Walsh et al. 2013a, 2018b*).

The negative oxygen balance (OB) of military high explosives provides a surrogate measurement of residue recovery from the snow surface in form of solid elemental carbon. This carbon is derived from the explosive itself and therefore should co-deposit along with unreacted solid explosive

material and may also promote deposition through agglomeration. Sampling for total carbon acts as a surrogate for residue recovery from the surface, assuming no exogenous carbon inputs. The trial performed during the 81 mm IMX-104 (approximate OB -40 %) live-fire tests recovered slightly more carbon than modeled by the CHEETAH thermochemical model (122 g/cartridge), which supported the assumption of complete recovery of residues from the surface. Exogenous carbon was avoided through selection of only ideal plumes (e.g., minimal cratering, no vegetation), and munition component inputs were estimated at a maximum of 7 grams/cartridge from the steel mortar body.

Measurement of emitted residues in conjunction with deposited residues surrounding the detonation point would provide the most complete testing solution, however air sampling adds additional complexity and uncertainty given its discrete nature and reliance on carbon emission factors, discussed in more detail in Section 8.3. Altogether, the lines of evidence presented here indicate that sampling deposited residues provide a near or completely quantitative estimate of residual explosive loading. Additionally, this deposited fraction is most likely to concentrate at impact area target locations where hundreds of detonations can accumulate and potentially result in groundwater or surface water impacts.

8.2 REPRESENTATION OF EXPLOSIVE TRAIN

Matching the study munition's explosive train during command-detonation testing is essential in replicating the residue loading that occurs during training. From the previous tests with the AFS and CFS of different booster masses, booster mass clearly had a strong effect on residue loading. However, even the AFS that matched the booster of the M734A1 and M783 fuzes underestimated the NTO loading rate for the 81 mm IMX-104, underestimated DNAN for the 60 mm munition, and underestimated RDX for both caliber munitions. Cartridge orientation may have a part in some of these biases, but another possible variable is the blasting cap used to initiate the cartridges in previous command-detonation tests.

For practicality in setup, tests with both the AFS and CFS used blasting caps to initiate the detonations, and the explosive masses used in these caps are substantially greater than masses used in the issued fuze's S&A device. Interestingly, the same fuze simulation setups were applied to both caliber IMX-104 munitions with no significant difference with live-fire total residue loading for the 60 mm munition and a four-fold underestimation for the 81 mm munition. It is unclear whether the blasting cap's increased explosive mass could affect filler mass consumption.

Future command-detonation tests can reduce uncertainty related to variations in the firing train by both matching the fuze booster and the initiation charge in the fuze S&A device. Commercial off-the-shelf exploding bridge-wire detonators (e.g., RP-3) may be able to provide a closer match than the military M6/M7 blasting caps in future command-detonation tests. Some munitions can be used with multiple different fuzes each with different output charges (e.g., PGK). In this case, matching the explosive train of the fuze that is most likely to be used during training would be most relevant. Finally, as cartridge orientation may also affect surface deposition, future tests should explore matching a nose-down vertical or angled projectile orientation.

8.3 TESTING ENVIRONMENT AND LOGISTICS

The inability for thermochemical models to predict residual post-detonation energetics requires an empirical testing approach to address potential environmental impacts during live-fire training. Further, loading rates have not yet been found to definitively scale with filler mass or caliber, so as of now each munition needs to be tested individually to provide an accurate estimate. There is therefore a desire to make this empirical testing as facile and cost-effective for integration in the acquisition process. Command detonation enables this testing to occur early, before a munition is a certified for live fire, however multiple integrated testing-sampling approaches have been developed each with their own pros and cons, presented in Table 25 and discussed below.

Table 25. Comparison of sampling method pros and cons.

Sampling Method	Advantages	Disadvantages
Deposition on snow	Sensitivity; 'clean' medium; visible deposition plume	Deposition only; freezing and snow cover environmental constraints
Deposition on soil/sand	All-weather capability; ability to leverage existing tests	Deposition only; low sensitivity; clean material requirement; intensive sample processing
Witness plates	Clean surface; ability to leverage existing tests	Assumes particle adherence; discrete or composite sampling approach
Open-air emission sampling	Captures fraction likely for atmospheric transport	Emission only; point sampling within plume (assumed homogeneity); reliance on carbon-balance calculation
Detonation chamber	Whole product sampling (all gas and fine particle emissions and deposited particles); ability to leverage existing tests	Net explosive weight limits; chamber cleanliness; representation of open-air conditions

Sampling deposited residues from snow is likely the most well-developed and widely applied method for assessing solid residues from detonations. The ability to see the soot and residue plume on the snow surface and apply representative MIS provides a comprehensive and extremely sensitive method. The main assumption with this approach, as discussed above, is that all released residues are deposited within the sampling area and an insignificant portion is emitted to air. The main logistic issue with testing on snow is the dependency on weather conditions at the study site. A minimum snow depth of 1–2 cm is required to reliably recover increments. Testing on bare ice has been performed typically when large residue fragments were expected that might penetrate light snow (e.g., M1122), with a key difference in collection being the whole population sweeping of the plume area instead of MIS. Potential particle loss through cracks in the ice and to the broom bristles make this method only particularly useful for high-depositing munitions. Potential future improvements to ease the logistic burden with testing on snow include: a dedicated testing location in a cold location; and snow-making equipment to ensure suitable depth of sampling medium.

Sampling deposited residues from soil or sand is similar in approach as for snow and has seen recent use in assessment of a 155 mm IMX-104 munition (*Persico et al. 2022*). Unlike snow, the soot/residue plume is not always apparent on sand/soil so a fixed dimension area (typically a circle) must be assigned, and this area can be informed by previous tests on snow of munitions with similar net explosive weight. The major drawback from this approach is the reduced sensitivity created by the sampling medium. Assuming a shallower sampling depth is needed from soil (1 cm instead of 2.5 cm on snow), sampling the same area as for snow (100 increments of 10 cm^2 = 1

m^2) would produce a soil sample with a mass of ~16 kg (compared to ~2 liters of melted snow). That soil must be milled to a fine particle size in entirety, sub-sampled, and solvent-extracted (i.e., EPA Method 8330B). The typical detection limit for energetic compounds in soil is 0.04 mg/kg (*Hewitt et al. 2009*), making the minimum detected mass by soil testing approximately 0.64 mg. Comparatively, over the same area, snow sampling has an estimated detection limit mass of 0.4 µg, or is roughly 1600 times more sensitive. In both cases, the minimum munition loading rate (mg/cartridge) for detection needs to be extrapolated from the ratio of sampled area to plume area. For compounds with higher toxicity thresholds (e.g., NTO), soil may provide sufficient sensitivity for decision making.

Collection of distributed residues from witness plates or other solid surfaces is common to the field of forensics. Limited data are available on this approach in the application to military explosives, however a well-detailed study (*Abdul-Karim et al. 2016*) successfully applied an array of steel witness plates surrounding detonations of spherical unconfined plastic explosive. This sampling method may be easy to implement in a testing regime, offering easy-to-clean surfaces for the collection of residues. Potential drawbacks are uncertainty related to individual compound adherence to the plates, discrete sampling approach (depending on array), and damage by fragments of cased munitions.

Open-air sampling of air emissions has been applied extensively to open-burning and open-detonation of munitions (*Aurell et al. 2015*; SERDP WP-1672; *Walsh et al. 2018b*). Volatile and semi-volatile compounds have often been the focus of these types of studies, however solid energetic residues have also been targeted through filters on sampling/sensor packages (i.e., the EPA Flyer). These airborne packages need to be positioned inside the emitted smoke plume from detonations, with tethered balloons, wire rigging, and UAVs successfully applied. To avoid damaging over-pressure and fragmentation, the sampling/sensor package typically is positioned at a significant distance from the detonation point, and therefore likely misses energetic residues deposited to the immediately surrounding ground surface. From continuous measurements of CO/CO_2 and sampling of energetic particles, all at discrete points in the plume, emission factors of the energetic compounds can be calculated using the carbon-balance approach. This approach assumes all munition item carbon is converted to CO and CO_2, which may then require correction for energetic compound emission factors from detonation of explosive fillers with negative oxygen balance. Application of this method in conjunction with a deposition method could provide a near-complete assessment of all detonation products.

Testing in closed- or controlled-air environments such as blast chambers are appealing for their complete containment or capture of released detonation products. A 16.5 m diameter hemisphere called the BangBox was used by EPA and DOD to assess air emissions from some common conventional military explosives and smaller munition items (*Mitchell and Suggs, 1998*). Fans were used to circulate air within the blast chamber to homogenize emissions for air sampling. Another blast chamber was referenced in Walsh et al. (*2018b*) for the M720A1 PAX-21 munition, where solid residues were reported recovered from the chamber interior. This type of testing likely provides the best, most complete assessment of total energetic residues; however potential issues arise from chamber contamination/cleaning, potential over-pressurization effects, and, most importantly, net explosive weight limits (e.g., 220 g for the BangBox) that may prevent application to many common munitions.

9. REFERENCES

Abdul-Karim, N., C.S. Blackman, P.P. Gill, E.M. Wingstedt, and B.A.P. Reif. 2014. Post-Blast Explosive Residue – A Review of Formation and Dispersion Theories and Experimental Research. RSC Advances, 4 (97): 54354-54371. DOI: 10.1039/C4RA04195J

Abdul-Karim, N., C.S. Blackman, P.P. Gill, and K. Karu. 2016. The Spatial Distribution Patterns of Condensed Phase Post-Blast Explosive Residues Formed During Detonation. Journal of Hazardous Materials, 316: 204-213. DOI: 10.1016/j.jhazmat.2016.04.081

Arthur, J. D., N. W. Mark, S. Taylor, J. Šimůnek, M. L. Brusseau, and K. M. Dontsova. 2018. Dissolution and Transport of Insensitive Munitions Formulations IMX-101 and IMX-104 in Saturated Soil Columns. Science of the Total Environment, 624: 758–768. DOI: 10.1016/j.scitotenv.2017.11.307

Aurell, J., B.K. Gullett, D. Tabor, R.K. Williams, W. Mitchell, and M.R. Kemme. 2015. Aerostat-Based Sampling of Emissions from Open Burning and Open Detonation of Military Ordnance. Journal of Hazardous Materials 284: 108–120. DOI: 10.1016/j.jhazmat.2014.10.029

Bagge-Hansen, M., et al. 2019. Detonation synthesis of carbon nano-onions via liquid carbon condensation. Nature Communications, 10: 3819. DOI: 10.1038/s41467-019-11666-z

Beal, S.A. and M.F. Bigl. 2022. Particle Size Characteristics of Energetic Materials Distributed from Low-Order Functioning Mortar Munitions. Journal of Energetic Materials. DOI: 10.1080/07370652.2022.2155730

Bigl, M. F., S.A. Beal, M.R. Walsh, C.A. Ramsey, and K. A. Burch. 2020. Sieve Stack and Laser Diffraction Particle Size Analysis of IMX-104 Low-Order Detonation Particles. ERDC/CRREL TR-20-3. U.S. Army Engineer Research and Development Center, Cold Regions Research and Engineering Laboratory, Hanover, NH. DOI: 10.21079/11681/35515.

Brown, R.C., C.E. Kolb, J.A. Conant, J. Zhang, D.M. Dussault, T.L. Rush, B.E. Conway, J.W. Morris, and J. Touma. 2004. Source Characterization Model (SCM): A Precitive Capability for the Source Terms of Residual Energetic Materials from Burning and/or Detonation Activities. SERDP Project CP-1159. Available at: https://serdp-estcp.org/projects/details/18a8f8d3-979c-4a7d-af16-5ef2c96b6115 (Accessed 6 January 2023).

Chendorain, M.D., L.D. Steward, and B. Packer. 2005. Corrosion of Unexploded Ordnance in Soil-Field Results. Environmental Science and Technology 39 (8): 2442–2447. DOI: 10.1021/es049300x.

Chow, T.M., M.R. Wilcoxon, M.D. Piwoni, and S.W. Maloney. 2009. Analysis of new generation explosives in the presence of U.S. EPA Method 8330 energetic compounds by high-performance liquid chromatography. Journal of Chromatographic Science, 47: 40-43. DOI: 10.1093/chromsci/47.1.40

DOD. 2021. Department of Defense (DoD) Department of Energy (DOE) Consolidated Quality Systems Manual (QSM) for Environmental Laboratories. Version 5.3. Washington, DC: DoD and DOE. Available at: https://denix.osd.mil/edqw/documents/manuals/qsm-version-5-4-final/ (Accessed 4 January 2023)

Fried, L.E. and P.C. Souers. 1994. CHEETAH: A Next Generation Thermochemical Code. Lawrence Livermore National Laboratory, Livermore, CA. DOI: 10.2172/95184 Available at: https://www.osti.gov/servlets/purl/95184 (Accessed 4 January 2023)

Furnish, M.D., S. Root, and P. Samuels. 2014. Equation-of-State and Shock Homogeneity of IMX-101 and IMX-104. SAND2014-15499C. Sandia National Laboratories, Albuquerque, NM. Available at: https://www.osti.gov/servlets/purl/1315117 (Accessed 4 January 2023)

Hewitt, A.D., T.F. Jenkins, T.A. Ranney, J.A. Stark, M.E. Walsh, S. Taylor, M.R. Walsh, D.J. Lambert, N.M. Perron, N.H. Collins, and R. Karn. 2003. Estimates for Explosives Residue from the Detonation of Army Munitions. ERDC/CRREL TR-03-16. US Army Engineer Research and Development Center, Cold Regions Research and Engineering Laboratory, Hanover, NH. Available at: https://apps.dtic.mil/sti/citations/ADA417513 (Accessed 4 January 2023)

Hewitt, A. D., T. F. Jenkins, M. E. Walsh, M. R. Walsh, and S. Taylor. 2005. RDX and TNT Residues from Live-Fire and Blow-in-Place Detonations. Chemosphere 61 (6): 888–894. DOI: 10.1016/j.chemosphere.2005.04.058.

Hewitt, A.D., T.F. Jenkins, M.E. Walsh, S.R. Bigl, and S. Brochu. 2009. Validation of Sampling Protocol and the Promulgation of Method Modifications for the Characterization of Energetic Residues on Military Testing and Training Ranges. ERDC/CRREL TR-09-6. US Army Engineer Research and Development Center, Cold Regions Research and Engineering Laboratory, Hanover, NH. Hanover, NH. Available at: https://apps.dtic.mil/sti/citations/ADA517341 (Accessed 24 January 2023)

Hunter, L.E., D.E. Lawson, S.R. Bigl, B.N. Astley, C.F. Snyder, and F.E. Perron. 2000. Geological Investigations and Hydrogeological Model of Fort Richardson, Alaska. ERDC/CRREL TR-00-18. US Army Engineer Research and Development Center, Cold Regions Research and Engineering Laboratory, Hanover, NH. Hanover, NH. Available at: https://apps.dtic.mil/sti/citations/ADA383061 (Accessed 4 January 2023)

Jenkins, T. F., M. E. Walsh, P. H. Miyares, A. D. Hewitt, N. H. Collins, and T. A. Ranney. 2002. Use of Snow-Covered Ranges to Estimate Explosives Residues from High-Order Detonations of Army Munitions. Thermochimica Acta 384 (1–2): 173–185. DOI: 10.1016/S0040-6031(01)00803-6

Le Campion, L., M.T. Adeline, and J. Ouazzani. 1997. Separation of NTO related 1,2,4-triazole-3-one derivatives by a high performance liquid chromatography and capillary electrophoresis. Propellants, Explosives, Pyrotechnics 22: 233-237. DOI: 10.1002/prep.19970220410

MA ARNG (2019) Joint Base Cape Cod Cleanup Update. Massachusetts Army National Guard. Available at: https://www.massnationalguard.org/JBCC/afcee-documents/jbcc_cleanup_update_092619.pdf (Accessed 29 December 2022)

Mitchell, W.J. and J.C. Suggs. 1998. Emission Factors for the Disposal of Energetic Materials by Open Burning and Open Detonation (OB/OD). EPA/600/R-98/103, US Environmental Protection Agency, Research Triangle Park, NC. Available at: https://www.epa.gov/sites/default/files/2015-02/documents/1998_emission_factors_for_the_disposal_of_energetic_materials_by_ob-od.pdf (Accessed 4 January 2023)

NOAA. 2023. Alaska Snow Data. National Weather Service, National Oceanic and Atmospheric Administration, US Dept of Commerce. Available at: https://www.weather.gov/aprfc/Snow_Depth (Accessed 24 January 2023)

Persico, F., T. Temple, M. Ladyman, W. Gilroy-Hirst, E. Guiterrez-Carazo, and F. Coulon. 2022. Quantitative Environmental Assessment of Explosive Residues from the Detonation of Insensitive High Explosive Filled 155 mm Artillery Shell. Propellants, Explosives, Pyrotechnics 47 (3): e202100220. DOI: 10.1002/prep.202100220

R Core Team (2022). R: A language and environment for statistical computing. R Foundation for Statistical Computing, Vienna, Austria. https://www.R-project.org/.

Taylor, S., A.D. Hewitt, J. Lever, C. Hayes, L. Perovich, P. Thorne, and C. Daghlian. 2004. TNT particle size distributions from detonated 155-mm howitzer rounds. Chemosphere 55: 357-367. DOI: 10.1016/j.chemosphere.2003.11.031.

Taylor, S., D.B. Ringelberg, K. Dontsova, C.P. Daghlian, M.E. Walsh, and M.R. Walsh. 2013. Insights into the Dissolution and the Three-Dimensional Structure of Insensitive Munitions Formulations. Chemosphere 93:1782-1788. DOI: 10.1016/j.chemosphere.2013.06.011

Taylor, S., K. M. Dontsova, M. E. Walsh, and M. R. Walsh. 2015. Outdoor Dissolution of Detonation Residues of Three Insensitive Munitions (IM) Formulations. Chemosphere 134: 250–256. DOI: 10.1016/j.chemosphere.2015.04.041

Taylor, S., M.E. Walsh, J.B. Becher, D.B. Ringelberg, P.Z. Mannes, and G.W. Gribble. 2017. Photo-degradation of 2,4-Dinitroanisole (DNAN): An Emerging Munitions Compound. Chemosphere 167: 193-203. DOI: 10.1016/j.chemosphere.2016.09.142

Walsh, M. E. 2016. Analytical Methods for Detonation Residues of Insensitive Munitions. Journal of Energetic Materials 34 (1): 76–91. DOI: 10.1080/07370652.2014.999173.

Walsh, M.R., M.E. Walsh, C.M. Collins, S.P. Saari, J.E., Zufelt, A.B., Gelvin, and J.W. Hug. 2005a. Energetic Residues from Live-Fire Detonations of 120-mm Mortar Rounds. ERDC/CRREL TR-05-15. US Army Engineer Research and Development Center, Cold Regions Research and Engineering Laboratory, Hanover, NH. Available at: https://apps.dtic.mil/sti/citations/ADA441147 (Accessed 4 January 2023)

Walsh, M.R., S. Taylor, M.E. Walsh, S.R. Bigl, K. Bjella, T.A. Douglas, A. Gelvin, D. Lambert, N. Perron, and S. Saari. 2005b. Residues from Live Fire Detonations of 155-mm Howitzer Rounds. ERDC/CRREL TR-05-14. US Army Engineer Research and Development Center, Cold Regions Research and Engineering Laboratory, Hanover, NH. Available at : https://apps.dtic.mil/sti/citations/ADA436330 (Accessed 4 January 2023)

Walsh, M.R., M.E. Walsh, C.A. Ramsey, R.J., Rachow, J.E. Zufelt, C.M. Collins, A.B. Gelvin, N.M. Perron, and S.P. Saari. 2006. Energetic Residues Deposition from 60-mm and 81-mm Mortars. ERDC/CRREL TR-06-10. US Army Engineer Research and Development Center, Cold Regions Research and Engineering Laboratory, Hanover, NH. Available at: https://apps.dtic.mil/sti/citations/ADA449108 (Accessed 4 January 2023)

Walsh, M. R., M. E. Walsh, and C. A. Ramsey. 2007. Measuring Energetics Residues on Snow. ERDC/CRREL TR-07-19. US Army Engineer Research and Development Center, Cold Regions Research and Engineering Laboratory, Hanover, NH. Available at: https://apps.dtic.mil/sti/citations/ADA472953 (Accessed 4 January 2023)

Walsh, M.R., C.M. Collins, and A.D. Hewitt. 2008. Energetic Residues from Blow-in-Place Detonation of 60-mm and 120-mm Fuzed High-Explosive Mortar Cartridges. ERDC/CRREL TR-08-19, US Army Engineer Research and Development Center, Cold Regions Research and Engineering Laboratory, Hanover, NH. Available at: https://apps.dtic.mil/sti/citations/ADA491353 (Accessed 4 January 2023)

Walsh, M. E., S. Taylor, A. D. Hewitt, M. R. Walsh, C. A. Ramsey, and C. M. Collins. 2010. Field Observations of the Persistence of Comp B Explosives Residues in a Salt Marsh Impact Area. Chemosphere 78: 467–473. DOI: 10.1016/j.chemosphere.2009.10.021

Walsh, M. R., M. E. Walsh, I. Poulin, S. Taylor, and T. A. Douglas. 2011a. Energetic Residues from the Detonation of Common US Ordnance. International Journal of Energetic Materials and Chemical Propulsion 10 (2): 169–186. DOI: 10.1615/IntJEnergeticMaterialsChemProp.2012004956.

Walsh, M. R., M. E. Walsh, and J. W. Hug. 2011b. A Simple Device for Initiating High Order Detonations. In Characterization and Fate of Gun and Rocket Propellant Residues on Testing and Training Ranges. Final Report, edited by M. R. Walsh, S. T., M. E. Walsh, G. Ampleman, R. Martel, I. Poulin, and S. Taylor. ERDC/CRREL TR-11-13. US Army Engineer Research and Development

Center, Cold Regions Research and Engineering Laboratory, Hanover, NH. https://apps.dtic.mil/sti/citations/ADA548745 (Accessed 4 January 2023)

Walsh, M.R., M.E. Walsh, and C.A. Ramsey. 2012. Measuring Energetic Contaminant Deposition Rates on Snow. Water Air Soil Pollution 223: 3689-3699. DOI: 10.1007/s11270-012-1141-5

Walsh, M. R., M. E. Walsh, C. A. Ramsey, S. Taylor, D. Ringelberg, J. Zufelt, S. Thiboutot, G. Ampleman, and E. Diaz. 2013a. Characterization of PAX-21 Insensitive Munition Detonation Residues. Propellants, Explosives, Pyrotechnics 38 (3): 399–409. DOI: 10.1002/prep.201200150.

Walsh, M.R., M.E. Walsh, C.A. Ramsey, S. Brochu, S. Thiboutot, and G. Ampleman. 2013b. Perchlorate contamination from the detonation of insensitive high explosive rounds. Journal of Hazardous Materials 262: 228-233. DOI: 10.1016/j.jhazmat.2013.08.045

Walsh, M.R., M.E. Walsh, and Ø.A. Voie. 2014a. Presence and Persistence of White Phosphorus on Military Training Ranges. Propellants, Explosives, Pyrotechnics 39: 922-931. DOI: 10.1002/prep.201400107

Walsh, M. R., M. E. Walsh, C. A. Ramsey, S. Thiboutot, G. Ampleman, E. Diaz, and J. E. Zufelt. 2014b. Energetic Residues from the Detonation of IMX-104 Insensitive Munitions. Propellants, Explosives, Pyrotechnics 39 (2): 243–250. DOI: 10.1002/prep.201300095.

Walsh, M.R., S, Thiboutot, and B. Gullet. 2017a. Characterization of residues from the detonation of insensitive munitions. Final Report, SERDP Project ER-2219. Available at: https://serdp-estcp.org/projects/details/155e3d44-16bc-4cf8-850e-f68a00300eb3 (Accessed 4 January 2023)

Walsh, M.R., T. Temple, M.F. Bigl, S.F. Tshabalala, N. Mai, and M. Ladyman. 2017b. Investigation of Energetic Particle Distribution from High-Order Detonations of Munitions. Propellants, Explosives, Pyrotechnics 42: 932-941. DOI: 10.1002/prep.201700089

Walsh, M. R., M. F. Bigl, M. E. Walsh, E. T. Wrobel, D. L. Zaloga, S. A. Beal, and T. Temple. 2018a. Physical Simulation of Live-Fire Detonations Using Command-Detonation Fuzing. Propellants Explosives Pyrotechnics 43 (6): 602–608. DOI: 10.1002/prep.201700316.

Walsh, M. R., B. Gullet, M. E. Walsh, M. F. Bigl, and J. Aurell. 2018b. Improving Post-Detonation Energetics Residues Estimations for the Life Cycle Environmental Assessment Process for Munitions. Chemosphere 194: 622–627. DOI: 10.1016%2Fj.chemosphere.2017.11.072.

Yehle, L.A. H.R. Schmoll and E. Dobrovolny. 1991. Geologic Map of the Anchorage B-8 SW Quadrangle, Alaska. USGS Open File Report 91-143, US Geological Survey, Denver, CO. Available at: https://pubs.usgs.gov/of/1991/0143/report.pdf (Accessed 4 January 2023)

APPENDICES

The data presented in these appendices detail the live-fire tests conducted as part of this ESTCP project only. Associated sample and QC data for command-detonation tests are presented in the SERDP project ER-2219 Final Report and references therein. For the live-fire tests, every attempt was made to match the methods (i.e., sampling, processing, analysis, and QA/QC) and acceptance criteria of prior command-detonation tests to eliminate operational variables.

APPENDIX A: POINTS OF CONTACT

POINT OF CONTACT Name	ORGANIZATION Name Address	Phone Fax E-mail	Role in Project
Samuel A. Beal	US Army ERDC-CRREL 72 Lyme Road Hanover, NH 03755	(603) 646-4125 samuel.a.beal@usace.army.mil	Principal Investigator
Matthew F. Bigl	US Army ERDC-CRREL 72 Lyme Road Hanover, NH 03755	(603) 646-4756 matthew.f.bigl@usace.army.mil	Co-Investigator

APPENDIX B: QUALITY ASSURANCE AND QUALITY CONTROL

B.1 CALIBRATION OF ANALYTICAL EQUIPMENT

Calibration of each analyte in each HPLC method followed EPA Method 8000D guidelines and DOD QSM 5.4 acceptance criteria. In brief, initial linear calibration curves forced through zero with equal weight were established from peak areas of 7 to 9 primary standard levels over the typical range of 0.05 to 10 mg/l. Regression coefficients (r^2) were greater than 0.9999. Initial calibration verification (ICV) using a secondary standard (separate lot # or separate manufacturer) was performed after initial calibration and after each sequence's continuing calibration verification (CCV), both typically in the concentration range of 0.5 to 2 mg/l. Acceptance criteria for the ICV and CCV, which was run every 10 samples, was ± 20 % of the true concentration.

B.2 QUALITY ASSURANCE SAMPLING

Background samples were collected prior to firing any munitions for the 60 mm munition and before, in between, and after all firing for the 81 mm munition. These samples were collected from approximately 40 m by 40 m areas (n = 3 for 60 mm munition; n = 4 for 81 mm munition) from the upper 2.5 cm of snow, in the same manner as plume samples, and serve to ensure the absence of pre-existing IMX-104 constituents on the testing surface. OTP samples collected from 0-3 m and 3-6 m outside the visible plume area from nearly each sampled plume assured the ITPs encompassed all deposited residues.

B.3 DECONTAMINATION PROCEDURES

Three two-person sampling teams collected all MIS samples. One team collected exclusively ITP samples, one team only OTP 3-6 m samples, and one team started each day with OTP 0-3 m samples before moving to collect ITP samples. This order of operation prevented cross contamination between plumes and between decision units. Footwear and lower pant shells were dry rinsed in clean snow at the end of each day. All sample containers were new and factory sealed. Sampling instruments were cleaned before and after each day of sampling with Micro-90 soap solution and MilliQ Type I water, and they were also cleaned between plumes with 50/50 methanol/water. Samplers wore nitrile gloves exchanged for fresh pairs between plumes.

B.4 SAMPLE DOCUMENTATION

Field samples were labeled following the example template in Table B1 using permanent marker on the outside of the bag and on a weatherproof sealable tag (Forestry Suppliers) affixed during bag closure with a cable tie. During processing, sample IDs were assigned to each field sample and these IDs were copied on associated processed sample storage glassware. All sample information was recorded in a field sampling notebook and electronic sample log by the PI, photographed, and then shipped by the co-PI. Receipt of samples at the organization's analytical laboratory and laboratory notetaking were performed by the project PI.

Table B1. Sample Tag Information.

Template	Example
Date: ____ Time: ____	1/22/21 1315
Munition Name	60-mm IMX-104
Plume # ____	Plume 2
Plume Type Replicate	ITP Rep 1 of 3
Scoop Size # Increments	10-cm 103 incs
Sampler Initials	SAB/MFB

APPENDIX C: QUALITY CONTROL DATA

C.1 METHOD BLANKS

Table C1. Filtration and SPE process blank concentrations in aqueous filtrate. All were below the method detection limits. NTO was not analyzed in SPE samples.

Field Test	QC Sample	Aqueous Concentration (mg/l)			
		HMX	RDX	DNAN	NTO
60 mm	Pre-Filter Blanks (*n* = 2)	<0.0001	<0.0001	<0.0001	<0.004
	Mid-Filter Blanks (*n* = 2)	<0.0001	<0.0001	<0.0001	<0.004
	Post-Filter Blanks (*n* = 2)	<0.0001	<0.0001	<0.0001	<0.004
	SPE Blanks (*n* = 3)	<0.0001	<0.0001	<0.0001	-
81 mm	Pre-Filter Blanks (*n* = 2)	<0.0001	<0.0001	<0.0001	<0.004
	Mid-Filter Blanks (*n* = 2)	<0.0001	<0.0001	<0.0001	<0.004
	Post-Filter Blanks (*n* = 2)	<0.0001	<0.0001	<0.0001	<0.004
	SPE Blanks (*n* = 4)	<0.0001	<0.0001	<0.0001	-

Table C2. Filtration process blank concentrations in filter extractions. All were below the method detection limits.

Field Test	QC Sample	Filter Extract (mg/l)			
		HMX	RDX	DNAN	NTO
60 mm	Pre-Filter Blanks (*n* = 2)	<0.01	<0.01	<0.01	<0.004
	Mid-Filter Blanks (*n* = 2)	<0.01	<0.01	<0.01	<0.004
	Post-Filter Blanks (*n* = 2)	<0.01	<0.01	<0.01	<0.004
81 mm	Pre-Filter Blanks (*n* = 2)	<0.01	<0.01	<0.01	<0.004
	Mid-Filter Blanks (*n* = 2)	<0.01	<0.01	<0.01	<0.004
	Post-Filter Blanks (*n* = 2)	<0.01	<0.01	<0.01	<0.004

C.2 BACKGROUND SAMPLES

Table C3. Background sample concentrations in aqueous filtrate and filter extractions. Analytes in all background samples were below detection except for RDX in 60 mm Backgrounds 1 and 2 and NTO in 81 mm Background 4. RDX in 60 mm Backgrounds 1 and 2 was attributed to prior training with Comp B munitions, as TNT was also detected in these samples. Trace NTO in 81 mm Background 4, which was collected after all study munitions were fired, was attributed to nearby impact Plumes 6–8.

Field Test	Background	Aqueous (mg/l)				Filter Extract (mg/l)			
		HMX	RDX	DNAN	NTO	HMX	RDX	DNAN	NTO
60 mm	1	<0.0001	0.0115	<0.0001	<0.004	<0.01	0.453	<0.01	<0.004
	2	<0.0001	0.0087	<0.0001	<0.004	<0.01	0.940	<0.01	<0.004
	3	<0.0001	<0.0001	<0.0001	<0.004	<0.01	<0.01	<0.01	<0.004
81 mm	1	<0.0001	<0.0001	<0.0001	<0.004	<0.01	<0.01	<0.01	<0.004
	2	<0.0001	<0.0001	<0.0001	<0.004	<0.01	<0.01	<0.01	<0.004
	3	<0.0001	<0.0001	<0.0001	<0.004	<0.01	<0.01	<0.01	<0.004
	4	<0.0001	<0.0001	<0.0001	0.004	<0.01	<0.01	<0.01	<0.004

Table C4. Estimated analyte masses in the entire background DUs and normalized to DU area. Non-detects are listed as estimated detection limits, which vary based on analytical detection limits, number of increments, DU area, and sample volume (i.e., snow density).

Field Test	Background	Area (m^2)	Mass in Background DU (mg)				Mass per Area (mg/m^2)			
			HMX	RDX	DNAN	NTO	HMX	RDX	DNAN	NTO
60 mm	1	1612	<1.4	136	<1.4	<43	<0.0009	0.0845	<0.0009	<0.03
	2	1635	<1.4	127	<1.4	<45	<0.0009	0.0777	<0.0009	<0.03
	3	1613	<1.4	<1.4	<1.4	<42	<0.0009	<0.0009	<0.0009	<0.03
81 mm	1	1544	<1.7	<1.7	<1.7	<57	<0.0011	<0.0011	<0.0011	<0.04
	2	1578	<1.8	<1.8	<1.8	<55	<0.0011	<0.0011	<0.0011	<0.03
	3	1674	<0.7	<0.7	<0.7	<14	<0.0004	<0.0004	<0.0004	<0.008
	4	1655	<0.8	<0.8	<0.8	18	<0.0005	<0.0005	<0.0005	0.011

C.3 LABORATORY CONTROL SAMPLES

Table C5. Laboratory control sample recoveries. HMX, RDX, and DNAN were spiked at 4 µg/l in Type I water prior to SPE, and NTO was spiked at 0.5 mg/l in Type I water prior to direct aqueous analysis.

Field Test	LCS #	Recovery (%)			
		HMX	RDX	DNAN	NTO
60 mm	1	110	96	99	95
	2	106	98	100	96
	3	97	101	96	94
81 mm	1	93	95	95	96
	2	99	100	100	96
	3	70	68	69	100
	4	98	95	96	99

C.4 PROCESS SAMPLE TRIPLICATES AND MATRIX SPIKES

Table C6. Precision for aqueous sample triplicates.

Field Test	Sample ID	Type	Mean Concentration (mg/l)				RSD (%)			
			HMX	RDX	DNAN	NTO	HMX	RDX	DNAN	NTO
60 mm	21FRA020	OTP 0-3 m	<0.0001	<0.0001	<0.0001	0.004	-	-	-	14
	21FRA040	ITP	0.0002	0.0020	0.0048	0.621	10	16	19	0.8
	21FRA058	ITP	0.0004	0.0039	0.0091	1.52	8	3	2	1.5
81 mm	22FRA018	ITP	0.0005	0.0112	0.0197	3.26	0.6	0.7	0.9	0.6
	22FRA040	OTP 0-3 m	<0.0001	0.0002	0.0008	0.090	-	7	4	0.2
	22FRA060	ITP	0.0004	0.0152	0.0141	7.89	4	3	2	0.8
	22FRA082	ITP	0.0004	0.0112	0.0085	5.47	3	2	5	0.6

Table C7. Recoveries and precision for aqueous sample matrix spike (MS) and matrix spike duplicates (MSD). HMX, RDX, and DNAN were spiked at 0.004 mg/l prior to SPE and NTO was spiked into a direct aqueous aliquot at 0.5 mg/l (most) or 5 mg/l (81 mm ITP samples).

Field Test	Sample ID	Recovery (%)				RPD (%)			
		HMX	RDX	DNAN	NTO	HMX	RDX	DNAN	NTO
60 mm	21FRA020 MS	104	101	98	98	0.49	0.03	1.4	0.43
	21FRA020 MSD	103	101	96	99	-	-	-	-
	21FRA040 MS	104	104	111	96	2.0	3.5	0.23	2.1
	21FRA040 MSD	102	98	111	91	-	-	-	-
	21FRA058 MS	96	95	98	93	0.29	2.4	1.5	2.9
	21FRA058 MSD	96	100	103	81	-	-	-	-
81 mm	22FRA018 MS	101	95	75	83	4	2	0	2
	22FRA018 MSD	96	86	76	87	-	-	-	-
	22FRA040 MS	101	102	110	98	4	6	12	2
	22FRA040 MSD	97	96	94	101	-	-	-	-
	22FRA060 MS	97	109	83	82	2	2	2	2
	22FRA060 MSD	99	98	92	87	-	-	-	-
	22FRA082 MS	111	154	135	80	11	14	8	5
	22FRA082 MSD	98	99	110	90	-	-	-	-

C.5 OUTSIDE-THE-PLUME SAMPLES

Table C8. Proportion of energetic masses found in OTPs relative to ITPs. OTP masses below detection limits are listed as zero.

Field Test	Plume	OTP 0-3 m				OTP 3-6 m			
		HMX	RDX	DNAN	NTO	HMX	RDX	DNAN	NTO
60 mm	1	1.6E-01	0	0	5.4E-03	0	3.0E-01	0	1.3E-05
	2	4.0E-01	2.8E-02	1.4E-02	5.6E-03	1.7E-01	5.0E-02	0	0
	3	8.6E-02	0	2.3E-03	7.6E-06	0	0	0	1.0E-05
	4	0	7.7E-03	0	1.3E-06	0	0	0	1.4E-06
	6	0	0	1.1E-02	4.6E-03	0	0	0	0
	7	0	0	0	1.1E-03	7.1E-02	1.4E-02	0	1.7E-05
	8	1.4E-01	1.1E-01	0	2.1E-03	1.4E-01	0	0	0
	9	0	2.2E-01	0	1.7E-03	8.3E-02	0	0	1.6E-03
81 mm	1	3.8E-02	6.9E-03	1.4E-02	9.7E-03	0	3.3E-03	3.5E-03	2.5E-03
	2	4.5E-02	1.5E-02	2.7E-03	5.3E-03	6.4E-02	0	1.6E-03	3.4E-03
	3	0	5.7E-03	1.3E-02	6.6E-03	1.8E-01	0	2.3E-03	1.9E-03
	4	0	2.3E-02	4.5E-02	2.4E-02	3.1E-01	0	1.4E-02	1.0E-02
	5	1.5E-01	6.7E-02	1.0E-01	2.9E-02	8.2E-02	0	7.5E-03	5.2E-03
	6	4.6E-03	6.5E-03	1.0E-02	6.8E-03	1.2E-01	0	2.3E-03	2.1E-03
	7	0	5.0E-03	1.0E-02	3.9E-03	1.5E-01	0	6.8E-03	2.5E-03
	8	0	0	9.1E-03	6.1E-03	2.4E-01	0	0	1.3E-03
	9	0	1.3E-02	2.1E-02	1.4E-02	1.2E-01	0	7.4E-03	5.3E-03
	10	0	0	1.4E-02	5.1E-03	1.2E-01	0	0	2.5E-03
	11	0	4.0E-03	1.0E-02	3.1E-03	6.3E-02	0	0	1.2E-03
	12	0	0	6.7E-03	1.7E-03	5.8E-02	0	2.8E-03	1.3E-03
	13	0	0	2.8E-02	7.7E-03	0	0	0	2.1E-03

APPENDIX D: FIELD SAMPLE DATA

Table D1. Sampling and processing data for the 2021 live-fire test of 60 mm IMX-104 cartridges.

ID	Type	Plume Area (m^2)	Increments (n)	Filtrate (mL)	SPE Factor	Filter Extract (mL)
21FRA001	Background 1	1611.5	104	6850	100	20.0
21FRA002	Background 2	1634.6	106	7340	100	20.0
21FRA003	Background 3	1613.3	100	6460	100	20.0
21FRA004	Plume 1 OTP 3–6 1/1	409.0	97	6390	100	20.0
21FRA005	Plume 2 OTP 3–6 1/1	401.2	102	7070	100	20.0
21FRA006	Plume 3 OTP 3–6 1/3	412.1	81	5630	100	20.0
21FRA007	Plume 3 OTP 3–6 2/3	412.1	97	6645	100	20.0
21FRA008	Plume 3 OTP 3–6 3/3	412.1	97	6945	100	20.0
21FRA009	Plume 4 OTP 3–6 1/3	349.9	115	7840	100	20.0
21FRA010	Plume 4 OTP 3–6 2/3	349.9	96	7160	100	20.0
21FRA011	Plume 4 OTP 3–6 3/3	349.9	105	7210	100	20.0
21FRA012	Plume 6 OTP 3–6 1/1	310.3	93	6460	100	20.0
21FRA013	Plume 7 OTP 3–6 1/3	356.0	102	6450	100	20.0
21FRA014	Plume 7 OTP 3–6 2/3	356.0	84	5521	100	20.0
21FRA015	Plume 7 OTP 3–6 3/3	356.0	91	6510	100	20.0
21FRA016	Plume 8 OTP 3–6 1/1	437.8	85	5680	100	20.0
21FRA017	Plume 9 OTP 1/1	442.4	102	6320	100	20.0
21FRA018	Plume 1 OTP 0–3 1/1	326.5	76	5480	100	20.0
21FRA019	Plume 2 OTP 0–3 1/1	362.6	97	7480	100	20.0
21FRA020	Plume 3 OTP 0–3 1/3	359.5	101	7810	100	20.0
21FRA021	Plume 3 OTP 0–3 2/3	359.5	83	6260	100	20.0
21FRA022	Plume 3 OTP 0–3 3/3	359.5	92	6640	100	20.0
21FRA023	Plume 4 OTP 0–3 1/3	334.0	94	7500	100	20.0
21FRA024	Plume 4 OTP 0–3 2/3	334.0	85	7260	100	20.0
21FRA025	Plume 4 OTP 0–3 3/3	334.0	93	8200	100	20.0
21FRA026	Plume 6 OTP 0–3 1/1	255.7	93	7175	100	20.0
21FRA027	Plume 7 OTP 0–3 1/3	291.8	98	7245	100	20.0
21FRA028	Plume 7 OTP 0–3 2/3	291.8	83	6720	100	20.0
21FRA029	Plume 7 OTP 0–3 3/3	291.8	88	7568	87.4	20.0
21FRA030	Plume 8 OTP 0–3 1/1	314.8	88	7550	100	20.0
21FRA031	Plume 9 OTP 0–3 1/1	371.8	81	6200	100	20.0
21FRA032	Plume 1 ITP Rep 1/3	631.5	82	5580	100	20.0
21FRA033	Plume 1 ITP Rep 2/3	631.5	90	6375	100	20.0
21FRA034	Plume 1 ITP Rep 3/3	631.5	90	6310	100	20.0
21FRA035	Plume 2 ITP Rep 1/3	613.2	86	6680	100	30.0
21FRA036	Plume 2 ITP Rep 2/3	613.2	89	6890	100	20.0
21FRA037	Plume 2 ITP Rep 3/3	613.2	86	6765	100	30.0
21FRA038	Plume 3 ITP Rep 1/3	571.0	80	5640	100	20.0
21FRA039	Plume 3 ITP Rep 2/3	571.0	114	8480	100	20.0
21FRA040	Plume 3 ITP Rep 3/3	571.0	77	6190	100	20.0
21FRA041	Plume 4 ITP Rep 1/3	547.3	84	6660	100	20.0
21FRA042	Plume 4 ITP Rep 2/3	547.3	88	7220	100	20.0
21FRA043	Plume 4 ITP Rep 3/3	547.3	86	7125	100	20.0
21FRA044	Plume 5 ITP Rep 1/3	322.0	88	6410	100	20.0
21FRA045	Plume 5 ITP Rep 2/3	322.0	86	6000	100	20.0
21FRA046	Plume 5 ITP Rep 3/3	322.0	81	5320	100	20.0
21FRA047A	Plume 6 ITP Rep 2/3 Bag 1/2	460.4	156	7340	100	20.0
21FRA047B	Plume 6 ITP Rep 2/3 Bag 2/2	NA	NA	4120	100	20.0

ID	Type	Plume Area (m^2)	Increments (n)	Filtrate (mL)	SPE Factor	Filter Extract (mL)
21FRA048	Plume 6 ITP Rep 1/3	460.4	84	5580	100	20.0
21FRA049	Plume 6 ITP Rep 3/3	460.4	110	7000	100	20.0
21FRA050	Plume 7 ITP Rep 1/3	613.9	105	8140	100	30.0
21FRA051	Plume 7 ITP Rep 2/3	613.9	95	7860	100	20.0
21FRA052	Plume 7 ITP Rep 3/3	613.9	91	7940	100	20.0
21FRA053	Plume 8 ITP Rep 1/3	786.6	78	6320	100	20.0
21FRA054	Plume 8 ITP Rep 2/3	786.6	99	8000	100	20.0
21FRA055	Plume 8 ITP Rep 3/3	786.6	87	7050	100	20.0
21FRA056	Plume 9 ITP Rep 1/3	771.8	102	6760	100	20.0
21FRA057	Plume 9 ITP Rep 3/3	771.8	82	5965	100	20.0
21FRA058	Plume 9 ITP Rep 2/3	771.8	120	8680	100	20.0

Table D2. Sampling and processing data for the 2022 live-fire test of 81 mm IMX-104 cartridges.

ID	Type	Plume Area (m^2)	Increments (n)	Filtrate (mL)	SPE Factor	Filter Extract (mL)
22FRA001	Background 1	1543.7	98	8958	100	20.0
22FRA002A	Background 2 Bag 1/2	1577.7	117	8000	100	30.0
22FRA002B	Background 2 Bag 2/2	NA	NA	2110	100	NA
22FRA003	Plume 1 OTP 3-6	344.9	99	1978	100	20.0
22FRA004	Plume 2 OTP 3-6	389.0	105	2010	100	20.0
22FRA005	Plume 2 OTP 3-6	389.0	95	1455	100	20.0
22FRA006	Plume 2 OTP 3-6	389.0	108	1935	100	20.0
22FRA007	Plume 1 OTP 0-3	287.8	104	2540	100	20.0
22FRA008	Plume 2 OTP 0-3	344.1	73	1265	100	20.0
22FRA009	Plume 2 OTP 0-3	344.1	73	1748	100	20.0
22FRA010	Plume 2 OTP 0-3	344.1	92	1505	100	20.0
22FRA013	Plume 1 ITP	540.5	121	5075	100	30.0
22FRA014	Plume 1 ITP	540.5	89	3280	100	30.0
22FRA015	Plume 1 ITP	540.5	94	2785	100	20.0
22FRA016	Plume 2 ITP	843.4	119	2410	100	30.0
22FRA017	Plume 2 ITP	843.4	140	5630	100	50.0
22FRA018	Plume 2 ITP	843.4	122	3270	100	50.0
22FRA019	Background 3	1674.0	97	1960	100	20.0
22FRA020	Background 4	1654.9	99	2590	100	20.0
22FRA021	Plume 3 OTP 3-6	273.2	80	2595	100	30.0
22FRA022	Plume 3 OTP 3-6	273.2	76	2230	100	20.0
22FRA023	Plume 3 OTP 3-6	273.2	79	2550	100	20.0
22FRA024	Plume 4 OTP 3-6	313.6	95	3475	100	20.0
22FRA025	Plume 5 OTP 3-6	300.9	96	3430	100	20.0
22FRA026	Plume 6 OTP 3-6	365.6	87	2330	100	20.0
22FRA027	Plume 6 OTP 3-6	365.6	73	2390	100	20.0
22FRA028	Plume 6 OTP 3-6	365.6	89	2890	100	20.0
22FRA029	Plume 7 OTP 3-6	390.8	75	2630	100	20.0
22FRA030	Plume 8 OTP 3-6	403.3	83	2810	100	20.0
22FRA031	Plume 9 OTP 3-6	346.2	87	3410	100	20.0
22FRA032	Plume 10 OTP 3-6	332.0	86	3010	100	20.0
22FRA033	Plume 10 OTP 3-6	332.0	87	2900	100	20.0
22FRA034	Plume 10 OTP 3-6	332.0	88	2855	100	30.0
22FRA035	Plume 11 OTP 3-6	342.0	88	3115	100	20.0
22FRA036	Plume 12 OTP 3-6	386.2	85	2600	100	30.0

ID	Type	Plume Area (m^2)	Increments (n)	Filtrate (mL)	SPE Factor	Filter Extract (mL)
22FRA037	Plume 13 OTP 3-6	333.4	85	2410	100	20.0
22FRA038	Plume 3 OTP 0-3	238.8	88	2390	100	20.0
22FRA039	Plume 3 OTP 0-3	238.8	87	2215	100	20.0
22FRA040	Plume 3 OTP 0-3	238.8	80	2810	100	20.0
22FRA041	Plume 4 OTP 0-3	273.4	89	2425	100	20.0
22FRA042	Plume 5 OTP 0-3	275.1	91	3215	100	20.0
22FRA043	Plume 6 OTP 0-3	322.5	94	2580	100	20.0
22FRA044	Plume 6 OTP 0-3	322.5	91	2420	100	20.0
22FRA045	Plume 6 OTP 0-3	322.5	97	2250	100	20.0
22FRA046	Plume 7 OTP 0-3	369.6	76	2210	100	20.0
22FRA047	Plume 8 OTP 0-3	395.3	90	2200	100	20.0
22FRA048	Plume 9 OTP 0-3	321.0	101	2850	100	20.0
22FRA049	Plume 10 OTP 0-3	293.5	80	2000	100	20.0
22FRA050	Plume 10 OTP 0-3	293.5	96	2730	100	30.0
22FRA051	Plume 10 OTP 0-3	293.5	79	2150	100	20.0
22FRA052	Plume 11 OTP 0-3	313.8	108	2960	100	20.0
22FRA053	Plume 12 OTP 0-3	379.9	95	2770	100	20.0
22FRA054	Plume 13 OTP 0-3	304.6	98	3185	100	20.0
22FRA058	Plume 3 ITP	323.7	87	3070	100	30.0
22FRA059	Plume 3 ITP	323.7	88	3225	100	30.0
22FRA060	Plume 3 ITP	323.7	102	3820	100	30.0
22FRA061	Plume 4 ITP	425.7	92	2665	100	30.0
22FRA062	Plume 4 ITP	425.7	81	2725	100	30.0
22FRA063	Plume 4 ITP	425.7	125	4520	100	30.0
22FRA064	Plume 5 ITP	451.3	113	3860	100	30.0
22FRA065	Plume 5 ITP	451.3	93	3140	100	30.0
22FRA066	Plume 5 ITP	451.3	106	3835	100	30.0
22FRA067	Plume 6 ITP	567.7	104	3700	100	30.0
22FRA068	Plume 6 ITP	567.7	99	3810	100	30.0
22FRA069	Plume 6 ITP	567.7	105	3990	100	30.0
22FRA070	Plume 7 ITP	711.4	130	5955	100	40.0
22FRA071	Plume 7 ITP	711.4	96	4165	100	30.0
22FRA072	Plume 7 ITP	711.4	93	4160	100	30.0
22FRA073	Plume 8 ITP	672.3	118	3600	100	30.0
22FRA074	Plume 8 ITP	672.3	95	3190	100	30.0
22FRA075	Plume 8 ITP	672.3	92	2780	100	30.0
22FRA076	Plume 9 ITP	616.6	150	6305	100	40.0
22FRA077	Plume 9 ITP	616.6	96	3650	100	30.0
22FRA078	Plume 9 ITP	616.6	117	5210	100	30.0
22FRA079	Plume 10 ITP	444.7	90	3520	100	30.0
22FRA080	Plume 10 ITP	444.7	91	3170	100	40.0
22FRA081	Plume 10 ITP	444.7	90	3085	100	30.0
22FRA082	Plume 11 ITP	492.1	142	5010	100	40.0
22FRA083	Plume 11 ITP	492.1	90	3080	100	20.0
22FRA084	Plume 11 ITP	492.1	99	3810	100	30.0
22FRA085	Plume 12 ITP	553.4	145	4535	100	30.0
22FRA086	Plume 12 ITP	553.4	95	3230	100	30.0
22FRA087	Plume 12 ITP	553.4	96	3225	100	30.0
22FRA088	Plume 13 ITP	525.6	110	3905	100	30.0
22FRA089	Plume 13 ITP	525.6	101	3245	100	30.0
22FRA090	Plume 13 ITP	525.6	103	3045	100	20.0

Table D3. Analytical data for processed-aqueous SPE, direct aqueous, and filter extraction sample fractions from the 2021 live-fire test of 60 mm IMX-104 cartridges.

ID	SPE (mg/L)			Aqueous (mg/L)	Filter Extract (mg/L)			
	HMX	RDX	DNAN	NTO	HMX	RDX	DNAN	NTO
21FRA001	<0.01	1.15	<0.01	<0.004	<0.01	0.453	<0.01	<0.004
21FRA002	<0.01	0.867	<0.01	<0.004	<0.01	0.940	<0.01	<0.004
21FRA003	<0.01	<0.01	<0.01	<0.004	<0.01	<0.01	<0.01	<0.004
21FRA004	<0.01	0.124	<0.01	<0.004	<0.01	0.042	<0.01	0.006
21FRA005	0.013	0.025	<0.01	<0.004	<0.01	<0.01	<0.01	<0.004
21FRA006	<0.01	<0.01	<0.01	<0.004	<0.01	<0.01	<0.01	<0.004
21FRA007	<0.01	<0.01	<0.01	<0.004	<0.01	<0.01	<0.01	0.005
21FRA008	<0.01	0.01	<0.01	<0.004	<0.01	<0.01	<0.01	<0.004
21FRA009	<0.01	<0.01	<0.01	<0.004	<0.01	<0.01	<0.01	<0.004
21FRA010	<0.01	<0.01	<0.01	<0.004	<0.01	<0.01	<0.01	<0.004
21FRA011	<0.01	<0.01	<0.01	<0.004	<0.01	<0.01	<0.01	<0.004
21FRA012	<0.01	<0.01	<0.01	<0.004	<0.01	<0.01	<0.01	<0.004
21FRA013	<0.01	0.012	<0.01	<0.004	<0.01	<0.01	<0.01	0.008
21FRA014	<0.01	<0.01	<0.01	<0.004	<0.01	<0.01	<0.01	0.008
21FRA015	<0.01	<0.01	<0.01	<0.004	0.035	<0.01	<0.01	0.008
21FRA016	<0.01	<0.01	<0.01	<0.004	0.028	<0.01	<0.01	<0.004
21FRA017	<0.01	<0.01	<0.01	0.006	0.034	<0.01	<0.01	<0.004
21FRA018	<0.01	<0.01	<0.01	0.008	0.030	<0.01	<0.01	0.008
21FRA019	<0.01	0.014	0.023	0.010	0.112	<0.01	<0.01	0.004
21FRA020	<0.01	<0.01	<0.01	<0.004	0.031	<0.01	<0.01	0.008
21FRA021	<0.01	<0.01	0.011	<0.004	0.028	<0.01	<0.01	<0.004
21FRA022	<0.01	<0.01	<0.01	<0.004	<0.01	<0.01	<0.01	<0.004
21FRA023	<0.01	<0.01	<0.01	<0.004	<0.01	<0.01	<0.01	<0.004
21FRA024	<0.01	<0.01	<0.01	<0.004	<0.01	<0.01	<0.01	<0.004
21FRA025	<0.01	0.015	<0.01	<0.004	<0.01	<0.01	<0.01	<0.004
21FRA026	<0.01	<0.01	0.019	0.006	<0.01	<0.01	<0.01	0.004
21FRA027	<0.01	<0.01	<0.01	<0.004	<0.01	<0.01	<0.01	0.007
21FRA028	<0.01	<0.01	<0.01	<0.004	<0.01	<0.01	<0.01	0.004
21FRA029	<0.01	<0.01	<0.01	0.005	<0.01	<0.01	<0.01	0.007
21FRA030	0.011	0.056	<0.01	0.004	<0.01	<0.01	<0.01	<0.004
21FRA031	<0.01	0.165	<0.01	0.006	<0.01	<0.01	<0.01	<0.004
21FRA032	0.012	0.202	0.461	0.787	0.065	0.123	0.718	13.542
21FRA033	0.018	0.249	0.587	0.765	0.068	0.136	0.783	9.500
21FRA034	0.016	0.251	0.574	0.837	0.067	0.151	0.710	8.378
21FRA035	0.028	0.271	0.691	1.012	0.032	0.033	0.536	6.784
21FRA036	0.029	0.281	0.676	1.084	0.068	0.062	1.005	9.563
21FRA037	0.026	0.270	0.658	1.053	0.032	0.049	0.584	9.268
21FRA038	0.028	0.363	0.943	1.005	0.070	0.134	1.205	9.265
21FRA039	0.024	0.257	0.677	0.738	0.052	0.086	1.021	8.145
21FRA040	0.022	0.216	0.539	0.620	0.048	0.048	0.658	7.017
21FRA041	0.041	0.557	0.997	1.046	0.079	0.125	1.089	8.59
21FRA042	0.024	0.263	0.556	0.691	0.041	0.029	0.615	2.238
21FRA043	0.032	0.403	0.836	0.951	0.057	0.050	1.229	9.772
21FRA044	0.034	0.486	0.835	1.869	0.089	0.063	1.721	26.79
21FRA045	0.025	0.287	0.631	1.589	0.050	0.025	0.973	23.265
21FRA046	0.045	0.674	1.000	1.665	0.105	0.072	1.784	27.205
21FRA047A	0.016	0.192	0.529	0.623	0.051	0.030	0.888	6.284
21FRA047B	0.043	0.472	1.093	1.010	0.072	0.048	1.257	6.577
21FRA048	0.029	0.268	0.724	0.778	0.034	0.006	0.468	1.925

21FRA049	0.033	0.324	0.888	0.808	0.060	0.060	1.123	8.309
21FRA050	0.014	0.156	0.254	0.858	0.045	0.029	0.478	15.267
21FRA051	0.013	0.139	0.254	0.692	0.035	0.053	0.694	20.45
21FRA052	0.012	0.085	0.196	0.564	0.053	0.024	0.247	3.534
21FRA053	0.041	0.383	1.034	1.361	0.080	0.058	1.238	17.908
21FRA054	0.034	0.334	1.008	1.010	0.065	0.055	1.110	0.274
21FRA055	0.033	0.273	0.710	1.544	0.081	0.066	1.347	9.496
21FRA056	0.047	0.416	0.858	2.036	0.110	0.070	1.544	11.102
21FRA057	0.035	0.315	0.745	1.775	0.071	0.038	0.946	15.370
21FRA058	0.037	0.384	0.907	1.541	0.088	0.039	1.269	8.359

Table D4. Analytical data for processed-aqueous SPE, direct aqueous, and filter extraction sample fractions from the 2022 live-fire test of 81 mm IMX-104 cartridges.

ID	SPE (mg/l)			Aqueous (mg/l)	Filter Extract (mg/l)			
	HMX	RDX	DNAN	NTO	HMX	RDX	DNAN	NTO
22FRA001	<0.01	<0.01	<0.01	<0.004	<0.01	<0.01	<0.01	<0.004
22FRA002A	<0.01	<0.01	<0.01	<0.004	<0.01	<0.01	<0.01	<0.004
22FRA002B	<0.01	<0.01	<0.01	<0.004	NA	NA	NA	NA
22FRA003	<0.01	0.038	0.122	0.039	<0.01	<0.01	<0.01	0.054
22FRA004	0.023	<0.01	0.020	0.038	<0.01	<0.01	<0.01	0.073
22FRA005	0.025	<0.01	0.021	0.051	<0.01	<0.01	<0.01	0.075
22FRA006	0.021	<0.01	0.023	0.034	<0.01	<0.01	<0.01	0.031
22FRA007	0.034	0.078	0.449	0.150	<0.01	<0.01	0.048	0.457
22FRA008	0.022	<0.01	0.037	0.066	<0.01	<0.01	<0.01	0.108
22FRA009	0.024	<0.01	0.041	0.056	<0.01	0.154	<0.01	0.122
22FRA010	<0.01	<0.01	0.033	0.076	<0.01	<0.01	<0.01	0.167
22FRA013	0.140	3.676	6.476	5.538	0.295	0.411	8.339	23.773
22FRA014	0.140	3.656	6.617	5.518	0.207	0.265	6.754	22.112
22FRA015	0.163	4.276	7.761	5.675	0.264	0.294	6.755	13.563
22FRA016	0.052	1.354	1.677	3.500	0.063	0.068	2.155	22.439
22FRA017	0.048	1.226	2.136	3.059	0.039	0.051	1.111	4.861
22FRA018	0.055	1.119	1.970	3.262	0.033	0.021	1.379	13.285
22FRA019	<0.01	<0.01	<0.01	<0.004	<0.01	<0.01	<0.01	<0.004
22FRA020	<0.01	<0.01	<0.01	0.004	<0.01	<0.01	<0.01	<0.004
22FRA021	0.034	<0.01	0.023	0.025	<0.01	<0.01	<0.01	0.020
22FRA022	0.037	<0.01	<0.01	0.021	<0.01	<0.01	<0.01	0.053
22FRA023	0.030	<0.01	0.015	0.017	<0.01	<0.01	<0.01	0.054
22FRA024	0.034	<0.01	0.033	0.040	<0.01	<0.01	0.008	0.200
22FRA025	0.024	<0.01	0.061	0.022	<0.01	<0.01	0.016	0.059
22FRA026	0.022	<0.01	0.024	0.017	<0.01	<0.01	<0.01	0.014
22FRA027	0.042	<0.01	0.013	0.016	<0.01	<0.01	<0.01	0.009
22FRA028	0.027	<0.01	0.013	0.011	<0.01	<0.01	<0.01	0.005
22FRA029	0.021	<0.01	0.021	0.022	<0.01	<0.01	<0.01	0.034
22FRA030	0.013	<0.01	<0.01	0.005	<0.01	<0.01	<0.01	<0.004
22FRA031	0.015	<0.01	0.022	0.026	<0.01	<0.01	<0.01	0.019
22FRA032	0.016	<0.01	<0.01	0.006	<0.01	<0.01	<0.01	<0.004
22FRA033	0.013	<0.01	<0.01	0.006	<0.01	<0.01	<0.01	<0.004
22FRA034	<0.01	<0.01	<0.01	0.028	<0.01	<0.01	<0.01	0.010
22FRA035	0.010	<0.01	<0.01	0.009	<0.01	<0.01	<0.01	0.007
22FRA036	0.013	<0.01	0.014	0.009	<0.01	<0.01	<0.01	<0.004
22FRA037	<0.01	<0.01	<0.01	0.023	<0.01	<0.01	<0.01	0.008
22FRA038	<0.01	0.020	0.086	0.096	<0.01	<0.01	<0.01	0.085

22FRA039	<0.01	0.017	0.100	0.096	<0.01	<0.01	0.011	0.133
22FRA040	<0.01	0.017	0.084	0.091	<0.01	<0.01	<0.01	0.038
22FRA041	<0.01	0.029	0.139	0.138	<0.01	<0.01	0.057	1.150
22FRA042	0.022	0.141	0.963	0.132	0.044	0.028	0.130	0.257
22FRA043	<0.01	0.038	0.136	0.082	<0.01	<0.01	0.011	0.015
22FRA044	<0.01	0.021	0.085	0.057	<0.01	<0.01	<0.01	0.023
22FRA045	<0.01	0.012	0.055	0.044	<0.01	<0.01	<0.01	0.034
22FRA046	<0.01	0.011	0.035	0.044	<0.01	<0.01	<0.01	0.010
22FRA047	<0.01	<0.01	0.016	0.033	<0.01	<0.01	<0.01	0.007
22FRA048	<0.01	0.024	0.092	0.104	<0.01	<0.01	0.025	0.044
22FRA049	<0.01	<0.01	0.029	0.045	<0.01	<0.01	<0.01	0.031
22FRA050	<0.01	<0.01	0.020	0.042	<0.01	<0.01	<0.01	0.012
22FRA051	<0.01	<0.01	0.029	0.025	<0.01	<0.01	<0.01	0.022
22FRA052	<0.01	0.012	0.050	0.035	<0.01	<0.01	0.010	0.008
22FRA053	<0.01	<0.01	0.030	0.012	<0.01	<0.01	<0.01	0.020
22FRA054	<0.01	<0.01	0.042	0.079	<0.01	<0.01	0.036	0.025
22FRA058	0.054	1.915	1.869	8.813	0.140	0.211	3.162	43.029
22FRA059	0.042	1.511	1.550	7.558	0.091	0.208	2.612	34.593
22FRA060	0.037	1.524	1.411	7.961	0.111	0.257	2.472	32.478
22FRA061	0.037	0.702	0.873	3.560	0.061	0.113	1.836	22.454
22FRA062	0.030	0.575	0.849	2.960	0.062	0.082	1.375	18.811
22FRA063	0.019	0.509	0.506	2.923	0.080	0.131	1.507	22.173
22FRA064	0.089	1.580	3.475	3.185	0.182	0.220	4.829	21.422
22FRA065	0.049	1.102	2.496	2.462	0.157	0.249	4.337	26.255
22FRA066	0.041	1.126	2.126	2.514	0.170	0.281	4.414	14.339
22FRA067	0.045	1.281	1.296	3.440	0.122	0.189	2.663	9.763
22FRA068	0.041	1.368	1.232	3.756	0.136	0.286	3.527	14.250
22FRA069	0.036	1.186	1.285	3.286	0.125	0.230	3.122	17.266
22FRA070	0.025	0.711	0.489	3.672	0.055	0.116	1.544	7.221
22FRA071	0.019	0.682	0.424	3.843	0.061	0.136	1.462	3.368
22FRA072	0.016	0.518	0.237	3.877	0.044	0.104	1.064	6.067
22FRA073	0.021	0.348	0.361	2.749	0.026	0.057	0.731	4.243
22FRA074	0.015	0.256	0.161	2.486	0.020	0.038	0.595	4.035
22FRA075	0.013	0.230	0.188	2.005	0.017	0.038	0.532	7.301
22FRA076	0.020	0.508	0.559	2.438	0.062	0.195	1.932	5.379
22FRA077	0.029	0.656	0.649	2.643	0.057	0.113	1.764	5.925
22FRA078	0.019	0.499	0.494	2.515	0.078	0.165	1.976	8.006
22FRA079	0.019	0.370	0.170	3.164	0.034	0.075	0.697	6.062
22FRA080	0.023	0.375	0.233	3.296	0.023	0.040	0.576	6.939
22FRA081	0.028	0.490	0.234	4.302	0.042	0.098	0.756	10.330
22FRA082	0.041	1.118	0.848	5.474	0.069	0.143	1.803	13.384
22FRA083	0.039	1.347	0.938	4.857	0.138	0.202	2.397	7.070
22FRA084	0.033	1.170	0.913	5.447	0.101	0.333	2.877	15.152
22FRA085	0.039	1.118	1.237	4.279	0.131	0.267	2.496	15.114
22FRA086	0.047	1.076	1.210	4.322	0.137	0.158	2.363	9.853
22FRA087	0.039	1.094	1.082	3.627	0.083	0.159	2.587	3.613
22FRA088	0.034	0.849	0.479	6.389	0.051	0.106	1.130	5.146
22FRA089	0.026	0.597	0.355	4.783	0.051	0.109	1.100	5.650
22FRA090	0.036	0.820	0.504	6.617	0.049	0.109	1.143	6.078

APPENDIX E: DETAILED RESIDUE TESTING METHODOLOGY

E.1 COMMAND-DETONATION SETUP

This technology demonstration/validation highlights the importance of representative fuze simulation in accurately reproducing residue loading rates from live-fire high-order detonations. Critically, external initiation using demolition blocks or shaped charges does not represent residue production as it occurs from initiation through the fuze well (Walsh et al. 2014). An ideal fuze simulator has matching initiation, lead, and booster charges to the study munition's fuze. While M6 and M7 military blasting caps have been used previously, a commercial exploding bridge-wire detonator that matches the fuze's safe and arming device would be ideal.

Irrespective of initiation method, munition setup typically involves placing the study round nose-up on a steel plate the center of the test area. This orientation simplifies fuze simulator initiation rigging, however placement in a nose-down orientation using a minimal support just above the steel plate may offer more representative results. Vertical placement produces relatively even dispersion in all radial directions, whereas placement of the munition on its side tends to produce greater cratering and dispersion in two primary directions (Figure E1). Of note, previous tests have included both full cartridges with attached tailfins (and included base propellant charge) and just mortar bodies without tailfins. Ideal setup would include the tailfin with base propellant charge removed to best represent live fire, however the effect of potential residue afterburning from the propellant charge and the effect of additional heigh above surface (when tailfin included and orientated nose-up) have not been studied.

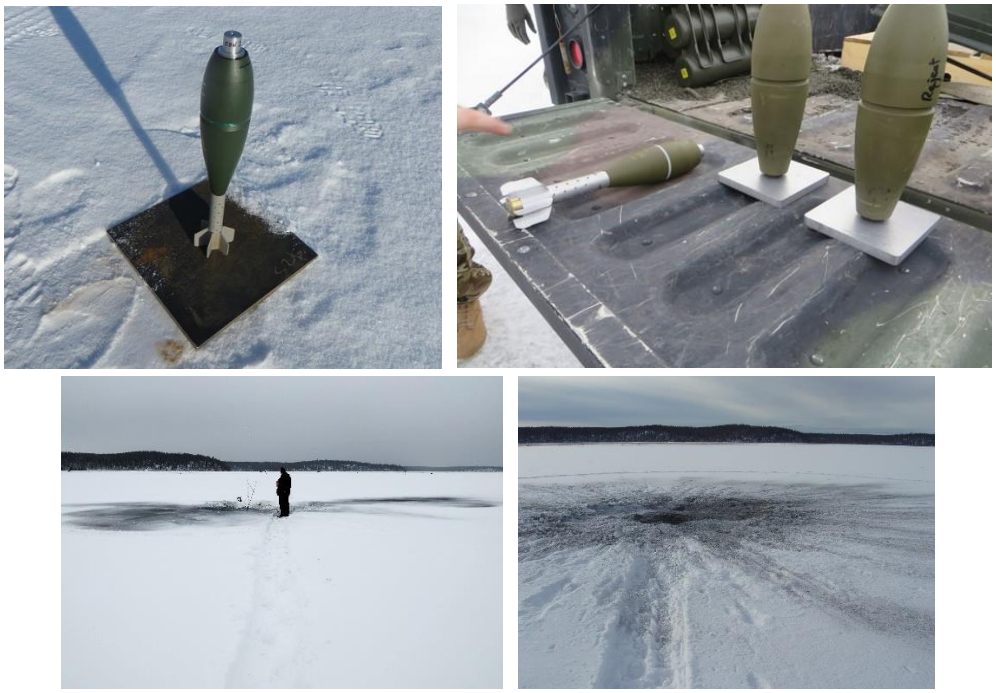

Figure E1. Clockwise from top left: an 81 mm cartridge with tailfin nose-up with CFS on a steel plate; a 60 mm mortar cartridge with tailfin and two 81 mm mortar round bodies mounted on aluminum support plates; symmetric dispersion of residue and soot from an 81 mm mortar cartridge with CFS in vertical position; and asymmetric dispersion of residue and soot from a horizontally placed 155 mm practice round with AFS.

Tests of individually resolved plumes from seven rounds have been the standard in providing an estimate and associated uncertainty for a study munition. The separation distance required between adjacent plumes varies based on explosive weight and wind conditions. For reference, average ITP areas were 250 m^2 and 770 m^2 for previous command-detonation tests of the 60 mm and 81 mm IMX-104 mortar cartridges using the AFS (Walsh et al. 2018), and the average ITP for 155 mm Comp B howitzer projectiles was 940 m^2 from live fire (Walsh et al. 2005 (tr-05-14)). In space-constrained testing locations, multiple rounds of the study munition can be fired with overlapping plumes. While the data from such tests represent the average loading residue loading rate, they cannot provide an estimate of inter-round variability and are also susceptible to failure if as few as one study round does not function high-order.

These command detonation setups are applicable to studying loading rates on any type of surface. However, the following sections address solely the sampling and processing of residues deposited on snow. This sampling medium provides the greatest sensitivity in residue estimates, but the methods may be adapted toward sampling on other surfaces such as soil and sand with higher detection limits.

E.2 RESIDUE SAMPLING

Demarcation of the DUs surrounding each detonation is first made for the ITP by subjectively walking the perimeter of the visibly discolored snow, often including a reasonable buffer to include disturbed snow from frag and create a shape that is amenable to easy sampling lane designation. For IMX munitions, an overly large ITP DU is usually not an issue given the relatively high loading rates from these munitions, however conventional munitions may require a tighter ITP to increase sensitivity. The OTP DUs can be marked using a tape measure and field workers walking parallel to the ITP edge.

Multi increment sampling of the ITP and OTP DUs differ in sampling directions (Figure E2). Sampling of the ITP starts at one edge of the plume and progresses in parallel lanes across the DU. Given a target of 100 increments per MI sample, spacing between increments should be initially estimated based on DU size. For most ITPs in the live-fire study, this spacing was 2 to 3 paces. Sampling lanes in the ITP are maintained using flagging along the ITP edge, moved after each sampling lane pass based on spacing. For OTPs, sampling lanes for the ring-shape DUs are continuous and sinusoidal, alternating between the inner and outer edges of the DU (Figure E2) for a complete circuit of the DU. If an insufficient number of increments are collected at the end of the full circuit, then a second circuit may be included in the same sample also with the option of changing the spacing for the second circuit. Replicate MI samples are collected from ITPs by collected the second replicate in sampling lanes perpendicular to the first replicate, and the third replicate collected at a 45-degree angle to first and second replicate sampling lanes. Replicate MI samples are collected from the OTP DUs using a sampling lane that is out of the phase to the other replicates.

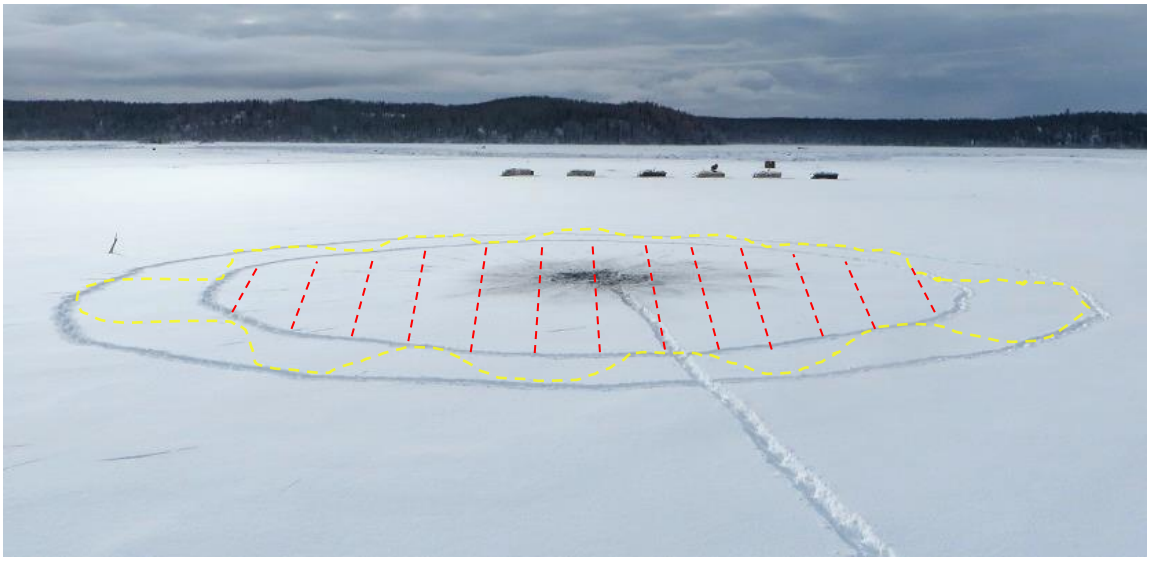

Figure E2. Conceptual first replicate sampling lanes for a plume ITP (red) and OTP (yellow).

Two-person sampling teams make collection of MI samples faster and more reliable. One person is responsible for scooping and maintaining sample lanes, and the second person carries the sampling bag and tracks number of sample increments (Figure E3). The second person also provides an independent check on maintenance of sampling lanes.

Figure E3. Two-person sampling team ITP sampling process on ERF.

The tools used for snow sampling are unique in having partial square sides (Figure E4). Tools with a 10 cm by 10 cm sampling surface and 2.5 cm depth have been used most often. The tool sampling surface area and number of increments are critical to calculating loading rates, and dimensionally consistent increment removal is required for precise residue estimates. In soft snow, increments can be collected easily in a single motion scoop. However, in hard snow (as was commonly encountered in the live-fire tests), initial outlining of a 10 cm by 10 cm area using the square sides of the scoop is sometimes required.

Figure E4. Left: outline chisel sampling on hard snow; right: one-motion scoop sampling on soft snow (note: larger 20-cm scoop pictured).

For sample tracking and documentation, each full MI sample is labelled with permanent marker on the bag surface and on the weatherproof yellow tag that is fastened with a cable tie to close the bag (Figure E5).

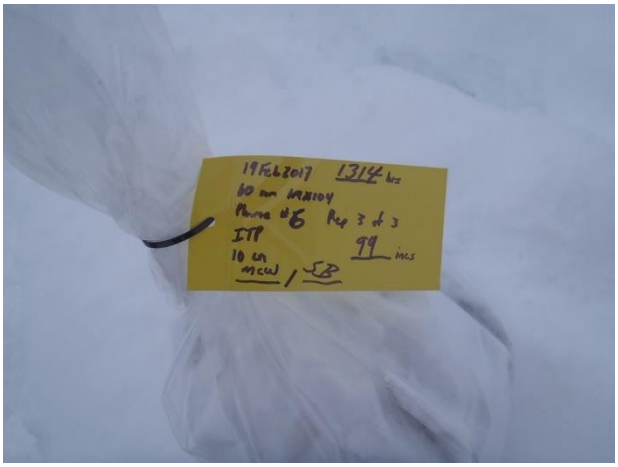

Figure E5. Labeled snow sample bag.

E.3 SAMPLE PROCESSING

Samples are melted in batches, enough to process during the following day, by letting melt overnight at room temperature. Placement of double-bagged samples in clean bins (Figure E6) allows samples to be recovered in case of the occasional bag puncture. For tracking, a sample ID is assigned on the reverse side of each sample tag and kept with the sample throughout processing. Pertinent processing data including filtrate volume, number of filters used, and processor's initials are also noted on the tag.

Figure E6. Sample melting in bins.

The melted samples, ideally still cold, are filtered through the glass filter vacuum apparatus (Figure E7). The sample is slowly poured into the top of the filtration apparatus fitted with a new glass fiber filter (Whatman GF/A) until the collection flask is full. When full, the contents are transferred to the 2000 ml mark on a clean volumetric cylinder then transferred to a clean 9 L glass jug. Additional sample is filtered in the same manner and combined in the 9 L jug until all sample has been filtered. Material adhered to the sides of the bag is rinsed to the bottom of the bag with Type I water and concentrated into V-shape in a bottom corner of the bag. This corner is cut off with clean scissors and then, with additional Type I water from a squirt bottle, rinsed into the filtration apparatus. Slow filtering caused by excess solids can be addressed during processing through replacement with a new filter.

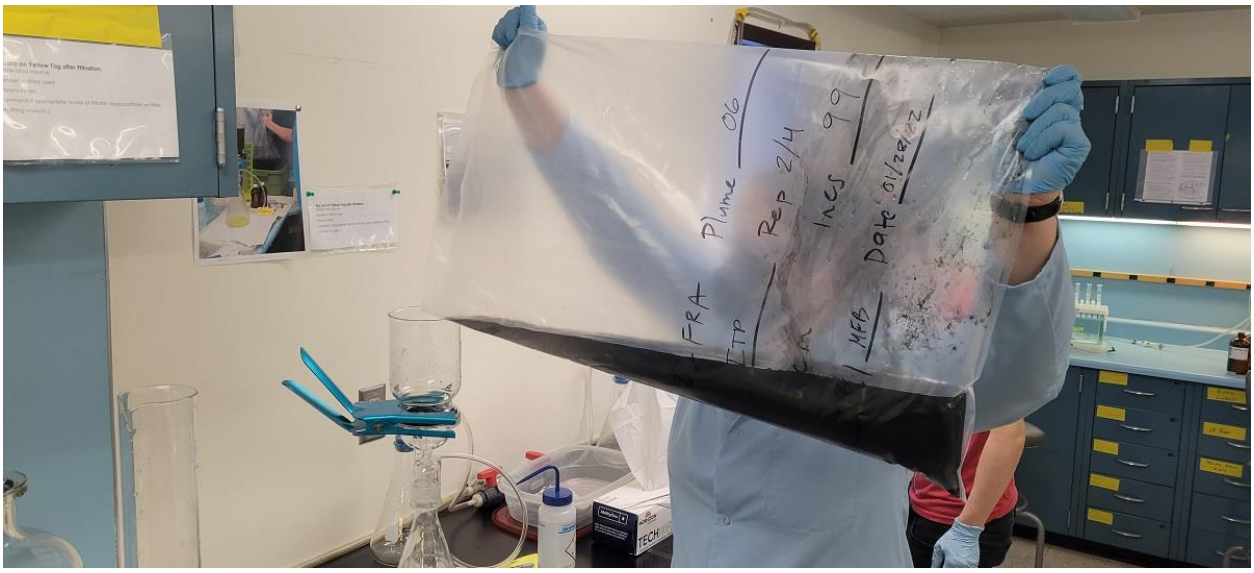

Figure E7. Sample filtration.

Once all filtrate is aggregated and total volume recorded, the aggregated filtrate is shaken to mix in the 9 L jug and then poured through a clean glass funnel into three bottles: one 500 ml glass

bottle for SPE; one 500 ml glass bottle for archive; and one 40 ml glass vial for direct analysis. Sample filters with adhered soot, frag, and other solids are folded in quarters and then combined in glass jars (Figure E8). Both solid and aqueous samples are kept refrigerated.

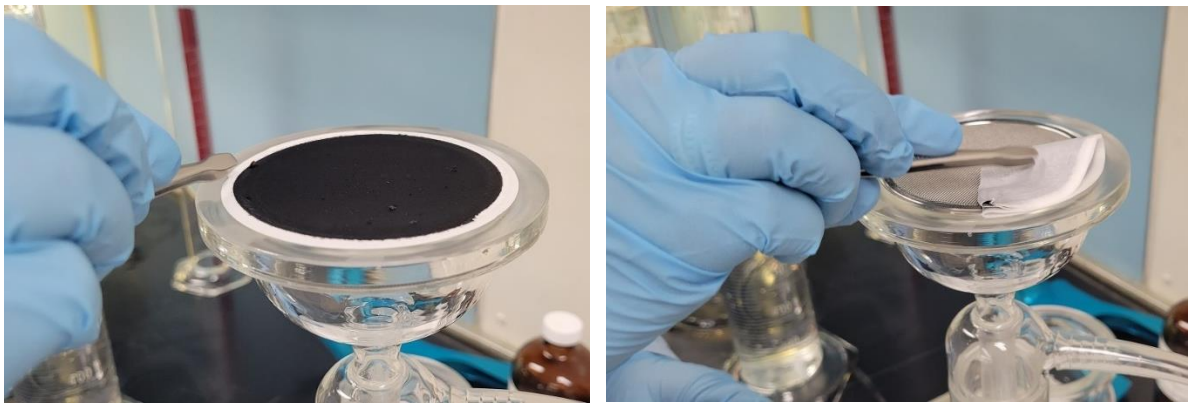

Figure E8. Glass fiber filter after sample filtration (left) and folding with clean tweezers to store in glass jar (right).

Solid-phase extraction is effective at concentrating the nonpolar energetics (i.e., HMX, RDX, TNT, and DNAN) but does not work particularly well for NTO and NQ (M.E. Walsh, 2016). However, NTO and NQ have strong UV absorption and are generally present at relatively high concentrations in residues allowing for sensitive direct aqueous analysis.

For the nonpolar compounds, SPE is performed on a vacuum manifold using large sample adapters. The SPE cartridges (Waters Sep-Pak Vac RDX 6 cc 500 mg) are first pre-conditioned with 15 ml acetonitrile (HPLC grade) under atmospheric pressure, keeping ~5 mm of acetonitrile above the SPE bed, and then washed with ~30 ml Type I water under vacuum at a slow drip rate (~8 ml/min), keeping the cartridge full of water prior to loading. Clean large sample adapters are then attached between the 500 ml aqueous sample bottles and SPE cartridges (Figure E9). Sample loading occurs under vacuum at a drip rate of ~8 ml/min so that samples are fully processed in ~1 hour. Once all of the sample has loaded, the adapters are removed, and the cartridges dried under vacuum for 45 minutes.

Figure E9. Solid-phase extraction of 500 ml aqueous samples. Left block has cartridges drying and right block has samples loading.

Elution of SPE cartridges is performed by adding 5.0 ml of acetonitrile to each cartridge at atmospheric (or slightly positive pressure, if stubborn, using a syringe), into clean graduated cylinders (Figure E10). Less than 5 ml of eluate is recovered, so each sample is brought to 5.00 ml using acetonitrile from a Pasteur pipet, such that this process concentrates compatible analytes 100 fold. SPE samples are stored in amber glass vials (7 ml), with a ~1 ml aliquot kept separately in a glass autosampler vial for archive. SPE samples are stored frozen (-18° C).

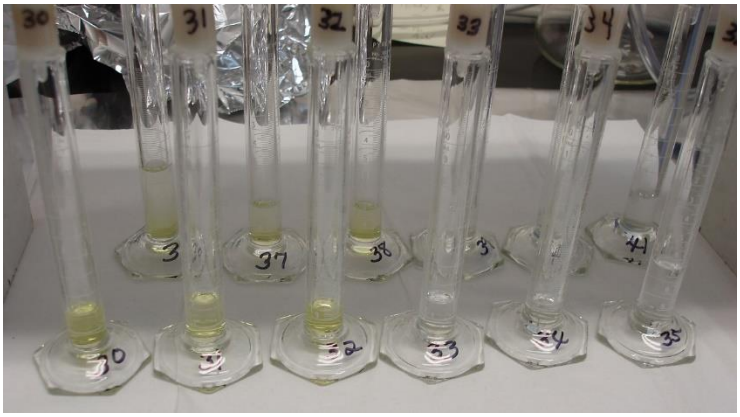

Figure E10. Collection of unusually colorful SPE eluate in 10 ml graduated cylinders.

All glassware (i.e., filtration apparatus, funnel, graduated cylinders) and stainless-steel components (i.e., tweezers, scissors, filter support) that comes in contact with samples is cleaned between use with a multipurpose cleaning solution (Micro-90) in tap water, with final rinsing using Type I water. The interior and exterior of SPE sample adapters are cleaned with methanol and then Type I water.

Laboratory control and matrix spike samples are prepared prior to SPE by spiking 500 ml of water or aqueous sample in a sample bottle. In this work, spikes used 1.00 ml of spike solution (2.0 mg/l in acetonitrile) delivered with an A glass pipet, yielding a concentration of 4.0 µg/l.

Filter samples are extracted with a solvent tailored to the target analytes. For Comp B and TNT munitions, this solvent is typically acetonitrile (T.F. Jenkins 1987), however the polar analytes NTO and NQ in IMX-101 and IMX-104 are sparingly soluble in common organic solvents. M.E. Walsh (2016) found that 1:1 (v/v) acetonitrile/water efficiently extracts both the polar and non-polar compounds in the IMX formulations. For tested conventional and IM formulations, enough extraction solvent to cover the filters completely (usually 20–60 ml) is sufficient to extract the study analytes using a shaker table for 18 hours. Numerous other extraction methods for soil are available but have not been demonstrated for munition residue concentrates.

Prior to analysis, each sample's matrix is adjusted to optimize peak shape for a given separation. This adjustment is made using volumetric glass pipets with mixing in a glass scintillation vial and aliquoting into a autosampler vial with a Pasteur pipet. Sample matrix should match the matrix of the standard used for calibration.

E.4 SAMPLE ANALYSIS

Typical analytical methods for explosives in soil and water are generally applicable to processed munition residue samples. Gas chromatography (e.g., EPA Method 8095) is useful for nonpolar analytes in organic solvents, but the flexibility and comparable sensitivity of HPLC (e.g., EPA Method 8330B) is generally preferred for quantifying the polar analytes in partially aqueous matrices. Instrument detection limits of less than 10 µg/l are typical by HPLC with UV detection for HMX, RDX, TNT, DNAN, NTO, and NQ.

Reverse-phase separations on C8 or C18 columns are effective for HMX, RDX, TNT, and DNAN but are generally unable to resolve NTO and NQ from the solvent peaks, especially when large volume injections of partially organic matrices are required for sensitivity. Alternative HPLC separation for NTO and NQ have been demonstrated effective using porous graphitic carbon columns (Hypercarb) and hydrophilic interaction chromatography (HILIC; *M.E. Walsh, 2016*). This two-column approach (plus two confirmations) for analyzing residues by HPLC are generalized in Table E1.

Table E1. Generalized HPLC methods for conventional and insensitive munition residues.

Study Explosive	Sample Fractions	Analytes	HPLC Methods
Comp B/TNT	SPE extract (ACN)	RDX, TNT	• Reverse Phase C8 or C18 • CN or Biphenyl
	Filter extract (ACN)	RDX, TNT	• Reverse Phase C8 or C18 • CN or Biphenyl
IMX-101/104	SPE extract (ACN)	HMX, RDX, DNAN	• Reverse Phase C8 or C18 • CN or Biphenyl
	Filter extract (1:1 ACN:H_2O)	HMX, RDX, DNAN	• Reverse Phase C8 or C18 • CN or Biphenyl
		NTO, NQ	• Porous Graphitic Carbon • HILIC
	Direct Aqueous (H_2O)	NTO, NQ	• Porous Graphitic Carbon • HILIC

Chromatographic conditions used for the live-fire tests are shown in Table E2. These isocratic methods were used to match previous command-detonation tests of the same munitions. Example chromatographs from live-fire 81 mm tests are shown in Figures E11-E14. Acidification of the

mobile phase to pH < 2, in this case using 0.1 % trifluoroacetic acid (TFA), is required to retain NTO in its protonated form. The porous graphitic carbon and HILIC methods shown for NTO are also applicable to measuring NQ, if present. NQ elutes slightly overlapping NTO with a 3/1 ACN/Water mobile phase, but it is baseline separated using 1/1 ACN/Water mobile phase (Figure E15). The reverse elution order of NQ and NTO can be achieved using the HILIC method with a mobile phase of 3/1 ACN/water and 0.1% acetic acid (Figure E16).

Table E2. Chromatographic conditions used in IMX-104 sample analysis. IPA is isopropanol, ACN is acetonitrile, MeOH is methanol, RT is retention time, and λ is detection wavelength.

Column	Mobile Phase (v/v)	Flow Rate (mL/min)	Temperature (°C)	Injection Volume (µL)	Injection Matrix (v/v)	RTs/λs (min/nm)
NovaPak C8 150 × 3.9 mm, 4 µm	15/85 IPA/Water	1.4	30	100	1/3 ACN/Water	HMX: 1.5/230 RDX: 2.8/230 DNAN: 6.7/295
Hypercarb 150 × 4.6 mm, 5 µm	3/1 ACN/Water 0.1 % TFA	1.5	28	100	3/1 ACN/Water	NTO: 1.7/321
Poroshell 120 EC-CN 150 × 3.0 mm, 2.7 µm	50/50 MeOH/Water	0.6	30	10	1/3 ACN/Water	HMX: 6.7/230 RDX: 4.1/230 DNAN: 2.9/295
XBridge BEH Amide 100 × 4.6 mm, 2.5 µm	97/3 ACN/Water 0.1 % TFA	0.5	28	20	3/1 ACN/Water	NTO: 3.3/320

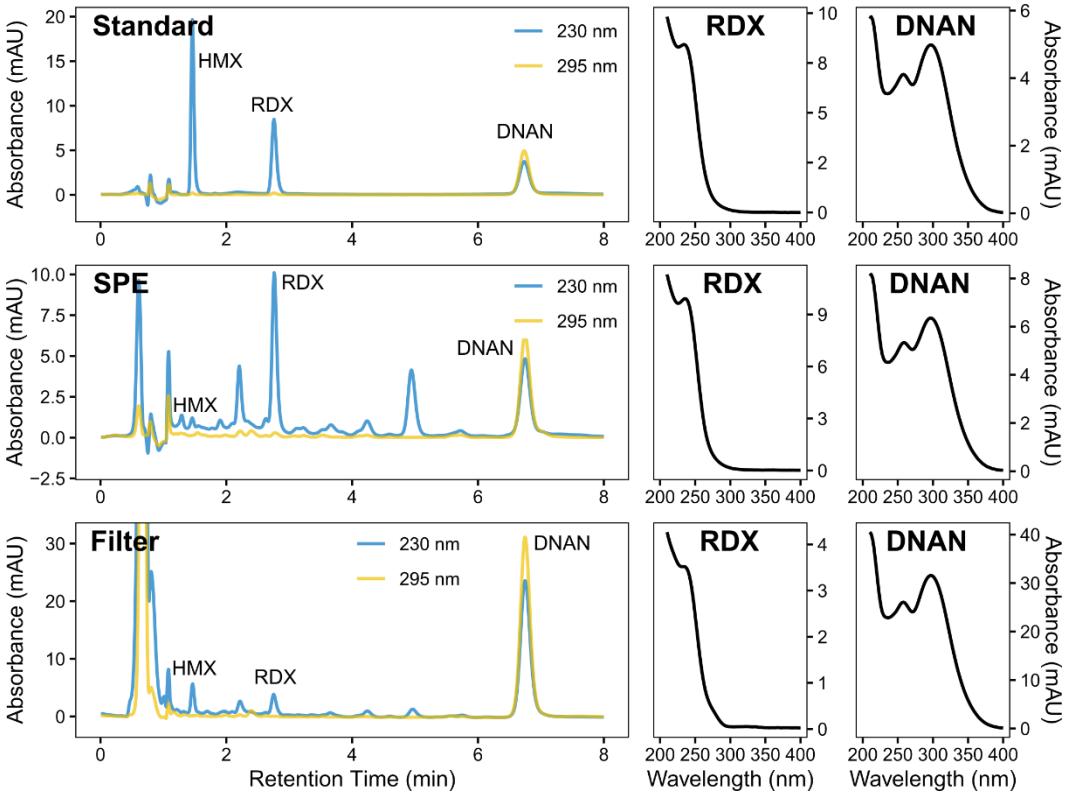

Figure E11. Example chromatography and UV spectra of a standard and samples using the C8 primary method for HMX, RDX, and DNAN.

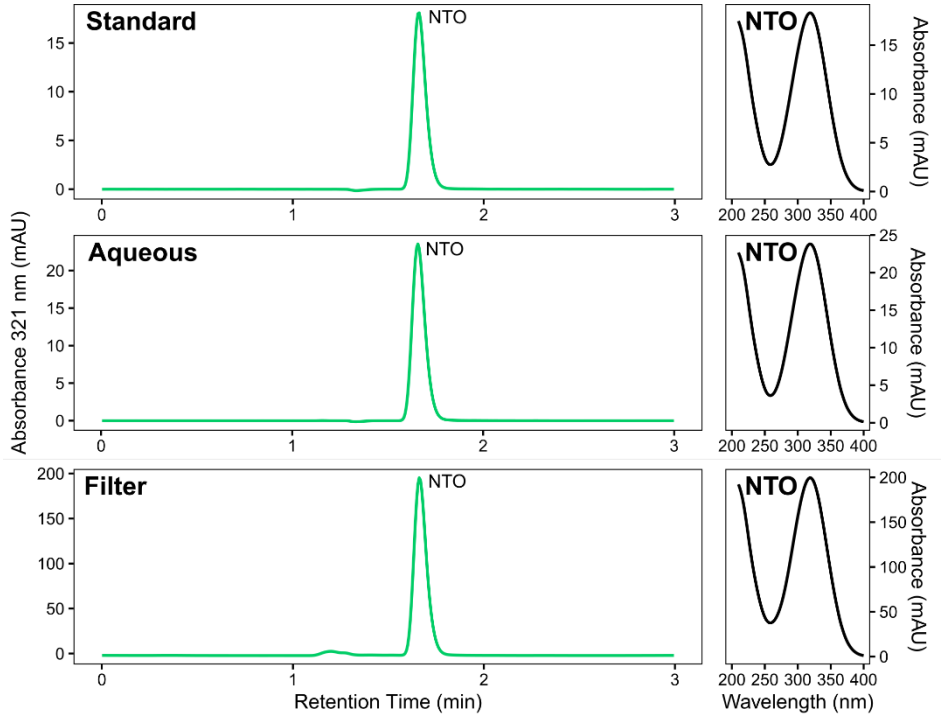

Figure E12. Example chromatography and UV spectra of a standard and samples using the Hypercarb primary method for NTO.

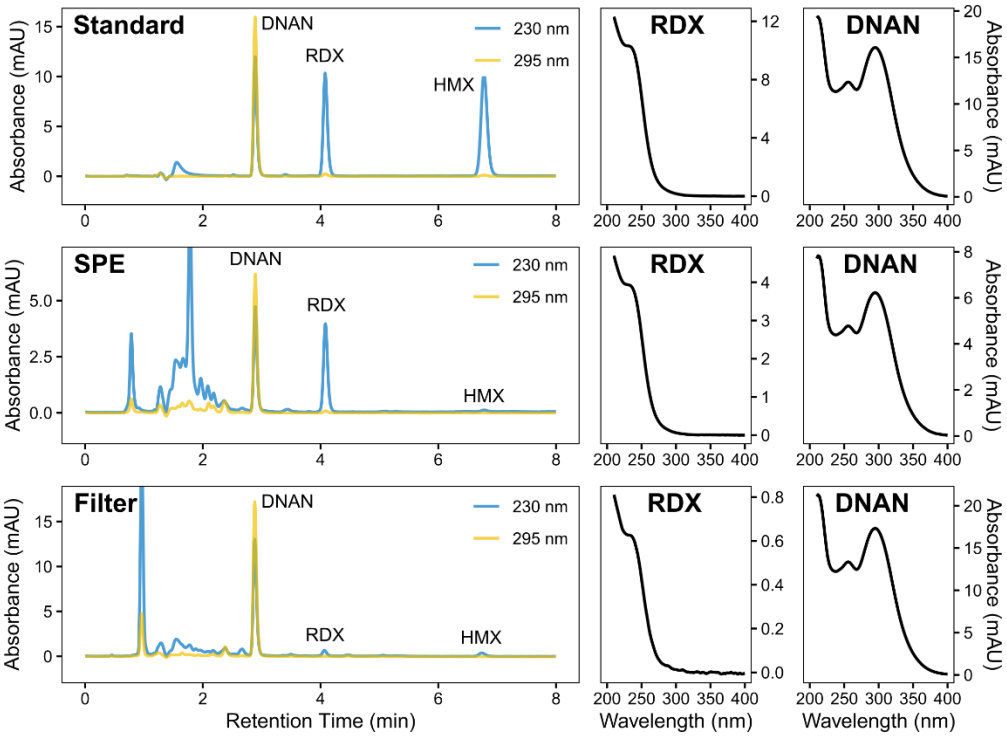

Figure E13. Example chromatography and UV spectra of a standard and samples using the CN confirmation method for HMX, RDX, and DNAN.

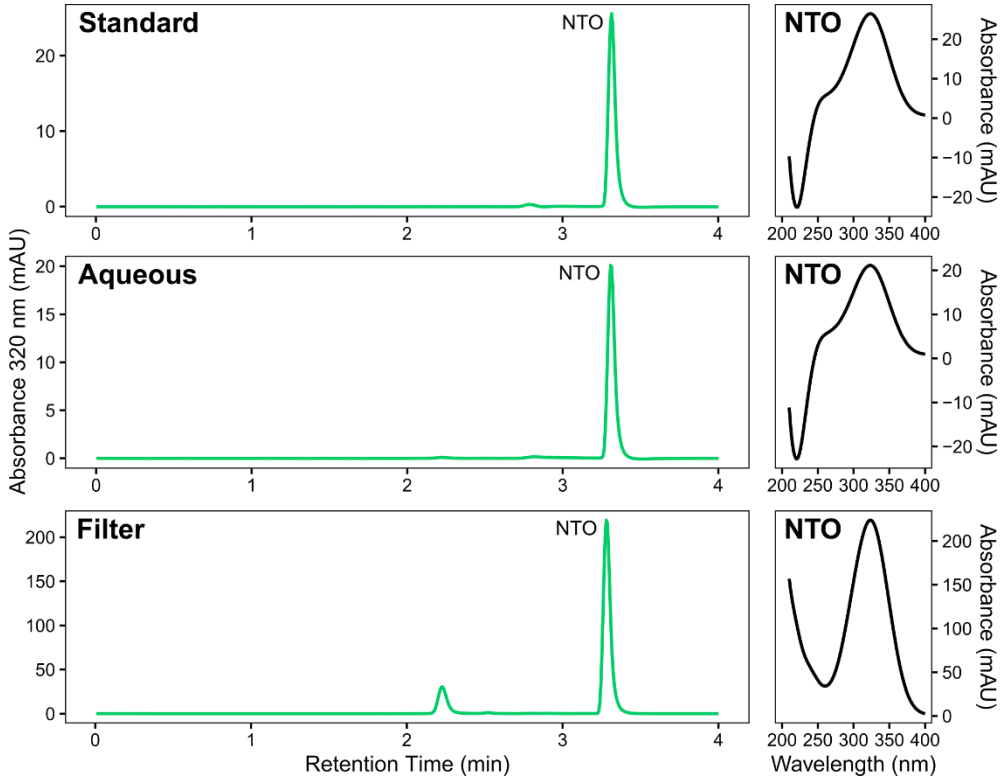

Figure E14. Example chromatography at 320 nm and UV spectra of a standard and samples using the HILIC confirmation method for NTO. Note: HMX, RDX, and DNAN elute prior to NTO.

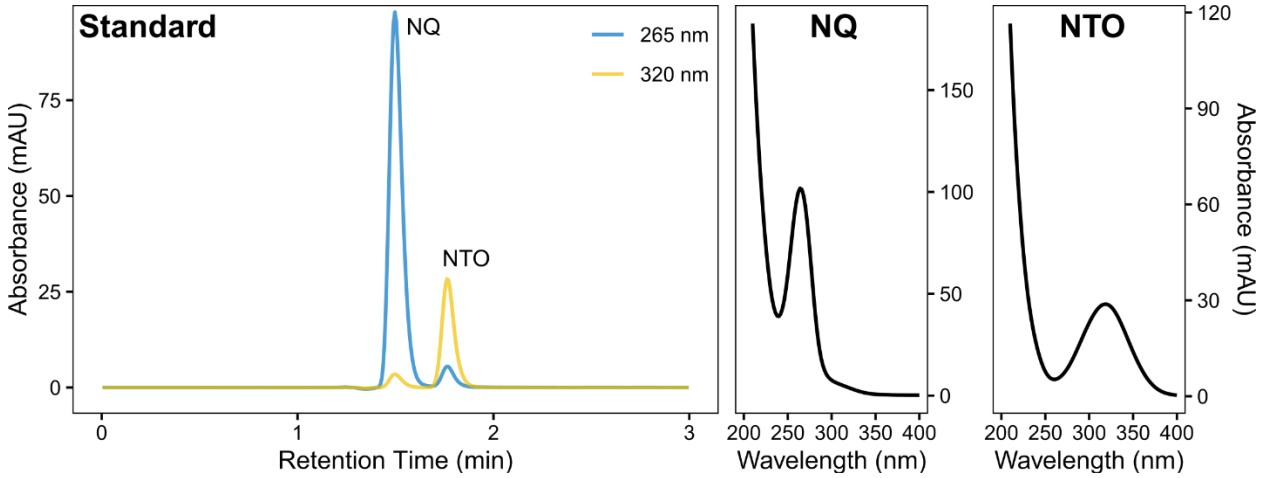

Figure E15. Example chromatography and UV spectra of a standard using the above Hypercarb method with a mobile phase of 1/1 (v/v) ACN/Water and 0.1 % TFA for NQ and NTO.

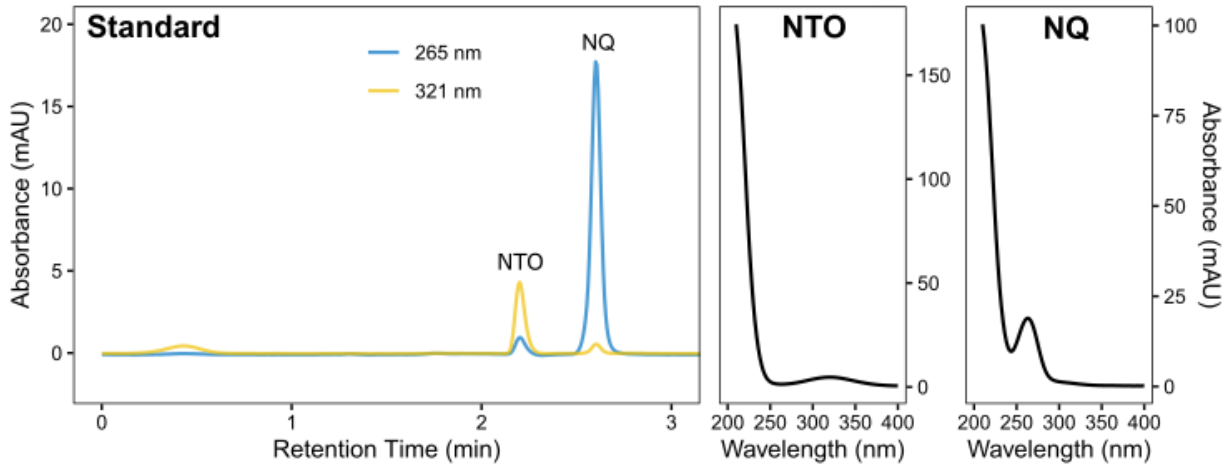

Figure E16. Example chromatography and UV spectra of a standard using the above HILIC method with a mobile phase of 3/1 (v/v) ACN/Water and 0.1% CH_3COOH for NQ and NTO.